

**Basics for Groundwater
Flow under Permafrost
Conditions in the Context
of Radioactive Storage**

Basics for Groundwater Flow under Permafrost Conditions in the Context of Radioactive Storage

Klaus-Peter Kröhn

December 2022

Remark

This report refers to the research project 02E11809A, funded by the Federal Ministry for the Environment, Nature Conservation, Nuclear safety and Consumer Protection (BMUV).

This work was conducted by Gesellschaft für Anlagen- und Reaktor sicherheit (GRS) gGmbH.

The author is responsible for the content of the report.

Keywords

Balance Equations, Equations of State, Geological Repository, Groundwater Flow, Heat Flow, Permafrost Conditions

Acknowledgements

Funding of this theoretical work within the project HYMNE (FKZ 02 E 11809A) by the German Federal Ministry for the Environment, Nature Conservation, Nuclear Safety and Consumer Protection (BMUV) is gratefully acknowledged. Many thanks are also due to my colleague Matthias Hinze for his remarkably thorough and constructive review of this report. Much obliged!

Abstract

Deep geological disposal of nuclear waste implies storage at a depth of several hundred metres below the surface and a safety assessment covering a long period of time. One of the main concerns for such a repository is the detrimental effect of groundwater on the technical and geotechnical barriers, a second one the migration of radionuclides with the groundwater into the biosphere in case of a possible failure of the waste canisters. Long-term safety assessment thus requires well-founded knowledge of the local and regional groundwater system as a basis for assessing the robustness of a repository in general and for predicting radionuclide migration in case of leakage from a damaged waste canister in particular.

An additional complexity to this requirement is introduced by the fact that all potential sites for a nuclear waste repository in Germany have several times been subject to permafrost conditions within the last million years. It is thus highly likely that groundwater flow at any chosen site will undergo such conditions during its envisioned lifetime. Under permafrost conditions, ground freezing to a large lateral as well as vertical extent has to be assumed. Against this background it can easily be imagined that formerly shallow flow paths can be blocked by the evolving ice.

The depth of the permafrost is basically a result of the interplay of the mean surface temperature, the geological structure of the top few hundred meters in the ground and heat flow from earth's interior. Changes between moderate and cold periods may therefore lead to radical changes in the groundwater flow system with a strong impact on potential pathways of radionuclides.

Further complexity is introduced by larger surface waters such as lakes and rivers as they may cause the formation of taliki. A talik is a layer or body of unfrozen ground occurring in a permafrost zone that may connect the surface water with a deep aquifer below the permafrost. As such, it may establish a hydraulic shortcut through the permafrost, thereby concentrating groundwater exchange between the surface and deep aquifers – and by that a potential outflow of radionuclides – to the few open taliki. At that, they represent a key feature in a groundwater flow system under permafrost conditions. Knowledge of size and location as well as the stability of taliki is thus vital for predicting possible radionuclide migration.

The approach of an ice shield and the subsequent ice coverage increase the complexity of influences on the groundwater system considerably again. The dynamics of the growth of the ice shield as well as the resulting mechanical load on the groundwater flow in the porous underground are additionally to be taken into account. Pressure melting under the ice shield may liquefy frozen groundwater and introduce an extra flow system.

However, including these effects does not contribute to the understanding of taliki and is therefore not necessary at this stage of investigation. The scope of this report is rather restricted to periglacial permafrost conditions in order to limit the incalculables concerning the referring groundwater flow. This appears to be even more reasonable as permafrost evolves anyway before an ice shield possibly arrives. The present work is therefore ultimately aiming on taliki as a comparatively poorly understood feature in a groundwater flow system under permafrost conditions.

In the field, taliki can be investigated only "as is". Hints about their geological history are hard to come by. However, broadening the understanding of the mechanisms that create taliki and keep them open over longer time periods might also be gained by numerical modelling. The work presented here intends to provide the basis for modelling exercises in that respect. This includes (a) the physics of a conceptual model, (b) a sound comprehension of the balance equations underlying a referring mathematical model, (c) a compilation of equations of state (EOS) with a particular view to subzero temperatures as well as the also required constitutive equations, and (d) a comparison with some formulations from the literature.

Moreover, work on bullet point (c) led to the development of new formulations for the EOS that are adapted to the temperature and pressure ranges expected for the problem at hand. Since these ranges are much more limited than those established for more general applications, the formulations developed here are simpler and easier to compute.

Zusammenfassung

Die Errichtung eines geologischen Endlagers für radioaktive Abfälle bedeutet unter anderem, dass die Einlagerungsorte mehrere hundert Meter unter der Oberfläche liegen und dass Sicherheitsbetrachtungen für einen großen Zeitraum erforderlich sind. Eines der Hauptprobleme für ein solches Endlager stellt der schädliche Einfluss von Grundwasser auf die technischen und geotechnischen Barrieren dar. Ein Zweites besteht für den Fall eines möglichen Versagens von Abfallbehältern in der Ausbreitung von Radionukliden mit dem Grundwasser in die Biosphäre.

Für Untersuchungen zur Langzeitsicherheit eines geologischen Endlagers ist es daher von entscheidender Bedeutung, die Grundwasserbewegungen sowohl lokal als auch regional möglichst gut zu charakterisieren insbesondere mit Blick auf eine Radionuklid-ausbreitung nach einem möglichen Behälterversagen. Diese für sich genommen bereits nicht triviale Aufgabe wird dadurch weiter erschwert, dass alle potenziellen Endlagerstandorte in Deutschland während der letzten Million Jahre wiederholt Permafrostbedingungen ausgesetzt waren. Aus diesem Grund ist anzunehmen, dass die Grundwasserbewegung an all diesen Orten während der projektierten Lebensdauer eines Endlagers über Zeiträume von Tausenden von Jahren hinweg durch Permafrostbedingungen beeinflusst sein werden.

Permafrostbedingungen implizieren ein Einfrieren des Bodens über weite Bereiche und bis zu einer erheblichen Tiefe. Somit ist leicht vorstellbar, dass das entstehende Eis im Boden vormals flach verlaufende Fließwege blockiert. Die Tiefe des Permafrosts ist im Wesentlichen durch das Zusammenspiel folgender Größen bestimmt: der mittleren Oberflächentemperatur, der geologischen Struktur insbesondere in dem mehrere hundert Meter mächtigen Bereich unter der Oberfläche und dem Wärmestrom aus dem Erdinneren. Wechsel zwischen gemäßigten und kalten Klimata können daher zu radikalen Änderungen der Grundwasserströmung und damit der potenziellen Ausbreitungspfade von Radionukliden führen.

Die Komplexität dieses Phänomens wird weiter dadurch erhöht, dass sich unter größeren Oberflächengewässern Taliki bilden können. Ein Talik ist ein Bereich ungefrorenen Bodens im Permafrost, dessen Größe von den örtlichen Bedingungen abhängt. Nicht selten sind Taliki hinreichend stark ausgeprägt, so dass sie den Permafrost durchdrin-

gen und dadurch Oberflächengewässer und tiefe Grundwasserstockwerke verbinden können. In diesen Fällen stellen sie einen hydraulischen Kurzschluss durch den Permafrost dar, der den Austausch von Oberflächenwasser und tiefen Grundwässern ermöglicht und damit einen potenziellen Radionuklidstrom örtlich konzentriert. Taliki bilden daher ein Schlüsselmerkmal in einem Grundwassersystem unter Permafrostbedingungen. Verständnis für Größe und Lage sowie die Stabilität von Taliki sind daher entscheidend für belastbare quantitative Vorhersagen einer möglichen Radionuklidausbreitung.

Das Herannahen eines Eisschildes und eine nachfolgende Eisüberdeckung erhöhen die Komplexität der Einflüsse auf das Grundwassersystem noch einmal erheblich. Zum einen ist die Wachstumsdynamik des Schildes zu berücksichtigen, zum anderen verändert die Auflast des Schildes die Druckverhältnisse für die Strömung im porösen Untergrund. Ferner kann Druckschmelzen zu Strömungsvorgängen unter dem Eisschild führen.

Für das grundsätzliche Verständnis der Talikbildung und –stabilität sind die Vorgänge im Umfeld eines Eisschildes jedoch nicht erforderlich. Der Fokus dieses Berichts richtet sich daher auf periglaziale Permafrostbedingungen, um die Anzahl der Unwägbarkeiten zu begrenzen, zumal sich Permafrost in jedem Fall bildet, noch bevor ein Eisschild gegebenenfalls eintrifft.

Allerdings sind Taliki im Feld nicht einfach zu untersuchen und spiegeln zudem auch nur den gegenwärtigen Zustand wider. Hinweise auf ihren geohistorischen Werdegang sind schwer zu finden. Wegen der zentralen Bedeutung von Taliki für das Grundwassersystem unter Permafrostbedingungen erscheint es daher sinnvoll, die Mechanismen, die zur Entstehung von Taliki führen und diese über lange Zeiten hinweg erhalten, alternativ durch numerische Modelle zu identifizieren.

Dieser Bericht soll für solche Arbeiten eine Basis schaffen. Dabei werden die folgenden vier Teilaspekte berührt: (a) ein Konzeptmodell der relevanten physikalischen Vorgänge, (b) ein grundlegendes Verständnis für die einem mathematischen Modell zugrunde liegenden Erhaltungsgleichungen, (c) eine Zusammenstellung der relevanten Zustandsgleichung mit besonderem Blick auf Formulierungen für den Temperaturbereich unter $0\text{ }^{\circ}\text{C}$ wie auch der ebenfalls erforderlichen konstitutiven Beziehungen und (d) ein Vergleich von unterschiedlichen Formulierungen aus der Literatur.

Darüber hinaus sind aus den Arbeiten an Punkt (c) heraus neue Formulierungen für die Zustandsgleichungen entstanden. Diese sind an das Spektrum der Temperaturen und Drücke angepasst, das im Rahmen dieses Berichts erwartet wird. Diese Einschränkung gegenüber den etablierten und sehr viel allgemeiner gültigen Beziehungen ermöglichte es, mit einfacheren und damit weniger rechenintensiven Formulierungen ähnlich gute Beschreibungen zu gewinnen.

Table of content

	Acknowledgements	I
	Abstract	II
	Zusammenfassung	IV
1	Introduction and motivation	1
1.1	Terminology.....	1
1.2	Characteristics and influences concerning permafrost	5
1.3	Geological repositories and permafrost conditions in Germany	7
1.4	Permafrost and groundwater flow	10
2	Problem definition	11
3	Physical particularities of freezing water.....	13
3.1	Changing the phase state of water	13
3.2	State variables at sub-zero temperatures	14
3.3	Freezing of water in porous media.....	14
4	Conceptual understanding	15
4.1	Phenomena.....	15
4.2	Groundwater flow	15
4.3	Interaction of groundwater flow and heat flow	17
5	General balance equations	19
5.1	Methodology.....	19
5.1.1	Introductory remark.....	19
5.1.2	Local derivation.....	19
5.1.3	Global derivation	20
5.1.4	General balance equation	22
5.2	Mass balance equation.....	23
5.2.1	Mass balance for water	23
5.2.2	Mass balance for ice	24
5.2.3	Mass balance for the whole system	25
5.3	Energy balance equation	25
5.3.1	Energy balance for water	25
5.3.2	Energy balance for ice	27
5.3.3	Energy balance for the matrix	28
5.3.4	Energy balance for the whole system.....	29

6	Processes, constitutive equations and equations of state	31
6.1	The “game board” and the “book of rules”.....	31
6.2	Processes.....	31
6.2.1	Rules for the mass balance.....	31
6.2.2	Rules for the energy balance	32
6.3	Constitutive equations	35
6.3.1	Porosity.....	35
6.3.2	Flow law.....	36
6.3.3	Saturation	37
6.3.4	Relative permeability for water	38
6.3.5	Non-advective heat flow.....	38
6.3.6	Dispersion.....	39
6.3.7	Summary of dependencies for the CEs.....	40
6.4	Equations of state.....	40
6.5	Reified balance equations.....	42
7	Case specific adaptations	47
7.1	Purpose and procedure	47
7.2	Case 1: Heat producing geological repositories.....	47
7.3	Case 2: Benchmarks from the INTERFROST-project.....	51
7.4	Case 3: Talik forming.....	53
7.5	Comparison of the developed equations.....	56
7.5.1	General remarks	56
7.5.2	Mass balance equations	56
7.5.3	Heat balance equations	58
8	Formulations from the literature	61
8.1	Approaches in different versions of COMSOL Multiphysics	61
8.1.1	Approaches used in /COM 16/	61
8.1.2	New features in /COM 21/.....	63
8.1.3	Approach from /ZOT 12/.....	65
8.1.4	Approach from /BAR 16/	66
8.1.5	Approach from /SCH 17/.....	68
8.1.6	Own attempt on case 2	71
8.2	Approach from /FER 17/.....	72
8.3	Approach from /GRE 18/	74
9	Comparison of approaches	77
9.1	Introductory remark.....	77
9.2	Balance equations	77
9.2.1	General observations.....	77
9.2.2	Groundwater flow equations.....	78
9.2.3	Heat flow equations.....	82

9.3	Equations of state	89
9.4	Constitutive equations	91
9.4.1	General observations	91
9.4.2	Porosity	91
9.4.3	Water/ice saturation	92
9.4.4	Relative permeability for water	95
10	Summary, conclusions and recommendations	101
10.1	Summary	101
10.2	Conclusions	103
10.2.1	General remarks	103
10.2.2	Comparison of the balance equations	104
10.2.3	Comparison of the EOS	106
10.2.4	Comparison of the CEs	107
10.3	Recommendations	108
	References	111
	Table of figures	123
	List of tables	125
A	Appendix: Formalized test case descriptions	127
A.1	Test case TH2 “Frozen inclusion thaw”	127
A.2	Test case TH3 “Talík Opening/Closure”	129
B	Appendix: State variables including subzero temperatures.....	133
B.1	Data and formulations	133
B.1.1	Density	135
B.1.2	Viscosity	138
B.1.3	Thermal conductivity	140
B.1.4	Heat capacity	144
B.2	Full range of primary variables T and p as considered in case 1	148
B.2.1	Density	148
B.2.2	Viscosity	149
B.2.3	Thermal conductivity	150
B.2.4	Heat capacity	151
B.3	Discussion of cases 1 to 3	153
B.3.1	Choice of formulations	153
B.3.2	Variability of EOS in cases 1 to 3	154
B.3.3	Choice of EOS in cases 1 to 3	158

C	Appendix: Treatment of freezing soils after /AUK 16/	161
C.1	General assumptions.....	161
C.2	Characterizing soil parameters	161
C.3	Effective hydraulic conductivity	162
C.4	Cryosuction	162
C.5	Freezing temperature	163
C.6	Water saturation	163
C.7	Explanation of variables.....	165
D	Appendix: Reference formulations from the literature	167
D.1	Density from /IAP 15/.....	167
D.2	Viscosity from /IAP 08/.....	171
D.3	Thermal conductivity from /IAP 11/	174
D.4	Heat capacity from /IAP 15/	177

1 Introduction and motivation

1.1 Terminology

The following definitions concern the underground as well as groundwater conditions and form the conceptual basis of this report. They are taken from /VEV 05/ and illustrated in Fig. 1.1 and Fig. 1.2. The sequence of the definitions is chosen to be informative in the sense of increasing insight rather than being alphabetical. Additions to the text from /VEV 05/ are marked as “Note”.

Permafrost: Ground (soil or rock and included ice and organic material) that remains at or below 0 °C for at least two consecutive years¹.

Note: The term “*permafrost*” refers to temperature only. The top of the *permafrost* may therefore be located at any depth below the surface.

Geothermal gradient: The rate of temperature increase with depth in the subsurface.

Note: In the vicinity to the ground surface the vertical temperature evolution is distorted by the seasonal temperature variations.

Cryotic ground: Soil or rock at temperatures of 0 °C or lower.

Note: The terms “*cryotic*” and “*non-cryotic*” refer to the temperature of 0 °C as opposed to the terms “*frozen*” and “*unfrozen*” that depend on the local melting point of water.

Active layer: The layer of ground that is subject to annual thawing and freezing in areas underlain by *permafrost*.

Permafrost table: The upper boundary surface of permafrost.

Note: The depth of the permafrost tables depends on a number of conditions. Best known is the relation to the thickness of the *active layer*.

¹ In the Russian literature, the definition involves three years of temperatures below 0 °C /VEV 05/.

Permafrost base: The lower boundary surface of *permafrost*, above which temperatures are perennially below 0 °C (*cryotic*) and below which temperatures are perennially above 0 °C (*non-cryotic*).

Cryopeg: A layer of *unfrozen* ground that is perennially *cryotic* (forming part of the *permafrost*), in which freezing is prevented by freezing-point depression due to the dissolved-solids content of the pore water.

Comment by /VEV05/: Three types of *cryopeg* can be distinguished on the basis of their position with respect to *permafrost*:

1. a *basal cryopeg* forms the basal portion of the *permafrost* (see Fig. 1.1);
2. an *isolated cryopeg* is entirely surrounded by perennially *frozen* ground;
3. a *marine cryopeg* is found at the top in coastal or subsea perennially *frozen* ground; *marine cryopegs* may also be basal and/or isolated.

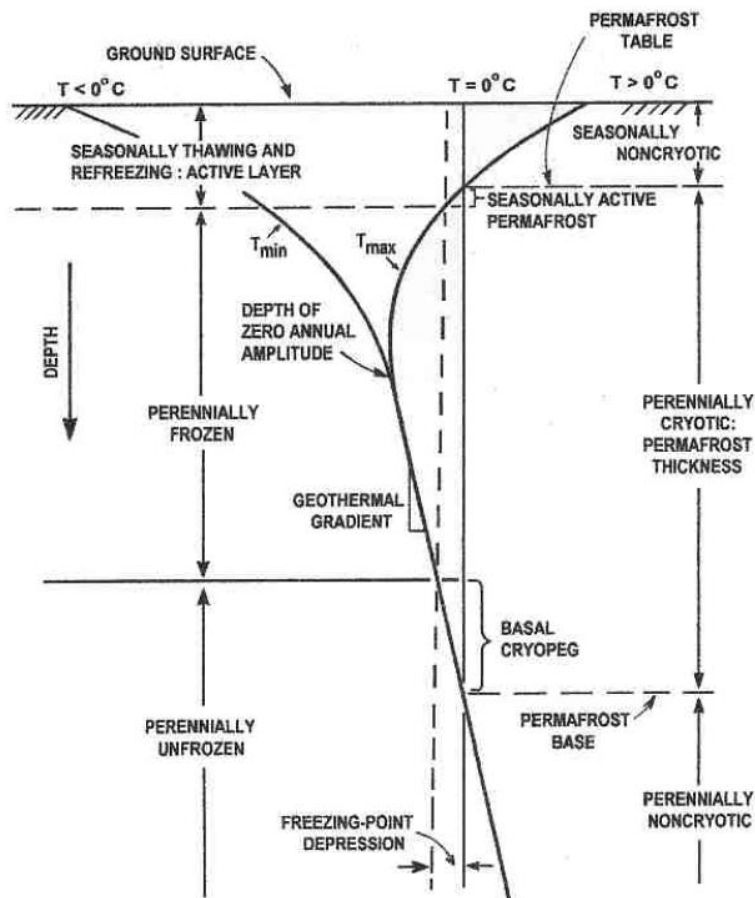


Fig. 1.1 Ground conditions in relation to temperature and depth; from /VEV 05/

Continuous permafrost: *Permafrost* occurring everywhere beneath the exposed land surface throughout a geographic region with the exception of widely scattered sites,

Note: Typically defined as underlying 90-100% of the landscape /IPA 21/, /BRO 97/

Discontinuous permafrost: *Permafrost* occurring in some areas beneath the exposed land surface throughout a geographic region where other areas are free of *permafrost*.

Note: Typically defined as underlying 50-90% of the landscape /IPA 21/, /BRO 97/

Sporadic discontinuous permafrost: *Permafrost* underlying 10 to 35 / 5 to 30 percent² of the exposed land surface.

Comment by /NEV05/: Individual areas of *permafrost* are completely surrounded by *unfrozen* ground.

Note: Typically defined as underlying 10-50% of the landscape /BRO 97/

Isolated patches of permafrost: *Permafrost* underlying less than 10 percent of the exposed land surface.

Note: As defined in /BRO 97/ or /HEG 09/

Talik: A layer or body of *unfrozen* ground occurring in a *permafrost* area due to a local anomaly in thermal, hydrological, hydrogeological, or hydrochemical conditions.

Comment by /NEV05/:

- *Taliki* may have temperatures above 0 °C (*non-cryotic*) or below 0° C (*cryotic*, forming part of the *permafrost*).
- Some *taliki* may be affected by seasonal freezing.
- Several types of *taliki* can be distinguished on the basis of
 - their relationship to the *permafrost* (closed, open, lateral, isolated and transient)
 - the mechanism responsible for their *unfrozen* condition (hydrochemical, hydrothermal and thermal *taliki*)³:

² North American/Russian definition

³ The sequence of the talik characterizations has been altered to provide an order with reference to cryotic and non-cryotik ground conditions.

closed talik - a *non-cryotic* talik occupying a depression in the *permafrost table* below a lake or river (also called "lake *talik*" and "river *talik*"); its temperature remains above 0° C because of the heat storage effect of the surface water;

hydrothermal talik - a *non-cryotic talik*, the temperature of which is maintained above 0 °C by the heat supplied by groundwater flowing through the *talik*;

thermal talik - a *non-cryotic talik*, the temperature of which is above 0 °C due to the local thermal regime of the ground;

isolated talik - a *talik* entirely surrounded by perennially *frozen* ground; usually *cryotic* (see *isolated cryopeg*), but may be *non-cryotic* (see *transient talik*);

lateral talik - a *talik* overlain and underlain by perennially *frozen* ground; can be *non-cryotic* or *cryotic*;

open talik - a *talik* that penetrates the *permafrost* completely, connecting suprapermafrost and subpermafrost water, (e.g., below large rivers and lakes). It may be *non-cryotic* (see *hydrothermal talik*) or *cryotic* (see *hydrochemical talik*).

SYNONYMS (not recommended): through talik, penetrating talik, perforating talik, piercing talik;

transient talik - a *talik* that is gradually being eliminated by freezing, e.g., the initially *non-cryotic* closed *talik* below a small lake which, upon draining of the lake, is turned into a transient isolated *talik* by *permafrost* aggradation.

hydrochemical talik - a *cryotic talik* in which freezing is prevented by mineralized groundwater flowing through the *talik*.

Note: The difference between *cryopegs* and *hydrochemical taliki* is somewhat fuzzy. However, while *cryopegs* are usually found at the fringe of the *permafrost* (or isolated within), *taliki* rather form connections through the *permafrost*.

Note further: While the terminology for classifying *taliki* used by /VEV 05/ is stringent, *taliki* are often labeled differently and less differentiated in the literature. An example is given by the illustration from /PAB 12/ where the expressions "open", "closed" and

“through” *talik* are used instead of “isolated”, “closed” and “open” *talik* as defined by /NEV 05/.

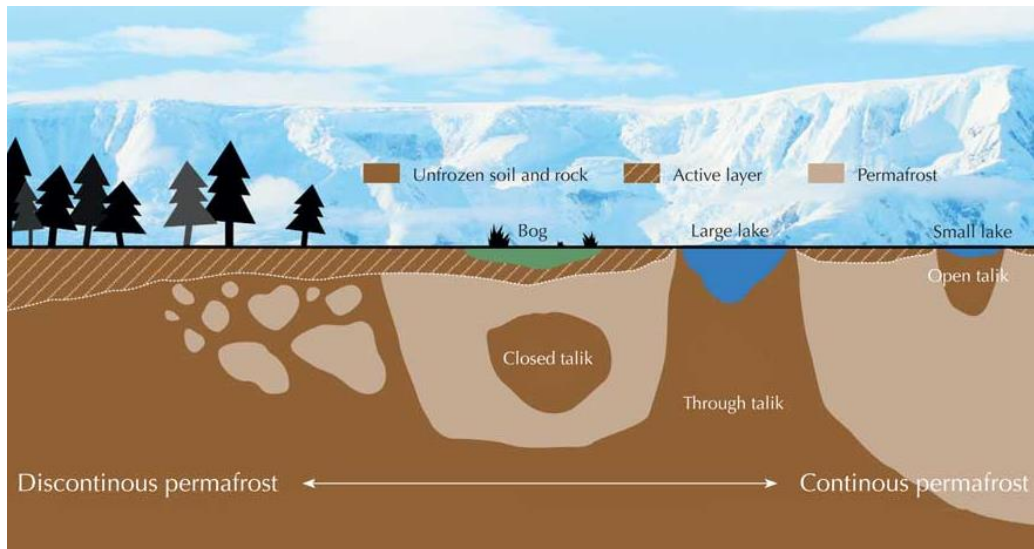


Fig. 1.2 Types of permafrost and taliki; from /PAB 12/

1.2 Characteristics and influences concerning permafrost

Permafrost underlies about 15 % of the exposed land surface area in the Northern Hemisphere and 11 % of the global surface /OBU 21/. At that, the literature ascribes the vast majority of permafrost affected underground (more than 97 %) to the Northern Hemisphere. Continuous, discontinuous and the sporadic permafrost zones together with isolated patches are roughly divided into shares of 50, 20 and 30 %, respectively, of the total permafrost area /HEG 09/. Besides being differentiated by the mean annual temperature and the associated permafrost structure, permafrost is sometimes also named after the location of occurrence like alpine permafrost or subsea permafrost.

By definition, permafrost is any type of ground that shows a temperature below 0 °C for a period of at least two years (see section 1.1). This temperature is not to be confused, though, with the annual mean soil surface temperature as the depth of the 0°C-isoplane may vary. Where the surface is open to the atmosphere, seasonal freezing and thawing may occur which defines the so-called “active layer”, to be found above the actual permafrost. Furthermore, there may be insulation of the surface by vegetation, snow and other mechanisms which requires the mean annual surface temperature to be lower than

0 °C for permafrost to develop. Below temperate glaciers there may be no permafrost at all due to pressure-melting /SHA 88/.

Generally, sporadic, discontinuous, and continuous permafrost can be found at decreasing temperatures. The temperature below which continuous permafrost can be expected is generally assumed to be about -5 °C (e.g. /IPA 21/, /TFL 21/, /WIK 21/b). The temperature separating discontinuous and sporadic permafrost may lie at -2 °C /TFL 21/.

Freezing of the ground is countered by geothermal heat coming up from earth's core. Where the opposing effects result locally in a temperature of 0 °C, the permafrost base can be found (see section 1.1).

There are several causes for earth's heat production such as radioactive decay which is believed to account for half of the heat production if not even somewhat more, residual heat from planetary accretion, and latent heat from core crystallization. The hottest spot can be found at the centre of earth from which the temperature decreases towards the surface. However, the core temperature as well as temperatures at the boundaries of the distinct layers constituting earth's interior are still subject to quite some uncertainty. A radial temperature profile from earth's centre to its surface clearly forms a complex curve due to the convection of the liquid mantle and outer core but can only be reliably quantified to a certain extent (see Fig. 1.3).

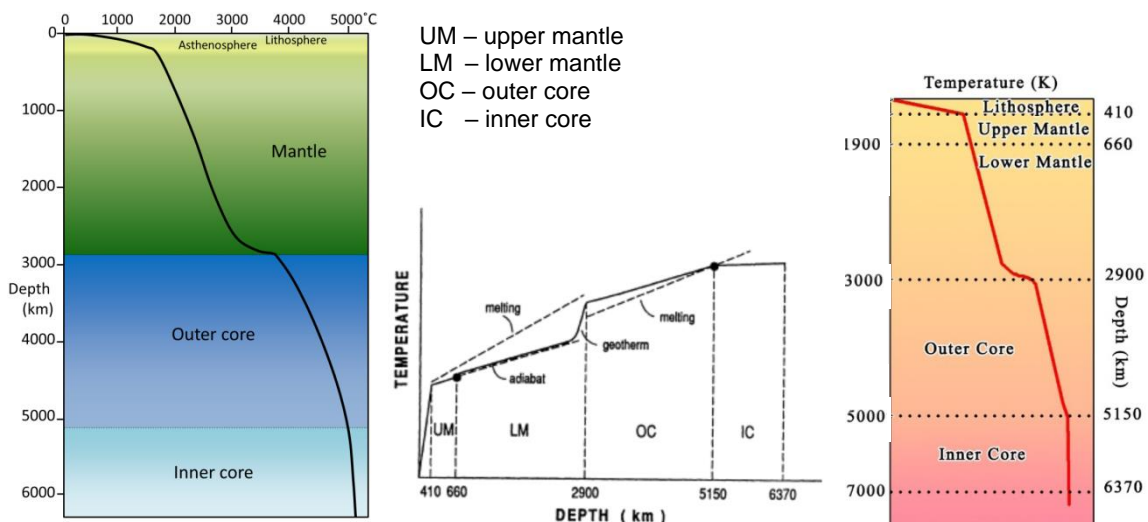


Fig. 1.3 Radial temperature profiles for the earth;
left: from /EAR 19/, middle: from /BOE 96/; right: from /MIK 14/

However, in earth's very upper part – the solid crust – down to a few hundred kilometres depth, the curve is rather linear and well described by the geothermal gradient as heat flow is basically due to conduction only in this region. In principle, the geothermal gradient is a constant, but it varies to a certain extent over earth's surface. While the global mean of the geothermal gradient amounts to about 29,8 K/km /SDW 21/, extreme values as high as 9 °C/100 m and as low as 1 °C/100 m have been found as well /WIK 21a/. The actual value depends on different local factors like geology, mineralogy, morphology and, if applicable, volcanic activity. Ultimately, however, the local thermal conductivity of earth's crust decides about the steepness of the geothermal gradient. As a general rule, the steepness is inversely related to the thermal conductivity.

1.3 Geological repositories and permafrost conditions in Germany

Deep geological disposal of nuclear waste implies (1) storage at a depth of several hundred metres below surface and (2) a safety assessment that covers a long period of time. In Germany a time span of 1,000,000 years has to be considered (e.g. /STA 17/). One of the main concerns for such a repository is the detrimental effect of groundwater on the technical and geotechnical barriers, a second one the migration of radionuclides with the groundwater into the biosphere in case of a possible failure of the waste canisters. With a view to those hazards, a multi-barrier system including technical barriers such as the waste canisters, geotechnical barriers, fabricated barriers from natural materials like bentonite or crushed salt (depending on the host rock) and the natural, geological barrier posed by the host rock is envisaged for a repository for radioactive waste as depicted in Fig. 1.4.

For long-term safety considerations, a well-founded knowledge of the local and regional groundwater system is therefore required in any case. This is obviously of vital importance for predicting radionuclide migration in case of leakage from a damaged waste canister.

Potential sites for repositories in Germany require a suitable host rock that is a formation with low hydraulic conductivity. Three possible host rocks qualifying in this respect have been identified in Germany (not in ranking order): rock salt, claystone and granite. According to older investigations, these formations can be found either in the North German lowlands, in Southern Germany within or adjacent to the Alpine foothills or in the

East in the range of the Erzgebirge (see Fig. 1.5, left) /BGR 12/. In the framework of the ongoing site selection process, even 54 % of the area of Germany are presently under investigation /BGE 20/ (see. Fig. 1.6).

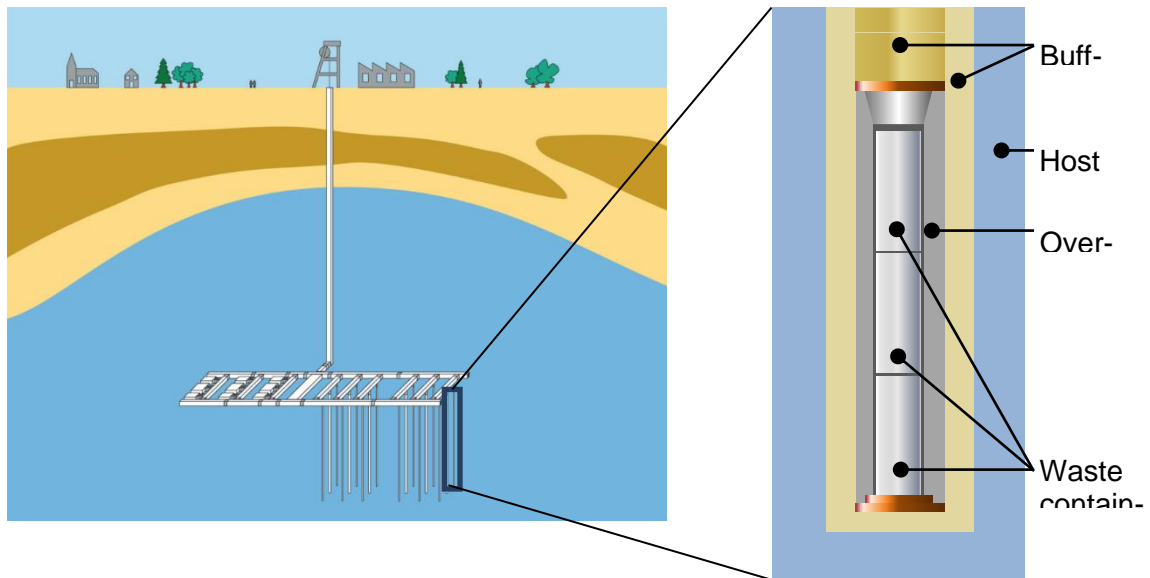


Fig. 1.4 Multi-barrier system envisaged for a deep geological repository

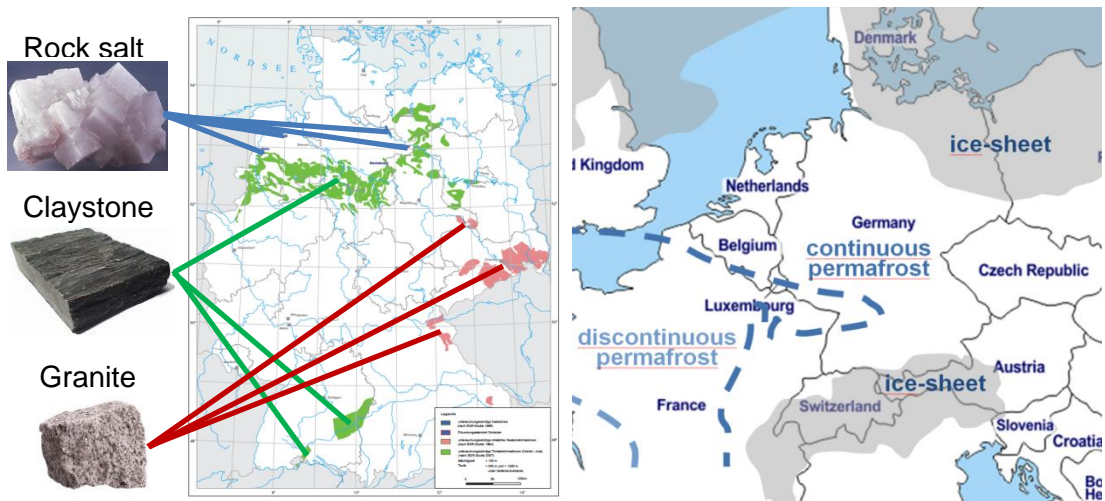


Fig. 1.5 Potential sites for a deep geological repository (left) /BGR 12/ and permafrost conditions during the latest ice age (right); after /VAN 93/ and /REN03/

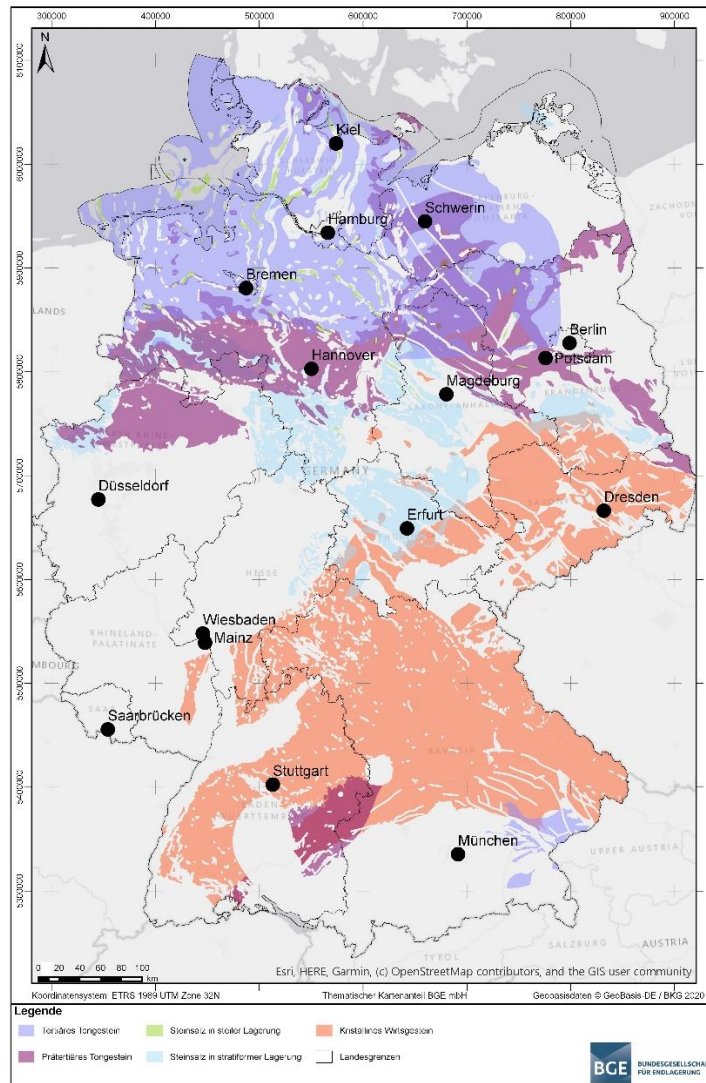


Fig. 1.6 Potential sites for a deep geological repository; present state of the site selection process in Germany /BGE 20/

During the latest cold period, the Weichselian glacial (Würm glacial stage for the Alpine region), all of Germany with a small exception to the mid-west has experienced either continuous permafrost and or even coverage by an ice shield (see Fig. 1.5, right; e.g. /VAN 93/ and /REN 03/). At one time or another, all potential sites for a nuclear waste repository have thus been under permafrost conditions. It has to be assumed that this will also happen in the future during the lifetime of any geological repository in Germany.

1.4 Permafrost and groundwater flow

Ground freezing to a large lateral as well as vertical extent has to be assumed under permafrost conditions. Changes between moderate and cold periods may lead to radical changes in the groundwater flow system with a strong impact on a potential radionuclide migration as illustrated in Fig. 1.7. The sketch illuminates the situation for a geological repository in granite below a slopy area that includes lakes and rivers. In this situation, groundwater flow is driven by different heights of surface water levels and precipitation that result in hydraulic pressure gradients.

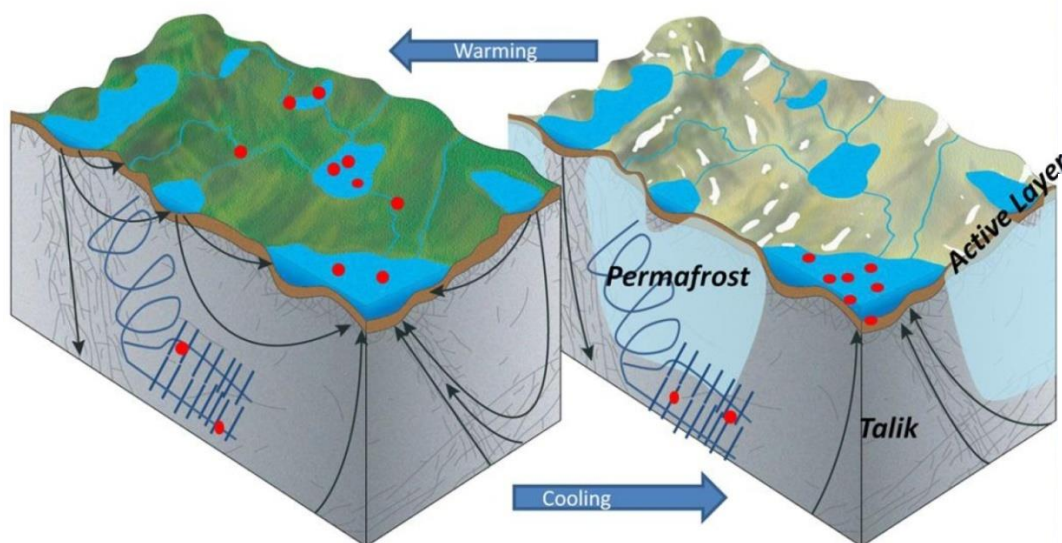


Fig. 1.7 Impact of permafrost on radionuclide migration; from /JOH 16/

During warmer climates, groundwater flow is thus characterized by a comparatively shallow flow system where the water can be imagined to seek paths of the least flow resistance. Groundwater taking up radionuclides from a leaking waste canister may therefore distribute them over quite a large area. In general, the flow can quite well be described as its relevant features, in particular the boundary conditions, can be considered to be more or less well known.

Under permafrost conditions, by contrast, many of the shallow flow paths are blocked by the evolving ice. Flow from above ground to the next available aquifer in the subsurface and vice versa is restricted to locations with open taliki forcing the water deeper downwards and concentrating a potential outflow of radionuclides to the few open taliki.

2 Problem definition

While isolated as well as closed taliki are not really of concern, open taliki form hydraulic shortcuts between deep unfrozen aquifers and ground surface. At that, they represent a key feature in a groundwater flow system under permafrost conditions. Knowledge of size and location as well as stability of taliki is thus vital for predicting possible radionuclide migration. On the whole, conditions for talik development are investigated in relation to climate warming, though (e.g. /PAR 18/).

Consequences for the potential migration paths of radionuclides in case of a canister breach are therefore presently hard to predict. Highly adverse appears to be the possibility that contaminated waters may be able to reach the surface via open taliki while remaining highly concentrated with pollutants.

Taliki often form below larger surface waters such as lakes and rivers, e.g. /DEL 98/, /KEL 98/, /SKB 06/, raising the suspicion that they are hydrothermal taliki (see section 1.1) by nature. They are thus not accessible to direct observation but can be detected by laborious field work (e.g. /JOH 16/). Understanding of the mechanisms that create taliki and keep them open over longer times might be gained by numerical modelling, though.

Following this idea implies that the simplest physically conceivable configuration should be investigated in order to get the most meaningful results. The present work is therefore restricted to periglacial permafrost conditions. The effects of an approaching ice cap and the subsequent ice coverage introduce undesirable additional levels of complexity to the permafrost conditions that precede the coming of an ice shield anyway.

The present work intends to provide the basis for a modelling exercise that aims at understanding of the mechanisms about talik forming and talik persistence. This includes the physics of a conceptual model as well as a sound comprehension of the related underlying mathematical model. As many different mathematical formulations can be found in the literature, it is of particular importance to be able to identify the physics that are represented by these formulations in order to make an appropriate choice.

3 Physical particularities of freezing water

3.1 Changing the phase state of water

Melting of ice is a phase change from the solid to the liquid phase of water at melting temperature. The process does not change the temperature but requires a certain amount of heat. The amount of heat that is taken up by the ice from the environment for melting is called “latent heat of fusion”. It is mass-specific and can be calculated with the help of the “specific heat of fusion” L which is given in units of energy per units of mass.

The reverse process of freezing of water⁴ sets the “latent heat of solidification” free which can be calculated using the “specific heat of solidification” L' . The absolute value of L is the same as of L' . Per definition, the latent heat of fusion is always a positive value, and the latent heat of solidification is always negative.

The fact that the impact of latent heat is proportional to the local mass of water/ice implies that in a porous medium, it is also related to the porosity. /BAR 16/ elaborates on that aspect, pointing out that this effect has been identified to be very small in granite, though, due to its low porosity /MOT 06/. However, in the active layer it plays a considerable role as melting and freezing get slowed down by absorption and release of heat during phase changes /MCK 07/.

The thermodynamic properties of water and ice such as density, thermal conductivity, or specific heat are temperature-dependent to a certain extent. However, particularly big differences in these properties can be observed when the phase state changes between water and ice. At a temperature of 0 °C, the volumetric expansion due to freezing amounts to almost 10 % which requires particular care when determining the fractions of coexisting water and ice.

⁴ As a convention for this report, liquid water is simply referred to as “water“ while solid water is called “ice“.

3.2 State variables at sub-zero temperatures

While density, specific heat, thermal conductivity and the viscosity (of water) are well investigated at temperatures above 0 °C for water (e.g. /KRÖ 10/) and below 0 °C for ice, data for water below 0 °C are less available. The best approximation stems from measurements on supercooled water that is water cooled below 0 °C without solidification. This can be achieved using demineralised water removing potential nuclei for crystallization from the liquid. As water can be cooled down to a little less than -48 °C by this method (e.g. /MOO 11/), the temperature-dependence of the state variables is actually measurable in the temperature range that is of interest here. The results of a literature search are presented and discussed in Appendix B.1.

3.3 Freezing of water in porous media

In pure water, the liquid freezes abruptly when its temperature falls below 0 °C. Decreasing temperatures in the underground, however, lead initially to freezing only of a part of the water where the fraction of still liquid water decreases continuously with temperature. Groundwater flow has been found even in the two-digit subzero temperature range. The function that relates the fraction of unfrozen water to the temperature is known as the soil freezing characteristic curve (SFCC) which is specific for a given soil.

It is generally agreed that two physical phenomena on the microscale are relevant for this effect (see /REM 04/, /WET 06/, and /ZHO 14/). Both are based on the effect of premelting. Premelting occurs at the interface between two phases and leads to a quasi-liquid film on the surface of a solid that is at a temperature below the melting point. The thickness of this film is temperature-dependent.

The first relevant premelting effect is called curvature-induced premelting and is caused by surface tension of the water meniscus between soil particles. The second one results from repulsive forces between ice and solid grains, forming a little gap into which the liquid water can be sucked. From a macroscopic point of view, the fraction of water in a porous medium below a temperature of 0°C is therefore temperature-dependent.

4 Conceptual understanding

4.1 Phenomena

Neglecting mechanical effects from expansion during freezing as well as from water flow, ground freezing is a thermal problem that is basically controlled by the mean ground surface temperature, heat production from earth's core and the thermal properties of the geological units (see Fig. 4.1, left).

Much more challenging is the simulation of the development of taliki which is a delicate process and requires a thermo-hydraulic (TH-)coupling. Open taliki connect deep aquifers with the rock surface and thus form a key feature in a frozen groundwater flow system. However, development of an open talik may be influenced by the actual groundwater flow system to an unknown extent in which case talik forming is site specific.

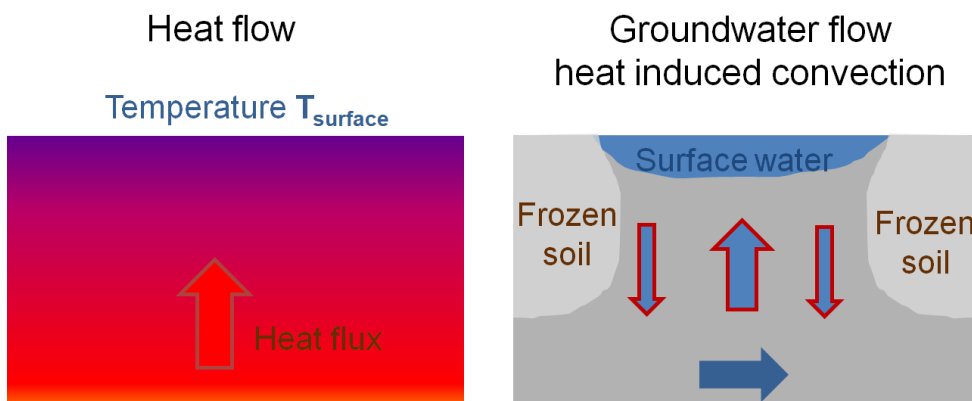


Fig. 4.1 Relevant processes for groundwater flow under permafrost conditions

4.2 Groundwater flow

Groundwater flow in general involves a porous matrix of solids and a theoretically unlimited number of fluids in the pore space. These fluids can be liquids as well as gases. Here, the considerations are restricted to a solid matrix being fully saturated with water for temperatures above 0 °C. For temperatures decreasing below the freezing point, the water exists partly as a liquid and partly as solid ice where the fraction of water decreases with temperature until basically all water becomes frozen. The relation between temperature and water fraction is called “soil freezing characteristic curve (SFCC)”.

Where water and ice coexist, the volume occupied by the two phases can be characterized by the saturation with unfrozen water S_w and the ice saturation S_i , respectively⁵, which are defined as the volumetric fraction of the respective phase of the total pore volume.

$$S_w = \frac{V_w}{V_p} \quad \text{and} \quad S_i = \frac{V_i}{V_p} \quad (4.1)$$

S_w - saturation of the pore space with unfrozen water [-]

S_i - saturation of the pore space with ice [-]

V_w - volume of the unfrozen water [m³]

V_i - volume of the ice [m³]

V_p - pore volume [m³]

Consequently, the two saturations defined in (4.1) add up to 1:

$$S_w + S_i = 1 \quad (4.2)$$

Groundwater flow occurs in the pore space of a porous matrix⁶. The physics described above therefore suggest that the groundwater system under freezing conditions can be regarded as a two-phase, single-component system. The component water exists either in a liquid state as water or in a solid state as ice and phase changes are possible according to the prevailing temperature. Neglecting furthermore the movement of ice, flow of water can be considered to be a special form of unsaturated flow where ice is displacing water like water displaces air in a conventional unsaturated flow problem.

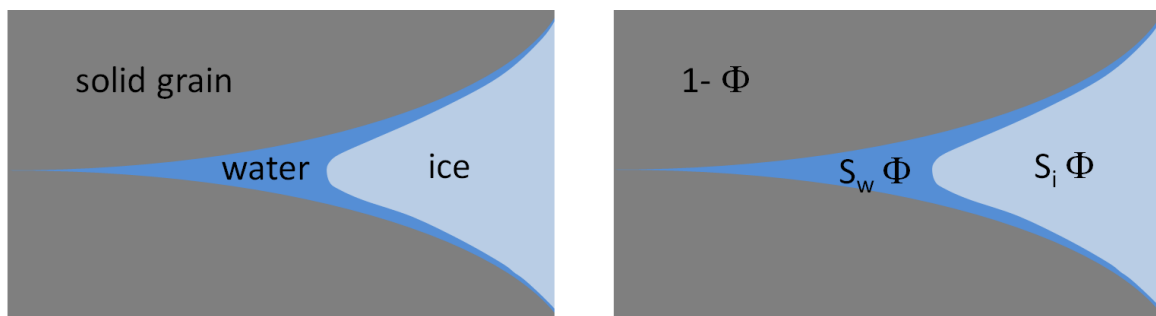


Fig. 4.2 Principle sketch illustrating porosity Φ and saturations S

⁵ Note that the indices w for water, i for ice and m for the solid matrix will be used throughout this report.

⁶ In a fractured porous medium this applies of course also to the open fractures.

4.3 Interaction of groundwater flow and heat flow

Freezing and melting in the underground implies transient thermal processes that interact with the groundwater flow in a rather complex way. On the one hand, the properties of water that are controlling flow are dependent on the transient temperature field and on the other hand, heat gets transported with the water by advection and possibly by convection. Phase changes draw or release energy thereby influencing the temperature field even further. The concomitant volumetric changes cause the water to be either squeezed out of or to be sucked into the pore space. A model of groundwater flow under freezing conditions thus requires a concept where thermo-hydraulic processes are fully coupled. If porosity changes are considered by frost heave or thawing settlement, a coupling to further mechanical processes may be in order. This, however, is beyond the scope of this report.

5 General balance equations

5.1 Methodology

5.1.1 Introductory remark

There are at least two principal methods to derive a balance equation. One would be centred on an infinitesimal volume, looking at infinitesimal changes from one side of this volume to the other. This is called here “local derivation”. The other method would be based on a finite volume, being rather a “global derivation”. Both methods will shortly be illustrated in the following two subsections by deriving the continuity equation. Due to a personal preference of the author, the mass balance as well as the energy balance equation is derived later on from the finite volume approach. Note that this choice is not imperative.

5.1.2 Local derivation

For the sake of simplicity, the continuity equation will be derived in this section in one dimension only. Basis is the infinitesimal volume element that is sketched in Fig. 5.1. The x-component of a mass flux \dot{m}_x through this element can be written as

$$\dot{m}_x = \rho(x) \cdot v_x(x) \cdot dy \cdot dz \quad (5.1)$$

where $\rho(x)$ stands for the density of water and $v_x(x)$ for the x-component of the flow velocity.

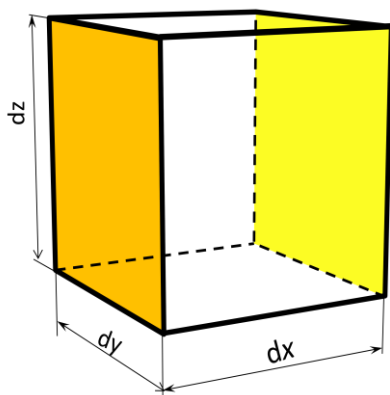


Fig. 5.1 Infinitesimal volume element

The difference between entering and leaving mass flux would then read

$$d\dot{m}_x = \dot{m}_{x,out} - \dot{m}_{x,in} = \frac{\partial[\rho(x) \cdot v_x(x)]}{\partial x} dx \cdot dy \cdot dz \quad (5.2)$$

Note that $d\dot{m}_x$ is positive if more mass is transported out of the control volume than in. Any non-zero value leads with time to a mass accumulation or loss \dot{m}_{CV} in the infinitesimal control volume dV .

$$\dot{m}_{CV} = \frac{\partial \rho}{\partial t} dV \quad (5.3)$$

By equating (5.2) and (5.3) appropriately, the basic continuity equation in one dimension is found:

$$\frac{\partial \rho}{\partial t} + \frac{\partial(\rho \cdot v_x)}{\partial x} = 0 \quad (5.4)$$

5.1.3 Global derivation

The derivation based on a finite volume is given in detail for instance in /GÄR 87/. In the following, only the gist of it is summarized. Illustrated in Fig. 5.2 is the situation where a finite control volume $V(t)$ that is defined by its surface $S(t)$, is transported by a flow field $\mathbf{v}(x, t)$. After a certain time Δt , the surface of the control volume and so the control volume itself has moved into a new temporary position. The control volume is assumed to contain a mass-related extensive⁷ quantity $Z(t)$ that may also change with time. Quantity $Z(t)$ can be written as an integral of the related density $z(x, t)$ over the control volume:

$$Z(t) = \int_{V(t)} z(x, t) dV \quad (5.5)$$

- $Z(t)$ - extensive variable in $V(t)$ with the appropriate dimension <dim> [<dim>]
- $V(t)$ - moving 3D-domain [m^3]
- $z(x, t)$ - density of $Z(t)$ [<dim>/ m^3]
- t - time [s]

⁷ additive like mass itself, impuls or energy

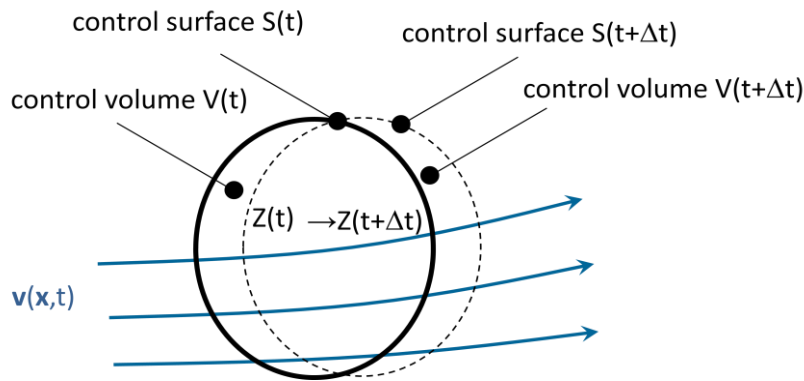


Fig. 5.2 Macroscopic control volume being carried with the flux

Equation (5.5) is a rather tricky expression as the amount of Z as well as the control volume V is a function of time. However, applying Reynold's transport theorem states that the change of Z with time can be expressed as

$$\dot{Z} = \frac{d}{dt} \int_V z dV = \int_V \left[\frac{\partial z}{\partial t} + \nabla \cdot (\mathbf{v}_a z) \right] dV \quad (5.6)$$

\mathbf{v}_a - (interstitial⁸) flow velocity [m/s]

G - spatially fixed control volume [m³]

in a fixed volume G or in a case where there is no production of Z

$$\int_G \left[\frac{\partial z}{\partial t} + \nabla \cdot (\mathbf{v}_a z) \right] dV = 0 \quad (5.7)$$

Reifying this expression by setting the extensive quantity Z to the mass m of water in a porous medium

$$\begin{aligned} Z &= m \\ z &= \Phi \rho \end{aligned} \quad (5.8)$$

leads then directly to

$$\int_G \left[\frac{\partial(\Phi \rho)}{\partial t} + \nabla \cdot (\mathbf{v}_a \Phi \rho) \right] dV = 0 \quad (5.9)$$

which is equivalent to equation (5.4) under certain conditions concerning the derivability of the integrand /GÄR 87/.

⁸ In case of porous media

5.1.4 General balance equation

Equations (5.4) and (5.9) are continuity equations in the strict sense that there is no gain or loss of quantity Z which is the mass m of water in this specific case. In order to gain a certain generality of the balance equation (5.6), production⁹ of Z in the control volume G remains to be added. In principle, a gain or loss of Z can be caused by two mechanisms. The first one would be a production inside the control volume according to a rate \bar{r} ; the second one would be a flux \mathbf{J} of quantity Z over the surface S of the control volume. Note that \mathbf{J} cannot be related to advection as surface S is moving with the flow field \mathbf{v} . Looking at equation (5.6), the derivation shows that production can simply be added on the right-hand side of (5.7)

$$\int_G \left[\frac{\partial z}{\partial t} + \nabla \cdot (\mathbf{v}_a z) \right] dV = \int_V \bar{r} dV - \int_S \mathbf{n} \cdot \mathbf{J} dS \quad (5.10)$$

- \mathbf{J} - non-advective flow of Z across the surface S [$\text{dim}/(\text{m}^2 \text{ s})$]
- \mathbf{n} - surface normal (positive in the outward direction) [-]
- \bar{r} - production of Z in G [$\text{dim}/(\text{m}^3 \text{ s})$]

With the help of the Gauss theorem, the surface integral can be transformed into an integral over the enclosed volume. Subsuming both volume integrals as one general source term \hat{r}

$$\int_G \hat{r} dV = \int_G (\bar{r} - \nabla \cdot (\mathbf{J})) dV \quad (5.11)$$

- \hat{r} - generalized production term for Z in G [$\text{dim}/(\text{m}^3 \text{ s})$]

will prove to be useful when looking into the energy balance equations. However, a more practical and general form of the balance equation that just needs reifying the mass-related quantity Z would eventually read:

$$\int_G \left[\frac{\partial z}{\partial t} + \nabla \cdot (\mathbf{v}_a z + \mathbf{J}) \right] dV = \int_G \bar{r} dV \quad (5.12)$$

⁹ Production is defined here to represent sinks and sources alike, sinks just being sources with an opposite sign.

5.2 Mass balance equation

Groundwater flow can be described by a mass balance equation for water including ice in a porous medium. Since different parameters and physical laws apply to the different phase states of water, it is advantageous to write down separate balance equations for water and ice. Water and ice coexist on a microscopic level, that is on pore scale, while the general balance equation (5.12) is related to the macroscopic scale. It thus suffices to ascribe the balance equations for water and ice to the fraction of volume that is occupied by water and by ice, respectively. This will be done with respect to water first and afterwards with respect to ice before both equations are combined to a single balance equation for water covering both phase states. Note that leaving out an analogous equation for the matrix implies that no flow of the solid matrix material will be considered here.

5.2.1 Mass balance for water

Similar to the example in subsection 5.1.3, the mass of water is considered here as well but only with respect to a fraction of the pore space as defined by the saturation S_w :

$$\begin{aligned} Z(t) &= m_w \\ z(x, t) &= S_w \Phi \rho_w(x, t) \\ \mathbf{v} &= \mathbf{v}_{aw} \\ \mathbf{J} &= \mathbf{J}_w \\ \bar{r} &= r_{fw} \end{aligned} \tag{5.13}$$

m_w - mass of water [kg]

Φ - porosity [-]

S_w - volumetric fraction of the pore volume that is occupied by water [m³/m³]

ρ_w - density of water [kg/m³]

\mathbf{v}_{aw} - interstitial water velocity [m/s]

\mathbf{J}_{fw} - non-advective flow of water [kg/(m² s)]

r_{fw} - production of water [kg/(m³ s)]

In the most general form, the mass balance equation for water thus reads either

$$\int_G \left[\frac{\partial(S_w \Phi \rho_w)}{\partial t} + \nabla \cdot (\mathbf{v}_{aw} S_w \Phi \rho_w) - \hat{r}_{fw} \right] dV = 0 \quad (5.14)$$

\hat{r}_{fw} - generalized production term for water mass in G [kg/ (m³ s)]

or eventually

$$\int_G \left[\frac{\partial(S_w \Phi \rho_w)}{\partial t} + \nabla \cdot (\mathbf{v}_{aw} S_w \Phi \rho_w + \mathbf{J}_{fw}) - r_{fw} \right] dV = 0 \quad (5.15)$$

5.2.2 Mass balance for ice

Analogously to the procedure described in section 5.2.1, a balance equation for the ice can be derived. Starting with the definitions

$$Z(t) = m_i$$

$$z(\mathbf{x}, t) = S_i \Phi \rho_i(\mathbf{x}, t)$$

$$\mathbf{v} = \mathbf{v}_{ai} \quad (5.16)$$

$$\mathbf{J} = \mathbf{J}_{fi}$$

$$\bar{r} = r_{fi}$$

m_i - mass of ice [kg]

S_i - volumetric fraction of the pore volume that is occupied by ice [m³/m³]

ρ_i - density of ice [kg/m³]

\mathbf{v}_{ai} - interstitial ice velocity [m/s]

\mathbf{J}_i - non-advective flow of ice [kg/(m² s)]

r_{fi} - production of ice [kg/(m³ s)]

the balance equation for ice reads either

$$\int_G \left[\frac{\partial(S_i \Phi \rho_i)}{\partial t} + \nabla \cdot (\mathbf{v}_{ai} S_i \Phi \rho_i) - \hat{r}_{fi} \right] dV = 0 \quad (5.17)$$

\hat{r}_{fi} - generalized production term for ice mass in G [kg/ (m³ s)]

or eventually

$$\int_G \left[\frac{\partial(S_i \Phi \rho_i)}{\partial t} + \nabla \cdot (\mathbf{v}_{ai} S_i \Phi \rho_i + \mathbf{J}_{fi}) - r_{fi} \right] dV = 0 \quad (5.18)$$

5.2.3 Mass balance for the whole system

Adding up the balance equations (5.15) and (5.18) results in

$$\int_G \left[\frac{\partial(\Phi[S_w \rho_w + S_i \rho_i])}{\partial t} + \nabla \cdot (\Phi[\mathbf{v}_{aw} S_w \rho_w + \mathbf{v}_{ai} S_i \rho_i]) + \nabla \cdot (\mathbf{J}_{fw} + \mathbf{J}_{fi}) - r_{fw} - r_{fi} \right] dV = 0 \quad (5.19)$$

Note that up to this point, no adaptation to specifically stated problems has been introduced.

5.3 Energy balance equation

In the context of water flow, the solid matrix could be ignored as it does not contribute to water mass balance. In case of heat energy, by contrast, it must be appropriately accounted for. The heat energy balance will therefore be written down separately for water, ice and the solid matrix before getting coupled to form one balance equation for the whole system. As in the section 5.2, firstly, the balance equation for water will be derived.

5.3.1 Energy balance for water

The extensive state variable Z in this case is the heat content of the water Q_w which comes along with the following definitions

$$Z(t) = Q_w = c_{sw} m_w T_w^{10} \quad (5.20)$$

¹⁰ ignoring any volume work

$$z(x, t) = S_w \Phi c_{s w} \rho_w T_w$$

$$\mathbf{v} = \mathbf{v}_{a w}$$

$$\mathbf{J} = \mathbf{J}_{h w}$$

$$r = r_{h w}$$

Q_w - heat content of the water [J]

$c_{s w}$ - specific heat capacity of water [J/(kg K)]

T_w - temperature of the water [K]

$\mathbf{J}_{h w}$ - non-advective flow of heat in water [J/(m² s)]

$r_{h w}$ - production of heat in water [J/(m³ s)]

Note that in the context of heat transport, the transport of heat by water flow is called “convection”. The definitions (5.20) lead to the most general form of the energy balance equation for water:

$$\int_G \left[\frac{\partial(S_w \Phi c_{s w} \rho_w T_w)}{\partial t} + \nabla \cdot (\mathbf{v}_{a w} S_w \Phi c_{s w} \rho_w T_w + \mathbf{J}_{h w}) - r_{h w} \right] dV = 0 \quad (5.21)$$

Without losing its generality, balance equation (5.21) can be simplified by applying the product rule to the storage and the convective term in a suitable way

$$\int_G \left[S_w \Phi \rho_w \frac{\partial(c_{s w} T_w)}{\partial t} + c_{s w} T_w \frac{\partial(S_w \Phi \rho_w)}{\partial t} + (\mathbf{v}_{a w} S_w \Phi \rho_w) \cdot \nabla(c_{s w} T_w) \right. \\ \left. + c_{s w} T_w \nabla \cdot (\mathbf{v}_{a w} S_w \Phi \rho_w) + \nabla \cdot \mathbf{J}_{h w} - r_{h w} \right] dV = 0 \quad (5.22)$$

allowing insertion of the mass balance equation for water in the form of equation (5.14):

$$\int_G \left[S_w \Phi \rho_w \frac{\partial(c_{s w} T_w)}{\partial t} + (\rho_w \mathbf{v}_{a w} S_w \Phi) \cdot \nabla(c_{s w} T_w) + c_{s w} T_w \hat{r}_{f w} + \nabla \cdot \mathbf{J}_{h w} \right. \\ \left. - r_{h w} \right] dV = 0 \quad (5.23)$$

Next to the storage and the convection term, there is a new term in equation (5.23), the third one, that is quite uncommon in most formulations for the energy balance. It looks deceptively like a source term, but this is not entirely the case. Actually, this term stems from the storage and the convective term in the general formulation (5.21) which do not relate to production. It may be rather interpreted as the effect of water entering the domain without adding heat. The actual heat production by inflowing water must still be taken care of by the production term r_{hw} (see section 6.2.2).

5.3.2 Energy balance for ice

The procedure for ice starts analogously to that for water with the following definitions

$$\begin{aligned}
 Z(t) &= Q_i = c_{si} m_i T_i \\
 z(\mathbf{x}, t) &= S_i \Phi c_{si} \rho_i T_i \\
 \mathbf{v} &= \mathbf{v}_{ai} \\
 \mathbf{J} &= \mathbf{J}_{hi} \\
 \bar{r} &= r_{hi}
 \end{aligned}
 \tag{ 5.24 }$$

- Q_i - heat content of ice [J]
- c_{si} - specific heat capacity of ice [J/(kg K)]
- T_i - temperature of the ice [K]
- \mathbf{J}_{hi} - non-advective flow of heat in the ice [J/(m² s)]
- r_{hi} - production of heat in the ice [J/(m³ s)]

leading to the formulation

$$\int_G \left[\frac{\partial(S_i \Phi c_{si} \rho_i T_i)}{\partial t} + \nabla \cdot (\mathbf{v}_{ai} S_i \Phi c_{si} \rho_i T_i + \mathbf{J}_{hi}) - r_{hi} \right] dV = 0
 \tag{ 5.25 }$$

Storage and convection term in equation (5.25) can again be split into two terms each

$$\int_G \left[S_i \Phi \rho_i \frac{\partial(c_{si} T_i)}{\partial t} + c_{si} T_i \frac{\partial(S_i \Phi \rho_i)}{\partial t} + (\mathbf{v}_{ai} S_i \Phi \rho_i) \cdot \nabla(c_{si} T_i) \right. \\
 \left. + c_{si} T_i \nabla \cdot (\mathbf{v}_{ai} S_i \Phi \rho_i) + \nabla \cdot (\mathbf{J}_{hi}) - r_{hi} \right] dV = 0
 \tag{ 5.26 }$$

for further simplification by inserting the mass balance for ice in the form of (5.17)

$$\int_G \left[S_i \Phi \rho_i \frac{\partial(c_{s_i} T_i)}{\partial t} + (\mathbf{v}_{a_i} S_i \rho_i \Phi) \cdot \nabla(c_{s_i} T_i) + c_{s_i} T_i \hat{r}_{f_i} + \nabla \cdot (\mathbf{J}_{h_i}) - r_{h_i} \right] dV = 0 \quad (5.27)$$

The third, new term in (5.27) has appeared analogously to the third term in balance equation (5.23) for water. Its significance will be discussed in subsection 6.2.

5.3.3 Energy balance for the matrix¹¹

Finally, the heat balance equation for the matrix must be established. The necessary definitions look formally the same as in the previous two cases:

$$\begin{aligned} Z(t) &= Q_m = c_{s_m} m_m T_m \\ z(\mathbf{x}, t) &= (1 - \Phi) c_{s_m} \rho_m T_m \\ \mathbf{v} &= \mathbf{v}_{a_m} \\ \mathbf{J} &= \mathbf{J}_{h_m} \\ \bar{r} &= r_{h_m} \end{aligned} \quad (5.28)$$

- Q_m - heat content of the matrix [J]
- c_{s_m} - specific heat capacity of the matrix [J/(kg K)]
- m_i - mass of the matrix [kg]
- T_m - temperature of the matrix [K]
- ρ_m - density of the solids in the matrix [kg/m³]
- \mathbf{v}_{a_m} - velocity of the matrix [J/(m² s)]
- \mathbf{J}_{h_m} - non-advective flow of heat in the matrix [kg/(m² s)]
- r_{h_m} - production of heat in the matrix [kg/(m³ s)]

¹¹ The term “matrix” actually refers only to the solid matter that forms the skeleton of a matrix without the enclosed pore space. In that, this term is somewhat inaccurately used here. More to the point would be “the solid part of the matrix”.

The balance equation thus reads

$$\int_G \left[\frac{\partial((1-\Phi)c_{sm}\rho_m T_m)}{\partial t} + \nabla \cdot (\mathbf{v}_{am}(1-\Phi)c_{sm}\rho_m T_m + \mathbf{J}_{hm}) - r_{hm} \right] dV = 0 \quad (5.29)$$

The storage term is split into two terms providing the form

$$\int_G \left[(1-\Phi)\rho_m \frac{\partial(c_{sm} T_m)}{\partial t} + c_{sm} T_m \frac{\partial((1-\Phi)\rho_m)}{\partial t} + \nabla \cdot (\mathbf{v}_{am}(1-\Phi)c_{sm}\rho_m T_m + \mathbf{J}_{hm}) - r_{hm} \right] dV = 0 \quad (5.30)$$

but this time to differentiate between direct storage of energy in the matrix (first term) and changes in the energy density due to e.g. mechanically or thermally induced changes in the bulk density of the matrix (second term).

5.3.4 Energy balance for the whole system

The energy balance equation for the whole system can be obtained by adding up balance equations (5.23), (5.27), and (5.30) for the subsystems water, ice and matrix, respectively:

$$\int_G \left[S_w \Phi \rho_w \frac{\partial(c_{sw} T_w)}{\partial t} + S_i \Phi \rho_i \frac{\partial(c_{si} T_i)}{\partial t} + (1-\Phi)\rho_m \frac{\partial(c_{sm} T_m)}{\partial t} + (\mathbf{v}_{aw} S_w \rho_w \Phi) \cdot \nabla(c_{sw} T_w) + \mathbf{v}_{ai} S_i \rho_i \Phi \cdot \nabla(c_{si} T_i) + \nabla \cdot (\mathbf{v}_{am}(1-\Phi)c_{sm}\rho_m T_m) + c_{sw} T_w \hat{r}_{fw} + c_{si} T_i \hat{r}_{fi} + \nabla \cdot (\mathbf{J}_{hw} + \mathbf{J}_{hi} + \mathbf{J}_{hm}) \right] dV = \int_G [r_{hw} + r_{hi} + r_{hm}] dV \quad (5.31)$$

6 Processes, constitutive equations, and equations of state

6.1 The “game board” and the “book of rules”

Balance equations (5.19) and (5.31) for the mass of water and ice and the heat energy of the whole system, respectively, provide metaphorically a game board which is a frame for modelling groundwater flow under permafrost conditions. For playing a particular game i.e. providing a numerical tool for solving a particular type of problem, a “book of rules” must be compiled that reflects the modelling problem at hand. This book of rules concerns the processes or phenomena that are to be included as well as the constitutive equations (CEs) and the equations of state (EOS). It should go without saying that these rules have to be known by heart by the “player” meaning the modeler.

6.2 Processes

6.2.1 Rules for the mass balance

The processes that can be considered are given in all generality by the balance equation (5.12): storage, advection/convection, non-advective transport, and volume-related production. Not taking a mass balance of the solid mass of the matrix into account, as mentioned earlier, is already a first rule implying a matrix that does not change or move on the macroscopic scale.

As ice is assumed to be distributed over parts of the pore space, it will be treated as not moving as well, thus setting the flow velocity of ice to 0. However, changes in the mass of ice must be permitted. A balance equation for the mass of ice is therefore nevertheless required.

It is further assumed that non-advective mass exchange of water across the surface S of the moving control volume V does not lead to a change of water mass in V . Self-diffusion of water may thus occur but is not accounted for. The non-advective flux of water $J_{f w}$ is therefore set to zero. The same applies to the non-advective flux of ice $J_{f i}$.

Production of water from the continuum outside the model domain is considered as the classic sink/source term $\rho_w q_w$. Furthermore, a second source r_{Lw} is to be added that

relates to loss of water by freezing or gain of water by melting. No contribution comes from non-advective fluxes $J_{f w}$ as discussed above.

$$r_{f w} = \rho_w q_w + r_{Lw} \quad (6.1)$$

- q_w - volumetric production of water from outside the domain [$\text{m}^3/(\text{m}^3 \text{ s})$]
 r_{Lw} - production of water due to phase changes [$\text{kg}/(\text{m}^3 \text{ s})$]

For ice, the situation is even simpler as no flow of ice is considered and thus no production of ice in the classic sense needs to be taken care of. Gain from freezing or loss from melting still applies, though:

$$r_{f i} = r_{Li} \quad (6.2)$$

- r_{Li} - production of ice due to phase changes [$\text{kg}/(\text{m}^3 \text{ s})$]

Obviously, any mass gained due to a phase change in one phase is lost to the other phase by the same amount

$$r_{Lw} = -r_{Li} \quad (6.3)$$

so that the source term in equation (5.19) simply adds up to

$$r_{f w} + r_{f i} = \rho_w q_w \quad (6.4)$$

The mass balance equation (5.19) thus reads now

$$\frac{\partial(\Phi[S_w \rho_w + S_i \rho_i])}{\partial t} + \nabla \cdot (\mathbf{v}_{a w} \Phi S_w \rho_w) = \rho_w q_w \quad (6.5)$$

6.2.2 Rules for the energy balance

Water, ice and matrix coexist on pore-scale. The involved processes such as water flow and phase changes are slow processes in comparison to heat conduction on the micro-scale. Based on these observations, the assumption of a local thermal equilibrium is justified:

$$T = T_w = T_i = T_m \quad (6.6)$$

- T - local equilibrium temperature [K]

Since only the water phase is defined to be moving, convection can only occur in the water. No convection in the ice or in the matrix is thus considered.

The non-advective heat flux is explained in further detail in the subsection “Constitutive equations” (section 6.3).

The energy balance equation (5.31) shows still three sink/source terms that are related to the three phases water, ice and matrix. Possible sinks and sources are

- energy flux from or to the outside of the domain by local cooling or heating¹² r_{hQ}
- heat of entering water r_{hw}
- heat consumed or liberated by a phase change of water r_{hL}

which can be summed up as

$$r_{hw} + r_{hi} + r_{hm} = r_{hQ} + r_{hw} + r_{hL} \quad (6.7)$$

r_{hQ} - energy from a cooling or heating system [J/(s m³)]

r_{hw} - heat of entering water [J/(s m³)]

r_{hL} - production of heat due to phase changes [J/(s m³)]

Direct heat production r_{hQ} has simply to be specified by a dimensionally correct number. This particular source is macroscopically applied and thus affects all three phases which justifies ascribing the total heat input to just one of the three terms on the right-hand side of balance equation (5.31).

A bit more complex is the situation in case of the heat that comes with water entering the model domain. As shown earlier, this could be water crossing the model boundary or water being produced by a phase change (see eq. (6.1)). The related heat flux can thus be defined as

$$r_{hw} = c_{sw} (\rho_w q_w + r_{Lw}) \dot{T} \quad (6.8)$$

\dot{T} - temperature variable according to definition (6.9)

with

¹² e.g. heat from a canister containing radioactive waste

$$\begin{aligned}
\dot{T} &= T_{w\ in} && \text{for water sources} \\
\dot{T} &= T && \text{for water sinks} \\
\dot{T} &= 0 && \text{everywhere else}
\end{aligned}
\tag{6.9}$$

$T_{w\ in}$ - temperature of inflowing water [K]

Source term (6.8) can nicely be combined with the term $c_{s\ w} T_w \hat{r}_{f\ w}$ from balance equation (5.31) as the only difference lies in the temperature \dot{T} or T , respectively:

$$c_{s\ w}(\rho_w q_w + r_{Lw})(T - \dot{T}) \tag{6.10}$$

Expression (6.10) can formally be assigned to the source term on the right hand side of (5.31). The definition of \dot{T} shows that term (6.10) is only relevant in case of inflowing water where \dot{T} equals a specified temperature value or is possibly given by a time dependent function. In this case, both brackets in (6.10) represent a non-zero value. If water is lost by sinks or by freezing, temperature T equals \dot{T} , letting (6.10) vanish. If water is added by melting, the temperature $T_{w\ in}$ equals the ambient (melting) temperature T and the difference of T and \dot{T} equals zero again. Everywhere else, the water production terms $\rho_w q_w$ and r_{Lw} are equal to zero.

What remains to be defined is a sink/source term for latent heat due to phase changes. This term is a bit particular as it is caused by the interplay of water and ice but affects also the matrix. Instead of writing down separate production terms for each phase, just one term is therefore formulated to be inserted directly in the balance equation for the whole system. Since latent heat is a mass-related property, production of latent heat is related to the production of ice during freezing (or loss of water) by the specific heat L . Production of ice is written as

$$\frac{\partial m_i}{\partial t} = \int_G \frac{\partial(\rho_i S_i \Phi)}{\partial t} dV \tag{6.11}$$

and the related released amount of heat r_{hL} as

$$r_{hL} = L \frac{\partial(\rho_i S_i \Phi)}{\partial t} \tag{6.12}$$

L - specific heat of fusion [J/kg]; $L=334$ J/kg

All these rules transform the energy balance equation (5.31) into

$$\begin{aligned}
 & S_w \Phi \rho_w \frac{\partial(c_{s w} T)}{\partial t} + S_i \Phi \rho_i \frac{\partial(c_{s i} T)}{\partial t} + (1 - \Phi) \rho_m \frac{\partial(c_{s m} T)}{\partial t} \\
 & + (\mathbf{v}_{a w} S_w \rho_w \Phi) \cdot \nabla(c_{s w} T) + \nabla \cdot (\mathbf{J}_{h w} + \mathbf{J}_{h i} + \mathbf{J}_{h m}) \\
 & = r_{h Q} + c_{s w} \rho_w q_w (T - \dot{T}) + L \frac{\partial(\rho_i S_i \Phi)}{\partial t}
 \end{aligned} \tag{ 6.13 }$$

6.3 Constitutive equations

The next chapter in the book of rules concerns the constitutive equations (CEs). These are material-specific relations of physical quantities that generally describe reactions triggered by any form of initiation. In the end, they basically concern empirical material properties. In this respect, the balance equations presented up to this point are therefore more or less derived on general principles, leaving appropriate functions and material parameters still to be specified. A comparison of related approaches from the literature is discussed in section 9.4.

6.3.1 Porosity

The porosity of a porous medium can change due to forces on the matrix which may be macroscale mechanical forces from outside the domain in question or microscale forces from inside the pore space like hydraulic pressure. In these cases, the pressure must be related to the strength of the porous matrix to calculate a porosity change. A phenomenon particularly difficult to describe in a mathematical model is that of frost heave as it relates to a change in porosity that affects groundwater flow as well as freezing of water. Thermal expansion of the solid matrix would also affect the porosity. While all these effects on porosity are not pursued to greater depth here, a dependence of the porosity on water pressure and temperature is nevertheless accounted for in the balance equations as a matter of principle:

$$\Phi = \Phi(p_w, T) \tag{ 6.14 }$$

p_w - hydraulic pressure [Pa]

6.3.2 Flow law

A prominent CE is the flow law that relates the flow velocity of a fluid to a pressure gradient (or, in a porous medium, alternatively to the equivalent gradient of the hydraulic head). Widely used in the field of porous media flow is the generalized Darcy's law

$$\mathbf{v}_f = -\frac{\mathbf{k}}{\eta} \cdot (\nabla p_w - \rho \mathbf{g}) \quad (6.15)$$

- \mathbf{v}_f - Darcy velocity [m/s]
- \mathbf{k} - tensor of the absolute permeability [m²]
- η - viscosity [Pa s]
- \mathbf{g} - vector of the gravitational acceleration [m/s²]

The vector \mathbf{g} in the generalized Darcy's law is explained as

$$\mathbf{g} = \begin{bmatrix} 0 \\ 0 \\ -g \end{bmatrix} \quad (6.16)$$

- g - gravitational acceleration [m/s²]

For the problem at hand, Darcy's law is applied to the flow of water. Equation (6.15) reads then

$$\mathbf{v}_{f w} = -\frac{\mathbf{k}_w}{\eta_w} \cdot (\nabla p_w - \rho_w \mathbf{g}) \quad (6.17)$$

- \mathbf{k}_w - tensor of the effective water permeability [m²]

Note that the effective permeability \mathbf{k}_w for water replaces the absolute permeability accounting for the flow impediments by ice in the pore space. The effective permeability is defined as the product of the absolute permeability \mathbf{k} and a factor k_{rw} called relative permeability that is a function of the water saturation S_w and lies between 0 and 1:

$$\mathbf{k}_w = k_{rw}(S_w) \mathbf{k} \quad (6.18)$$

- k_{rw} - relative permeability for water [-]

Note further that with the viscosity η_w , the generalized Darcy's law introduces a new state variable in the mass balance equation that will be discussed together with the other state variables in section 6.3.7.

Note finally that the Darcy velocity or filter velocity refers to the flow velocity with respect to the bulk volume. In order to derive the interstitial water velocity v_a that is required for the balance equations, the Darcy velocity must be divided by that fraction of space in the porous medium that is available for flow. In case of single-phase flow, this fraction is equal to the porosity, in case of multi-phase flow it refers to the porosity times the phase saturation S . However, the total flow rate, that is the velocity times the referring cross-section, is not affected by the different formulations. Interstitial water velocity and filter velocity thus relate by

$$v_{aw} = \frac{v_{fw}}{S_w \Phi} \quad (6.19)$$

Alternatively, particularly in case of constant density and viscosity the alternative formulation in terms of hydraulic heads and conductivity can also be used:

$$v_{fw} = -K_w \cdot \nabla h \quad (6.20)$$

K_w - effective hydraulic conductivity for water [m/s]

h - hydraulic head [m]

where the hydraulic conductivity is again subject to a saturation-dependent reduction, an equivalent to the relative permeability. Common practice is to add the term ∇z to equation (6.20) to include density-dependent flow:

$$v_{fw} = -K_w \cdot (\nabla h + \nabla z) \quad (6.21)$$

6.3.3 Saturation

Water saturation can become less than 1 for temperatures below 0 °C only¹³ which is reflected by the SFCC. The SFCC is thus clearly a function of temperature. In case of high pressures, the melting temperature may be affected thus making the saturation also a function of pressure:

$$S_w = S_w(p_w, T) \quad (6.22)$$

A sound basis for an appropriate choice of CEs for groundwater flow under permafrost conditions is presently hard to come by. Against this background, the publication of

¹³ or the complimentary saturation with ice greater than 0, see eq.(4.2)

/AUK 16/ appears to be particularly helpful as it presents an analytical approximation to the thermal soil properties under freezing conditions, based on fractionated grain size distributions. Moreover, it also produces an approach to include the effect of pressure melting. This work is described shortly in appendix C. A typical common approach is to use an abstract function, though, that requires to be adapted to a concrete problem (cp. section 9.4).

6.3.4 Relative permeability for water

With adopting Darcy's law as a flow law, the relative permeability is also introduced as a CE. Like the saturation, the relative permeability becomes less than 1 for temperatures below the melting point. It is usually provided as an abstract function that must be adapted for a specific problem (cp. section 9.4). As it is directly dependent on the saturation, it can be indirectly a function of pressure and temperature:

$$k_{rw} = k_{rw}(S_w(p_w, T)) \quad (6.23)$$

6.3.5 Non-advective heat flow

In contrast to a fluid, thermal energy can also spread out in solid materials. The related process is called "heat conduction" and is accounted for in the heat balance equation as a non-advective process. It can mathematically be described by a generalized form of Fourier's first law for water, ice and the matrix, respectively.

$$J_{cond w} = -S_w \Phi \lambda_w \cdot \nabla T$$

$$J_{cond i} = -S_i \Phi \lambda_i \cdot \nabla T \quad (6.24)$$

$$J_{cond m} = -(1 - \Phi) \lambda_m \cdot \nabla T$$

$J_{cond w}$ - heat flux in the water due to conduction [J/(s m²)]

λ_w - tensor of the thermal conductivity of water [J/(s m K)]

$J_{cond i}$ - heat flux in the ice due to conduction [J/(s m²)]

λ_i - tensor of the thermal conductivity of ice [J/(s m K)]

$J_{cond m}$ - heat flux in the matrix due to conduction [J/(s m²)]

λ_m - tensor of the thermal conductivity of the matrix [J/(s m K)]

In case of water, the tensor of the thermal conductivity is clearly isotropic and can thus also be expressed as a scalar. By contrast, ice and particularly the solid matrix can show anisotropy with respect to heat conduction. This, however, is a theoretical consideration. For practical purposes, the thermal conductivity is assumed here to be isotropic for all three phases. It is therefore treated as a tensor in the differential equations for compatibility reasons where necessary but written as a scalar everywhere else.

Note that heat conduction thus introduces the thermal conductivity as the second additional state variable that will also be discussed in the next subsection.

Another heat spreading process is restricted to water. It is attributed to the hydrodynamic dispersion which is caused by the flow of water through the tortuous pore space. While heat conduction is physically related to advection on the microscopic scale, it can mathematically be described as a non-advective process on the macroscopic scale by application of an averaging procedure /BEA 72/. Note that dispersion constitutes a new CE (see below). The related heat flux $J_{disp w}$ is explained as

$$J_{disp w} = -S_w \Phi C_{S w} \rho_w \mathbf{D}_w \cdot \nabla T \quad (6.25)$$

\mathbf{D}_w - dispersion tensor [m²/s]

This leads eventually to

$$J_{h w} = J_{cond w} + J_{disp w}$$

$$J_{h i} = J_{cond i} \quad (6.26)$$

$$J_{h m} = J_{cond m}$$

6.3.6 Dispersion

Following /SCH 61/, the dispersion tensor \mathbf{D}_w is defined as

$$\mathbf{D}_w = \begin{bmatrix} \alpha_l |\mathbf{v}| & 0 & 0 \\ 0 & \alpha_t |\mathbf{v}| & 0 \\ 0 & 0 & \alpha_t |\mathbf{v}| \end{bmatrix} \quad (6.27)$$

α_l - longitudinal dispersion length [m]

α_t - transversal dispersion length [m]

if the water velocity vector is aligned with the x-axis. Otherwise \mathbf{D}_w requires an appropriate congruent transformation according to the direction of flow (e.g. /KRÖ 91/).

6.3.7 Summary of dependencies for the CEs

The CEs comprise three parameters, i.e. porosity, saturation, and relative permeability and three empirical laws, i.e. Darcy's law, Fourier's law and Scheidegger dispersion that may directly or indirectly be dependent on the considered primary variables pressure and temperature. Note, the dependencies include EOS that are discussed in the next subsection and are therefore not further explained here.

$$\begin{aligned}
 \Phi &= \Phi(p_w, T) \\
 S_w &= S_w(p_w, T) \\
 k_{rw} &= k_{rw}(S_w(p_w, T)) \\
 \mathbf{v}_{aw} &= \mathbf{v}_{aw}(\mathbf{v}_{fw}(k_{rw}(S_w(p_w, T))), S_w(p_w, T), \Phi(p_w, T), g, \rho_w, \eta_w, p_w) \quad (6.28) \\
 J_{condj} &= J_{condj}(S_j(p_w, T)^{14}, \Phi(p_w, T), \lambda_j, T), j = w, i, m \\
 J_{dispw} &= J_{dispw}(S_w(p_w, T), \Phi(p_w, T), \mathbf{D}_w(\mathbf{v}_{aw}, \alpha_l, \alpha_t), c_{sw}, \rho_w, T)
 \end{aligned}$$

Furthermore, two effects, the influence of gravity on flow and the impact of hydraulic dispersion on heat flow can be included by choosing a non-zero value for the related constants g , α_l , and α_t .

6.4 Equations of state

The next entry in the book of rules concerns the equations of state (EOS). They relate the state of matter which is described by state variables such as density or thermal conductivity to physical conditions like pressure or temperature¹⁵. In principle, EOS apply to a vast range of physical conditions that is far too broad to apply to a specific problem. Practical limits have thus to be defined that cover the expected conditions for the problem at hand to avoid excessive complexity. However, a careful choice is advisable as such limits also restrict the applicability of a model to other problems.

¹⁴ Where applicable

¹⁵ Another influencing quantity could be the salinity of the groundwater, but salinity as well as other possible physicochemical conditions are left to be incorporated at a later time if need arises.

Three possible applications are described and discussed in section 7. They impose different requirements to pressure and temperature ranges on the EOS. The first one is considered to be quite general in that maximum values are chosen according to extreme conditions envisaged for a repository for radioactive waste and the minimum values according to deep freezing conditions. The adopted maximum ranges for pressure and temperature in this case are therefore (see section 7.2)

$$\begin{aligned} 0.1 \text{ MPa} < p < 10 \text{ MPa} \\ -20 \text{ }^\circ\text{C} < T < 200 \text{ }^\circ\text{C} \end{aligned} \quad (6.29)$$

Two reports have been written in the past to compile formulations for state variables, /KRÖ 08/ and /KRÖ 10/. While all state variables that are of interest here were covered, the lowest temperature considered in these reports had only been 0 °C.

Additional data have therefore been collected and compiled in appendix B.1. Analytical functions based on these data have been formulated and their relation to the data from the literature is also presented in appendix B.1. As a general illustration, the EOS are depicted in Fig. 6.1 for atmospheric pressure using the analytical formulations.

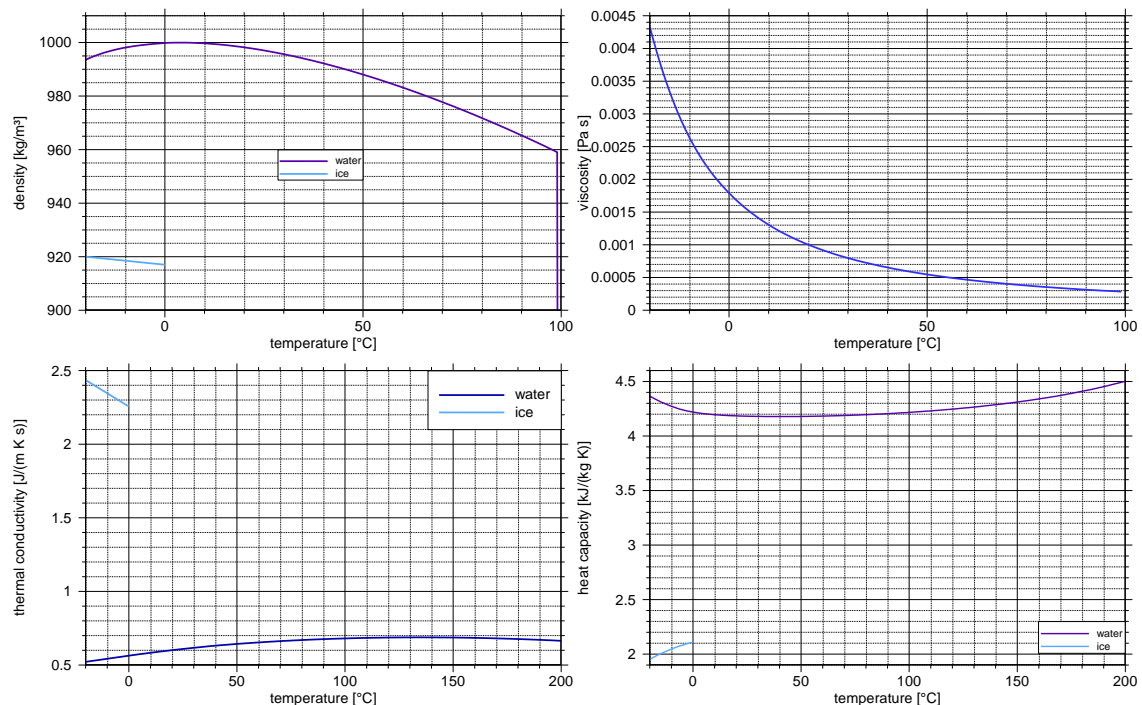


Fig. 6.1 Density (top left), viscosity (top right), thermal conductivity (bottom left), and heat capacity (bottom right) for water and ice, where applicable

Based on the discussion in Appendix B.3.2 the following dependencies are adopted to be possibly implemented in the balance equations:

$$\begin{aligned}
\rho_w &= \rho_w(p_w, T)^{16} & \rho_i &= \rho_i(T) & \rho_m &= \text{const.} \\
\eta_w &= \eta_w(p_w, T) \\
\lambda_w &= \lambda_w(p_w, T) & \lambda_i &= \lambda_i(T) & \lambda_m &= \lambda_m(T) \\
c_{sw} &= c_{sw}(p_w, T) & c_{si} &= c_{si}(T) & c_{sm} &= c_{sm}(T)
\end{aligned} \tag{6.30}$$

6.5 Reified balance equations

Introducing the CEs and the EOS as discussed in section 6.3 includes Darcy's law in form of equation (6.15) after applying relation (6.19) between interstitial and filter velocity. Applying also the relation between water and ice saturation (4.2), mass balance equation (6.5) can be written as

$$\begin{aligned}
&(S_i \rho_i + S_w \rho_w) \frac{\partial \Phi}{\partial t} + \Phi(\rho_w - \rho_i) \frac{\partial S_w}{\partial t} + S_w \Phi \frac{\partial \rho_w}{\partial t} + S_i \Phi \frac{\partial \rho_i}{\partial t} \\
&-\nabla \cdot \left(\rho_w \frac{k_{rw}}{\eta_w} \mathbf{k} \cdot (\nabla p_w - \rho_w \mathbf{g}) \right) = \rho_w q_w
\end{aligned} \tag{6.31}$$

As the primary variables in the balance equations for mass and heat are pressure and temperature, the derivatives with respect to time can be expanded to

$$\begin{aligned}
&(S_i \rho_i + S_w \rho_w) \left[\frac{\partial \Phi}{\partial p} \frac{\partial p}{\partial t} + \frac{\partial \Phi}{\partial T} \frac{\partial T}{\partial t} \right] + \Phi(\rho_w - \rho_i) \left[\frac{\partial S_w}{\partial p} \frac{\partial p}{\partial t} + \frac{\partial S_w}{\partial T} \frac{\partial T}{\partial t} \right] \\
&+ S_w \Phi \left[\frac{\partial \rho_w}{\partial p} \frac{\partial p}{\partial t} + \frac{\partial \rho_w}{\partial T} \frac{\partial T}{\partial t} \right] + S_i \Phi \frac{\partial \rho_i}{\partial T} \frac{\partial T}{\partial t} \\
&-\nabla \cdot \left(\rho_w \frac{k_{rw}}{\eta_w} \mathbf{k} \cdot (\nabla p_w - \rho_w \mathbf{g}) \right) = \rho_w q_w
\end{aligned} \tag{6.32}$$

Equation (6.32) calls for rearranging since temperature T is calculated by the energy balance equation. All related terms can therefore be considered to be permanently and

¹⁶ The discussions in Appendix B.3.2 are based on the pressure limitation (7.4) and result in a pressure dependence for the density of water that is less relevant. However, adopting the broader range (7.2) the pressure dependence becomes significant for the water density as well.

possibly iteratively updated source terms which are all assigned to the right-hand side of the balance equation:

$$\begin{aligned} & \left[(S_i \rho_i + S_w \rho_w) \frac{\partial \Phi}{\partial p} + \Phi (\rho_w - \rho_i) \frac{\partial S_w}{\partial p} + S_w \Phi \frac{\partial \rho_w}{\partial p} \right] \frac{\partial p}{\partial t} \\ & - \nabla \cdot \left(\rho_w \frac{k_{rw}}{\eta_w} \mathbf{k} \cdot (\nabla p_w - \rho_w \mathbf{g}) \right) = \rho_w q_w \quad (6.33) \\ & - \left[(S_i \rho_i + S_w \rho_w) \frac{\partial \Phi}{\partial T} + \Phi (\rho_w - \rho_i) \frac{\partial S_w}{\partial T} + S_w \Phi \frac{\partial \rho_w}{\partial T} + S_i \Phi \frac{\partial \rho_i}{\partial T} \right] \frac{\partial T}{\partial t} \end{aligned}$$

While the contribution of changes of porosity and densities can clearly be identified, the second term on the left-hand side in equation (6.33) as well as the second term on the right-hand side look a bit curious. They represent the effect of the different densities of water and ice on the water during a phase change as illustrated in Fig. 6.2. Water is pushed away in case of freezing by ice of less density and sucked towards the phase interface in case of melting. The key parameter to this effect is of course the saturation of ice (or the saturation of water) as it decides about the amount of ice in the pore space.

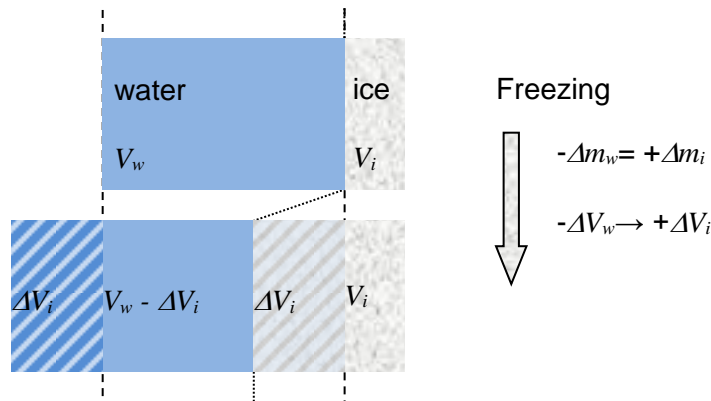


Fig. 6.2 Volumetric changes in water and ice during freezing

Another generally used CE is Fourier's first law in the heat conduction terms. Analogously to the procedure for the mass balance equation, the heat flow densities $J_{cond w}$, $J_{cond i}$ and $J_{cond m}$ will be inserted first into the energy balance equation (6.13) to provide easy comparability with other formulations. For the sake of simplicity, the flow law is not inserted in this case:

$$\begin{aligned}
& S_w \Phi \rho_w \frac{\partial(c_{s w} T)}{\partial t} + S_i \Phi \rho_i \frac{\partial(c_{s i} T)}{\partial t} + (1 - \Phi) \rho_m \frac{\partial(c_{s m} T)}{\partial t} \\
& + (\mathbf{v}_{a w} S_w \rho_w \Phi) \cdot \nabla(c_{s w} T) \\
& - \nabla \cdot [(S_w \Phi \boldsymbol{\lambda}_w + S_w \Phi c_{s w} \rho_w \mathbf{D}_w + S_i \Phi \boldsymbol{\lambda}_i + (1 - \Phi) \boldsymbol{\lambda}_m) \cdot \nabla T] \\
& = r_{hQ} + c_{s w} \rho_w q_w (T - \dot{T}) + L \frac{\partial(\rho_i S_i \Phi)}{\partial t}
\end{aligned} \tag{6.34}$$

Inserting now all the other CEs and the EOS leads to

$$\begin{aligned}
& S_w \Phi \rho_w \left[T \frac{\partial c_{s w}}{\partial t} + c_{s w} \frac{\partial T}{\partial t} \right] + S_i \Phi \rho_i \left[T \frac{\partial c_{s i}}{\partial t} + c_{s i} \frac{\partial T}{\partial t} \right] \\
& + (1 - \Phi) \rho_m \left[T \frac{\partial c_{s m}}{\partial t} + c_{s m} \frac{\partial T}{\partial t} \right] + (\mathbf{v}_{a w} S_w \rho_w \Phi) \cdot \nabla(c_{s w} T) \\
& - \nabla \cdot [(S_w \Phi \boldsymbol{\lambda}_w + S_w \Phi c_{s w} \rho_w \mathbf{D}_w + S_i \Phi \boldsymbol{\lambda}_i + (1 - \Phi) \boldsymbol{\lambda}_m) \cdot \nabla T] \\
& = r_{hQ} + c_{s w} \rho_w q_w (T_w - \dot{T}) + L \left[\rho_i S_i \frac{\partial \Phi}{\partial t} + \rho_i \Phi \frac{\partial S_i}{\partial t} + S_i \Phi \frac{\partial \rho_i}{\partial t} \right]
\end{aligned} \tag{6.35}$$

expanding even further to

$$\begin{aligned}
& S_w \Phi \rho_w \left[T \left(\frac{\partial c_{s w}}{\partial p} \frac{\partial p}{\partial t} + \frac{\partial c_{s w}}{\partial T} \frac{\partial T}{\partial t} \right) + c_{s w} \frac{\partial T}{\partial t} \right] + S_i \Phi \rho_i \left[T \frac{\partial c_{s i}}{\partial T} \frac{\partial T}{\partial t} + c_{s i} \frac{\partial T}{\partial t} \right] \\
& + (1 - \Phi) \rho_m \left[T \frac{\partial c_{s m}}{\partial T} \frac{\partial T}{\partial t} + c_{s m} \frac{\partial T}{\partial t} \right] + (\mathbf{v}_{a w} S_w \rho_w \Phi) \cdot \nabla(c_{s w} T) \\
& - \nabla \cdot [(S_w \Phi \boldsymbol{\lambda}_w + S_w \Phi c_{s w} \rho_w \mathbf{D}_w + S_i \Phi \boldsymbol{\lambda}_i + (1 - \Phi) \boldsymbol{\lambda}_m) \cdot \nabla T] \\
& = r_{hQ} + c_{s w} \rho_w q_w (T_w - \dot{T}) \\
& + L \left[\rho_i S_i \left(\frac{\partial \Phi}{\partial p} \frac{\partial p}{\partial t} + \frac{\partial \Phi}{\partial T} \frac{\partial T}{\partial t} \right) + \rho_i \Phi \left(\frac{\partial S_i}{\partial p} \frac{\partial p}{\partial t} + \frac{\partial S_i}{\partial T} \frac{\partial T}{\partial t} \right) + S_i \Phi \frac{\partial \rho_i}{\partial T} \frac{\partial T}{\partial t} \right]
\end{aligned} \tag{6.36}$$

Rearranging results in

$$\begin{aligned}
& S_w \Phi \rho_w \left[T \frac{\partial c_{s w}}{\partial T} \frac{\partial T}{\partial t} + c_{s w} \frac{\partial T}{\partial t} \right] + S_i \Phi \rho_i \left[T \frac{\partial c_{s i}}{\partial T} \frac{\partial T}{\partial t} + c_{s i} \frac{\partial T}{\partial t} \right] \\
& + (1 - \Phi) \rho_m \left[T \frac{\partial c_{s m}}{\partial T} \frac{\partial T}{\partial t} + c_{s m} \frac{\partial T}{\partial t} \right] \\
& - L \left[\rho_i S_i \frac{\partial \Phi}{\partial T} \frac{\partial T}{\partial t} + \rho_i \Phi \frac{\partial S_i}{\partial T} \frac{\partial T}{\partial t} + S_i \Phi \frac{\partial \rho_i}{\partial T} \frac{\partial T}{\partial t} \right] + (\mathbf{v}_{a w} S_w \rho_w \Phi) \cdot \nabla(c_{s w} T) \\
& - \nabla \cdot [(S_w \Phi \boldsymbol{\lambda}_w + S_w \Phi c_{s w} \rho_w \mathbf{D}_w + S_i \Phi \boldsymbol{\lambda}_i + (1 - \Phi) \boldsymbol{\lambda}_m) \cdot \nabla T] \\
& = r_{hQ} + c_{s w} \rho_w q_w (T_w - \dot{T})
\end{aligned} \tag{6.37}$$

$$\begin{aligned}
& +S_w \Phi \rho_w T \frac{\partial c_{sw}}{\partial p} \frac{\partial p}{\partial t} \\
& + L \left[\rho_i S_i \frac{\partial \Phi}{\partial p} \frac{\partial p}{\partial t} + \rho_i \Phi \frac{\partial S_i}{\partial p} \frac{\partial p}{\partial t} \right]
\end{aligned}$$

and finally in

$$\begin{aligned}
& \left(S_w \Phi \rho_w \left[T \frac{\partial c_{sw}}{\partial T} + c_{sw} \right] + S_i \Phi \rho_i \left[T \frac{\partial c_{si}}{\partial T} + c_{si} \right] \right. \\
& \left. + (1 - \Phi) \rho_m \left[T \frac{\partial c_{sm}}{\partial T} + c_{sm} \right] - L \left[\rho_i S_i \frac{\partial \Phi}{\partial T} + \rho_i \Phi \frac{\partial S_i}{\partial T} + S_i \Phi \frac{\partial \rho_i}{\partial T} \right] \right) \frac{\partial T}{\partial t} \\
& + (\mathbf{v}_{aw} S_w \rho_w \Phi) \cdot \nabla (c_{sw} T) \\
& - \nabla \cdot [(S_w \Phi \boldsymbol{\lambda}_w + S_w \Phi c_{sw} \rho_w \mathbf{D}_w + S_i \Phi \boldsymbol{\lambda}_i + (1 - \Phi) \boldsymbol{\lambda}_m) \cdot \nabla T] \\
& = r_{hQ} + c_{sw} \rho_w q_w (T_w - \hat{T}) + \\
& \left(S_w \Phi \rho_w T \frac{\partial c_{sw}}{\partial p} + L \left[\rho_i S_i \frac{\partial \Phi}{\partial p} + \rho_i \Phi \frac{\partial S_i}{\partial p} \right] \right) \frac{\partial p}{\partial t}
\end{aligned} \tag{6.38}$$

7 Case specific adaptations

7.1 Purpose and procedure

Defining limits for the independent primary variables pressure and temperature may allow for simplifications of the formulations for the CEs and the EOS. This can in turn allow for simplifying the time derivatives in the general form of the balance equations (5.19) and (5.31) or even for dropping terms in the quite complex form of equations (6.33) and (6.38).

Depending on the purpose at hand, the limits can be differently defined, introducing amendments in the book of rules leading to different simplifications. Furthermore, specific tasks might require accounting for a different sensitivity of the same secondary state variable within the same limits of pressure and temperature.

In the following subsections, possible applications – called case 1a, 1, 2, and 3 – of the mathematically coupled flow and heat transport equations derived in sections 5 and 6.5 are presented. The considered ranges of the primary variables and the following impact on the related processes are defined in each case and the consequences for the balance equations are discussed.

7.2 Case 1: Heat producing geological repositories

Many concepts for a geologic storage of radioactive waste restrict the admissible temperature on the surface of a waste canister to 100 °C. However, a maximum temperature of 200 °C is also considered in some cases. In order to cover all possible conditions in such a framework the maximum temperature is set to 200 °C.

Boiling of water is conceptually excluded from the presently discussed model. It should therefore be noted that the vapour pressure at 200 °C amounts to nearly 1.6 MPa (e.g. /KRÖ 10/). This vapour pressure is equivalent to the hydraulic pressure of a water column of about 150 m height. A phase change due to boiling at temperatures up to 200 °C is therefore not expected at depths significantly below 150 m below the water table. Geological storage is generally envisioned to be established at depths far greater than 150 m while the extreme temperatures occur in the immediate vicinity of the waste canis-

ters only. It is therefore not expected that allowing for a maximum temperature of even 200 °C at the repository would cause boiling anywhere in the host rock.

The lower bound of a suitable temperature range is controlled by the ambition to model groundwater flow under permafrost conditions. Keeping in mind that the temperature in the underground increases with depth lets expect that the lowest temperature will be found at the surface. Data from /JNC 00/ (see subsection 7.4) indicate that surface temperatures down to -20 °C suffice to create a permafrost thickness of up to 700 m in a granitic underground. Against this background, the lower temperature bound is tentatively set to -20 °C¹⁷. The following temperature range is therefore considered to be sufficient for a wide range of problems in the framework of radioactive waste storage:

$$-20\text{ }^{\circ}\text{C} < T < 200\text{ }^{\circ}\text{C} \quad (7.1)$$

While the minimum pressure should not drop below atmospheric pressure, the maximum pressure depends on the depth of the repository and the related hydrostatic pressure. While most envisaged geological repositories tend to aim at depths of less than 1000 m, geological storage in deep horizontal or vertical boreholes in several kilometres' depth are presently investigated as well, e.g. /FIN 20/, /MAL 20/. The maximum pressure could thus ad hoc be set to 50 MPa which is approximating the equivalent of a water column with a height of 5 km and thus covering an admissible pressure range of

$$0.1\text{ MPa} < p < 50\text{ MPa} \quad (7.2)$$

Conditions (7.1) and (7.2) define case 1a.

The dependencies of the CEs listed in (6.28) are in general tied to the primary variables pressure and temperature. In the same way, conditions (7.1) and (7.2) have also formed the basis for the definition of dependencies of the EOS in (6.30). For completeness and reference in this chapter, the dependencies are compiled in (7.3). Based on these assumptions balance equations (6.33) and (6.38) have been derived, which now define the most general case 1a.

¹⁷ Most data found in the literature would allow for a lower bound of -40 °C. This is felt to be beyond expectations for future climate conditions in present Germany, though. If need arises, an extension to such a low bound should not pose a problem.

$$\begin{aligned}
\Phi &= \Phi(p_w, T) \\
S_w &= S_w(p_w, T) \\
k_{rw} &= k_{rw}(S_w(p_w, T)) \\
\mathbf{v}_{aw} &= \mathbf{v}_{aw}(\mathbf{v}_{fw}(k_{rw}(S_w(p_w, T))), S_w(p_w, T), \Phi(p_w, T), g, \rho_w, \eta_w, p_w) \\
J_{condj} &= J_{condj}(S_j(p_w, T)^{18}, \Phi(p_w, T), \lambda_j, T), j = w, i, m \\
J_{dispw} &= J_{dispw}(S_w(p_w, T), \Phi(p_w, T), \mathbf{D}_w(\mathbf{v}_{aw}, \alpha_l, \alpha_t), c_{sw}, \rho_w, T) \\
\rho_w &= \rho_w(p_w, T) \quad \rho_i = \rho_i(T) \quad \rho_m = const. \\
\eta_w &= \eta_w(p_w, T) \\
\lambda_w &= \lambda_w(p_w, T) \quad \lambda_i = \lambda_i(T) \quad \lambda_m = \lambda_m(T) \\
c_{sw} &= c_{sw}(p_w, T) \quad c_{si} = c_{si}(T) \quad c_{sm} = c_{sm}(T)
\end{aligned} \tag{7.3}$$

While a maximum pressure of 50 MPa is suitable to include all conceivable cases including deep boreholes, it appears to be excessively high, though. More practical may be restricting the range to a maximum of 10 MPa which is equivalent to a water column of 1000 m height as this limit covers the majority of repository concepts. It also includes the extremely low permafrost bases found at depths of up to 700 m (see above). For practical purposes, a pressure range of

$$0.1 \text{ MPa} < p < 10 \text{ MPa} \tag{7.4}$$

defining case 1 appears to be more appropriate.

As the present work aims at permafrost conditions in the underground, some general simplifications appear to be in order. Where permafrost prevails, it is expected that there will be no mechanical load from ice shields. This does also exclude the possibility of pressure melting, thereby removing the dependency of saturation and thus relative permeability on pressure.

$$\begin{aligned}
S_w &= S_w(T) \\
k_{rw} &= k_{rw}(S_w(T))
\end{aligned} \tag{7.5}$$

¹⁸ Where applicable

It also removes a strong reason to include a dependence of the porosity on an external mechanical pressure. Internal mechanical pressure from hydraulic pressure or thermal expansion has up to now been taken into account. It has to be mentioned, though, that the density of a host rock is roughly twice as high as that of the groundwater even if the latter contains salts to a high degree. The lithostatic pressure of the rock thus increases about two times faster with depth than the hydrostatic pressure. In order to affect the porosity, any process leading to an increased hydraulic pressure must be of increasing strength with depth to compensate the much higher weight of the rock.

In case of thermal expansion, the highest influence must be expected in the immediate vicinity of the waste canisters. However, heat spreads out in all three dimensions which results in a strong temperature decrease with distance to the heat source. The biggest effect from thermal expansion can therefore be expected in the immediate vicinity of the waste canisters.

For completeness it should be mentioned here that the expansion of water during freezing may lead to an increase of porosity on the micro-scale which would result in frost heave on the macro-scale. Ignoring this phenomenon, as defined right at the beginning in section 4.1 causes a certain error when calculating the displacement of water in the pore space. However, this error is put up with here because the relevance of this effect is not entirely clear and taking it into account would increase the complexity of the problem by a considerable degree.

The reasoning about significant porosity changes is quite tentative and may not apply to a particular case. However, the porosity is set constant from here on, keeping in mind that the related expressions can easily be supplemented in case of need, based on their derivation in sections 5 and 6:

$$\Phi = \text{const.} \quad (7.6)$$

Based on these considerations, CEs and EOS look now like

$$\Phi = \text{const.}$$

$$S_w = S_w(T)$$

$$k_{rw} = k_{rw}(S_w(T))$$

$$\mathbf{v}_{aw} = \mathbf{v}_{aw}(\mathbf{v}_{fw}(k_{rw}(S_w(T))), S_w(T), \Phi, g, \rho_w, \eta_w, p_w)$$

$$J_{cond j} = J_{cond j}(S_j(T)^{19}, \Phi, \lambda_j, T), j = w, i, m \quad (7.7)$$

$$J_{disp w} = J_{disp w}(S_w(T), \Phi, \mathbf{D}_w(\mathbf{v}_{aw}, \alpha_l, \alpha_t), c_{sw}, \rho_w, T)$$

$$\rho_w = \rho_w(T) \quad \rho_i = const. \quad \rho_m = const.$$

$$\eta_w = \eta_w(p_w, T)$$

$$\lambda_w = \lambda_w(p_w, T) \quad \lambda_i = \lambda_i(T) \quad \lambda_m = \lambda_m(T)$$

$$c_{sw} = c_{sw}(p_w, T) \quad c_{si} = c_{si}(T) \quad c_{sm} = c_{sm}(T)$$

so that case 1 allows for a simplification of the balance equations to

$$-\nabla \cdot \left(\rho_w \frac{k_{rw}}{\eta_w} \mathbf{k} \cdot (\nabla p_w - \rho_w \mathbf{g}) \right) = \rho_w q_w - \left[\Phi(\rho_w - \rho_i) \frac{\partial S_w}{\partial T} + S_w \Phi \frac{\partial \rho_w}{\partial T} \right] \frac{\partial T}{\partial t} \quad (7.8)$$

and

$$\begin{aligned} & \left(S_w \Phi \rho_w \left[T \frac{\partial c_{sw}}{\partial T} + c_{sw} \right] + S_i \Phi \rho_i \left[T \frac{\partial c_{si}}{\partial T} + c_{si} \right] \right) \frac{\partial T}{\partial t} \\ & + (1 - \Phi) \rho_m \left[T \frac{\partial c_{sm}}{\partial T} + c_{sm} \right] - L \rho_i \Phi \frac{\partial S_i}{\partial T} \\ & + (\mathbf{v}_{aw} S_w \rho_w \Phi) \cdot \nabla (c_{sw} T) \\ & - \nabla \cdot [(S_w \Phi \lambda_w + S_i \Phi \lambda_i + (1 - \Phi) \lambda_m + S_w \Phi c_{sw} \rho_w \mathbf{D}_w) \cdot \nabla T] \\ & = r_{hQ} + c_{sw} \rho_w q_w (T_w - \dot{T}) + S_w \Phi \rho_w T \frac{\partial c_{sw}}{\partial p} \frac{\partial p}{\partial t} \end{aligned} \quad (7.9)$$

Note that mass balance equation (7.8) is formally at quasi steady-state if the right-hand side is considered to represent permanently updated source terms from the heat flow equation.

7.3 Case 2: Benchmarks from the INTERFROST-project

An international code comparison concerning groundwater flow under freezing conditions has been performed in the framework of the international INTERFROST-project /GRE 18/. It was based on several test cases where the latest two were 2D-problems considered to be “more complex scenarios“ taking heat flow, water flow and freez-

¹⁹ Where applicable

ing/melting of the water into account. The test cases were called TH2 “Frozen inclusion thaw” and TH3 “Talík Opening/Closure”. They are described in detail in appendices A.1 and A.2. The considered ranges of pressure and temperature can be taken from the initial and boundary conditions in the test case descriptions. They are covered by the following limitations:

$$\begin{aligned}
 -5 \text{ } ^\circ\text{C} < T < +5 \text{ } ^\circ\text{C} \\
 100\,000 \text{ Pa} < p < 100\,883 \text{ Pa}
 \end{aligned}
 \tag{7.10}$$

The test descriptions did neither include any water or heat sources nor a thermo-hydraulic heat dispersion. From the discussion of the pressure-dependences in case 1 it follows that any function of the pressure can be dropped in case 2 as well. For the rather narrow range of temperatures, many dependencies of the EOS on temperature can be neglected (see appendix B.3.2):

$$\begin{aligned}
 \Phi &= \text{const.} \\
 S_w &= S_w(T) \\
 k_{rw} &= k_{rw}(S_w(T)) \\
 \mathbf{v}_{aw} &= \mathbf{v}_{aw}(\mathbf{v}_{fw}(k_{rw}(S_w(T))), S_w(T), \Phi, g, \rho_w, \eta_w, p_w) \\
 J_{condj} &= J_{condj}(S_j(T)^{20}, \Phi, \lambda_j, T), j = w, i, m \\
 J_{dispw} &= 0 \\
 \rho_w &= \text{const.} \quad \rho_i = \text{const.} \quad \rho_m = \text{const.} \\
 \eta_w &= \eta_w(T) \\
 \lambda_w &= \lambda_w(T) \quad \lambda_i = \text{const.} \quad \lambda_m = \text{const.} \\
 c_{sw} &= \text{const.} \quad c_{si} = \text{const.} \quad c_{sm} = c_{sm}(T)
 \end{aligned}
 \tag{7.11}$$

All these assumptions allow for rewriting the balance equations (6.33) and (6.38) as

²⁰ Where applicable

$$-\nabla \cdot \left(\rho_w \frac{k_{rw}}{\eta_w} \mathbf{k} \cdot (\nabla p_w - \rho_w \mathbf{g}) \right) = -\Phi(\rho_w - \rho_i) \frac{\partial S_w}{\partial T} \frac{\partial T}{\partial t} \quad (7.12)$$

and

$$\left(S_w \Phi \rho_w c_{s w} + S_i \Phi \rho_i c_{s i} + (1 - \Phi) \rho_m \left[T \frac{\partial c_{s m}}{\partial T} + c_{s m} \right] - L \rho_i \Phi \frac{\partial S_i}{\partial T} \right) \frac{\partial T}{\partial t} + (\mathbf{v}_{a w} S_w \rho_w \Phi c_{s w}) \cdot \nabla T \quad (7.13)$$

$$-\nabla \cdot [(S_w \Phi \lambda_w + S_i \Phi \lambda_i + (1 - \Phi) \lambda_m) \cdot \nabla T] = 0$$

7.4 Case 3: Talik forming

Taliki are features in the permafrost which can form only when temperatures below the freezing point at ground surface are countered by the heat from earth's core over a long period of time. The base of the permafrost is thereby defined as the depth at which the temperature reaches the freezing point. The region covered by a numerical model investigating talik forming would thus essentially show temperatures below 0 °C except where it includes hydrogeological units below the permafrost. Tentatively, the relevant temperature range is therefore set to

$$-20 \text{ }^\circ\text{C} < T < +20 \text{ }^\circ\text{C} \quad (7.14)$$

Speculating on the basis of investigations from /JNC 00/, the depth of permafrost in middle Europe is expected to cover not more than a couple of hundred of meters. Locations that are more likely to experience severe permafrost conditions such as Canada, Alaska or Russia, have shown up to 700 m permafrost thickness, see Fig. 7.1. The pressure range of interest is therefore basically the same as in case 1:

$$0.1 \text{ MPa} < p < 10 \text{ MPa} \quad (7.15)$$

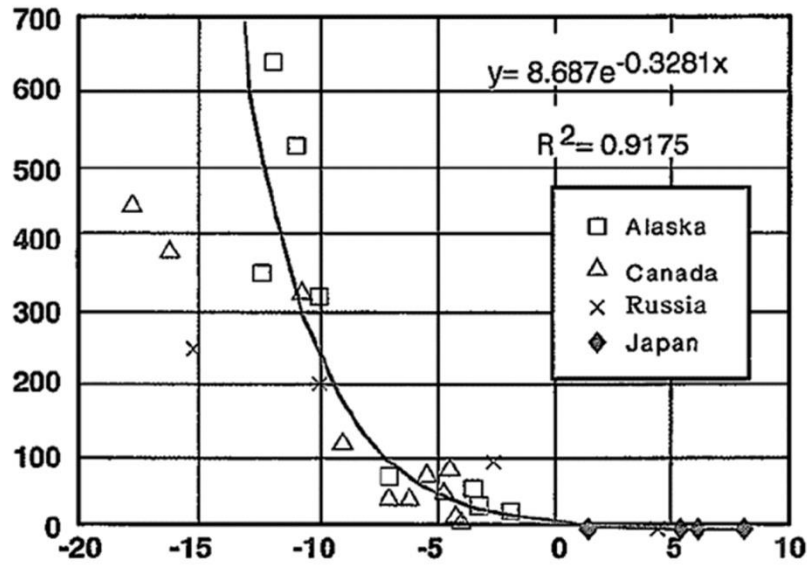


Fig. 7.1 Permafrost thickness over surface temperature; from /JNC 00/

Taliki are often located below large volumes of surface water such as lakes or rivers and can even connect these surface waters to unfrozen groundwater aquifers below the permafrost. It thus appears that water having a lower thermal conductivity than the rock has in principle an analogous influence on the development of taliki as surface features with lower thermal conductivity in general have on the thickness of permafrost (e.g. /NOS 22/).

There might be further processes relevant for this phenomenon, though, such as heat transport by convection or convection cells. In this case, the density anomaly of water leading to the highest density at 4 °C is likely to play a relevant role. If so, at least the CEs and EOS referring to water should be accurately reflected in a numerical model as little differences in the density may trigger convection cells. This leads to aggravated conditions for the CEs and EOS in comparison to case 1.

All things considered, case 3 is quite similar to case 1 despite the much more restricted temperature range because basically all processes, CEs and EOS need to be represented by a maximum of accuracy until their relevance for talik forming is clarified. Against this background, the following dependencies are adopted:

$$\Phi = \text{const.}$$

$$S_w = S_w(T)$$

$$k_{rw} = k_{rw}(S_w(T))$$

$$\mathbf{v}_{aw} = \mathbf{v}_{aw}(\mathbf{v}_{fw}(k_{rw}(S_w(T))), S_w(T), \Phi, g, \rho_w, \eta_w, p_w)$$

$$J_{cond j} = J_{cond j}(S_j(T)^{21}, \Phi, \lambda_j, T), j = w, i, m$$

(7.16)

$$J_{disp w} = J_{disp w}(S_w(T), \Phi, \mathbf{D}_w(\mathbf{v}_{aw}, \alpha_l, \alpha_t), c_{sw}, \rho_w, T)$$

$$\rho_w = \rho_w(p_w, T) \quad \rho_i = \rho_i(T) \quad \rho_m = \text{const.}$$

$$\eta_w = \eta_w(p_w, T)$$

$$\lambda_w = \lambda_w(p_w, T) \quad \lambda_i = \lambda_i(T) \quad \lambda_m = \lambda_m(T)$$

$$c_{sw} = c_{sw}(p, T) \quad c_{si} = c_{si}(T) \quad c_{sm} = c_{sm}(T)$$

With respect to a detailed hydraulic talik model, assumptions (7.16) may be adequate leading to the following form of the balance equations:

$$\begin{aligned} S_w \Phi \frac{\partial \rho_w}{\partial p} \frac{\partial p}{\partial t} - \nabla \cdot \left(\rho_w \frac{k_{rw}}{\eta_w} \mathbf{k} \cdot (\nabla p_w - \rho_w \mathbf{g}) \right) \\ = \rho_w q_w - \left[\Phi(\rho_w - \rho_i) \frac{\partial S_w}{\partial T} + S_w \Phi \frac{\partial \rho_w}{\partial T} + S_i \Phi \frac{\partial \rho_i}{\partial T} \right] \frac{\partial T}{\partial t} \end{aligned} \quad (7.17)$$

and

$$\begin{aligned} \left(S_w \Phi \rho_w \left[T \frac{\partial c_{sw}}{\partial T} + c_{sw} \right] + S_i \Phi \rho_i \left[T \frac{\partial c_{si}}{\partial T} + c_{si} \right] \right. \\ \left. + (1 - \Phi) \rho_m \left[T \frac{\partial c_{sm}}{\partial T} + c_{sm} \right] - L \left[\rho_i \Phi \frac{\partial S_i}{\partial T} + S_i \Phi \frac{\partial \rho_i}{\partial T} \right] \right) \frac{\partial T}{\partial t} \\ + (\mathbf{v}_{aw} S_w \rho_w \Phi) \cdot \nabla (c_{sw} T) \\ - \nabla \cdot [(S_w \Phi \lambda_w + S_i \Phi \lambda_i + (1 - \Phi) \lambda_m + S_w \Phi c_{sw} \rho_w \mathbf{D}_w) \cdot \nabla T] \\ = r_{hQ} + c_{sw} \rho_w q_w (T_w - \dot{T}) + S_w \Phi \rho_w T \frac{\partial c_{sw}}{\partial p} \frac{\partial p}{\partial t} \end{aligned} \quad (7.18)$$

²¹ Where applicable

7.5 Comparison of the developed equations

7.5.1 General remarks

Up to this point, rather different forms of balance equations have been presented, starting with a quite general form in section 5. These equations were further developed into a more specific form in section 6.5 that showed the dependencies on the CEs and the EOS explicitly and thereby formed the most general case 1a. In sections 7.2 to 7.4, the still quite general form was purpose-tailored to the cases 1, 2, and 3. The mass balance equations coming from this process are term-wise arranged in Tab. 7.1 for comparison, the heat flow equations in Tab. 7.2 and Tab. 7.3. Since it is planned to set up a numerical model with COMSOL Multiphysics /COM 21/ for case 2 at a later stage (see also section 8.1.6), the referring pre-set terms are included in this comparison.

7.5.2 Mass balance equations

The differences between the formulations are mainly caused by the storage term. Here, a lot of dependencies become visible. Since two equations are coupled that have different primary variables, i.e. pressure and temperature, the storage term consists of derivatives with respect to both primary variables. A derivative with respect to the variable that is not the primary variable in the considered equation can be looked at as a source term that is continually updated with every new iteration step. In that sense, parts of the original storage term therefore contribute to the source term of the same equation and are therefore assigned to the right-hand side.

The almost deceptively clear **storage term** in the general form (5.19) expands into a great variety of terms in case 1a. The same applies also for other right-hand side terms which have the same origin. However, the simplifications discussed above lead to a situation for cases 1 and 2 where the storage term vanishes.

Tab. 7.1 Groundwater flow equations from this work

Groundwater flow equation					Case	Equation
Storage term	Advective term	Non-advective term	Source term	Other right-hand side terms		
$\frac{\partial(\Phi[S_w \rho_w + S_i \rho_i])}{\partial t}$	$+\nabla \cdot (\Phi[\mathbf{v}_{a w} S_w \rho_w + \mathbf{v}_{a i} S_i \rho_i])$	$+\nabla \cdot (\mathbf{J}_{f w} + \mathbf{J}_{f i})$	$r_{f w} + r_{f i}$	(-)	general form	(5.19)
$\left[(S_i \rho_i + S_w \rho_w) \frac{\partial \Phi}{\partial p} + \Phi(\rho_w - \rho_i) \frac{\partial S_w}{\partial p} + S_w \Phi \frac{\partial \rho_w}{\partial p} \right] \frac{\partial p}{\partial t}$	$-\nabla \cdot \left(\rho_w \frac{k_{rw}}{\eta_w} \mathbf{k} \cdot (\nabla p_w - \rho_w \mathbf{g}) \right)$	(-)	$\rho_w q_w$	$-\left[(S_i \rho_i + S_w \rho_w) \frac{\partial \Phi}{\partial T} + \Phi(\rho_w - \rho_i) \frac{\partial S_w}{\partial T} + S_w \Phi \frac{\partial \rho_w}{\partial T} + S_i \Phi \frac{\partial \rho_i}{\partial T} \right] \frac{\partial T}{\partial t}$	case 1a	(6.33)
(-)	$-\nabla \cdot \left(\rho_w \frac{k_{rw}}{\eta_w} \mathbf{k} \cdot (\nabla p_w - \rho_w \mathbf{g}) \right)$	(-)	$\rho_w q_w$	$-\left[\Phi(\rho_w - \rho_i) \frac{\partial S_w}{\partial T} + S_w \Phi \frac{\partial \rho_w}{\partial T} \right] \frac{\partial T}{\partial t}$	case 1	(7.8)
(-)	$-\rho_w \nabla \cdot \left(\frac{k_{rw}}{\eta_w} \mathbf{k} \cdot (\nabla p_w - \rho_w \mathbf{g}) \right)$	(-)	(-)	$-\Phi(\rho_w - \rho_i) \frac{\partial S_w}{\partial t} \frac{\partial T}{\partial t}$	case 2	(7.12)
$S_w \Phi \frac{\partial \rho_w}{\partial p} \frac{\partial p}{\partial t}$	$-\nabla \cdot \left(\rho_w \frac{k_{rw}}{\eta_w} \mathbf{k} \cdot (\nabla p_w - \rho_w \mathbf{g}) \right)$	(-)	$\rho_w q_w$	$-\left[\Phi(\rho_w - \rho_i) \frac{\partial S_w}{\partial T} + S_w \Phi \frac{\partial \rho_w}{\partial T} + S_i \Phi \frac{\partial \rho_i}{\partial T} \right] \frac{\partial T}{\partial t}$	case 3	(7.17)
$\frac{\partial(\Phi \rho_w)}{\partial t}$	$-\nabla \cdot \left(\rho_w \frac{\mathbf{k}}{\eta} \cdot (\nabla p + \rho_w \mathbf{g}) \right)$	(-)z	$Q_m = \rho_w q_w$	(-)	COMSOL	(8.39)

By comparison, the **advective term** looks similar in all formulations except in case 2 where the water density is a constant and is taken out from under the differential operator. **Non-advective terms** have been excluded right from the beginning. The **source term** for groundwater is always the same except in case 2 where it is dropped by definition.

The **other right-hand side terms** are apparently not part of the general form, the game board, but pop up when a game becomes reified by rules in form of CEs and EOS and further specified by the amendments in form of limits of the primary variables i.e. temperature and pressure. It is thus that case 1a showing the highest degree of generality among the cases considered here, can be used as a starting point for reducing the other right-hand side terms based on the assumptions (7.7) for case 1, (7.11) for case 2 and (7.16) for case 3. Applying these assumptions leads to the case-specific choice of other right-hand side terms as listed in Tab. 7.1.

7.5.3 Heat balance equations

The **storage term** in the heat flow equations derived here is considerably more complex in any reified form than in the general form (see Tab. 7.2). At that, the most complex formulation can of course be found for case 1a, the most general reified case. As the set of terms varies significantly with the case in question, it appears that the storage term is particularly sensitive to the applied rules and amendments.

The **convective terms** as well as the **conductive terms** as compiled in Tab. 7.3 are, by contrast, the same in all formulations except in case 2 where the specific heat of water is constant and thus simplifies the convective term. Furthermore, thermo-hydraulic dispersion has not been considered in case 2, simplifying the conductive term.

Also, the **source terms** sorted by their physical meaning (direct heat source, inflowing heat, from storage term) look very much alike even if with two exceptions:

- (1) No heat source is defined in case 2.
- (2) The terms originating in the storage term but not being dependent on the temperature are subject to the same sensitivity to rules and amendments as the storage

term itself. A related case-dependent variation of formulations does therefore not come as a surprise.

Tab. 7.2 Heat flow equations (this work) – storage term (relates to Tab. 9.2)

Heat flow equation	Case	Equation
Storage term		
$S_w \Phi \rho_w \frac{\partial(c_{s w} T_w)}{\partial t} + S_i \Phi \rho_i \frac{\partial(c_{s i} T_i)}{\partial t} + (1 - \Phi) \rho_m \frac{\partial(c_{s m} T_m)}{\partial t}$	general form	(5.31)
$\left(S_w \Phi \rho_w \left[T \frac{\partial c_{s w}}{\partial T} + c_{s w} \right] + S_i \Phi \rho_i \left[T \frac{\partial c_{s i}}{\partial T} + c_{s i} \right] + (1 - \Phi) \rho_m \left[T \frac{\partial c_{s m}}{\partial T} + c_{s m} \right] - L \left[\rho_i S_i \frac{\partial \Phi}{\partial T} + \rho_i \Phi \frac{\partial S_i}{\partial T} + S_i \Phi \frac{\partial \rho_i}{\partial T} \right] \right) \frac{\partial T}{\partial t}$	case 1a	(6.38)
$\left(S_w \Phi \rho_w \left[T \frac{\partial c_{s w}}{\partial T} + c_{s w} \right] + S_i \Phi \rho_i \left[T \frac{\partial c_{s i}}{\partial T} + c_{s i} \right] + (1 - \Phi) \rho_m \left[T \frac{\partial c_{s m}}{\partial T} + c_{s m} \right] - L \rho_i \Phi \frac{\partial S_i}{\partial T} \right) \frac{\partial T}{\partial t}$	case 1	(7.9)
$\left(S_w \Phi \rho_w c_{s w} + S_i \Phi \rho_i c_{s i} + (1 - \Phi) \rho_m \left[T \frac{\partial c_{s m}}{\partial T} + c_{s m} \right] - L \rho_i \Phi \frac{\partial S_i}{\partial T} \right) \frac{\partial T}{\partial t}$	case 2	(7.13)
$\left(S_w \Phi \rho_w \left[T \frac{\partial c_{s w}}{\partial T} + c_{s w} \right] + S_i \Phi \rho_i \left[T \frac{\partial c_{s i}}{\partial T} + c_{s i} \right] + (1 - \Phi) \rho_m \left[T \frac{\partial c_{s m}}{\partial T} + c_{s m} \right] - L \left[\rho_i \Phi \frac{\partial S_i}{\partial T} + S_i \Phi \frac{\partial \rho_i}{\partial T} \right] \right) \frac{\partial T}{\partial t}$	case 3	(7.18)
$((1 - \Phi) \rho_m c_{s m} + \Phi \rho c_s) \frac{\partial T}{\partial t}$	COMSOL	(8.42)

Tab. 7.3 Heat flow equations (this work) – convective, conductive, and source terms (relates to Tab. 9.3, Tab. 9.4, and Tab. 9.5)

Convective term	Case	Equation
$+(\mathbf{v}_{a_w} S_w \rho_w \Phi) \cdot \nabla(c_{s_w} T_w) + (\mathbf{v}_{a_i} S_i \rho_i \Phi) \cdot \nabla(c_{s_i} T_i)$ $+\nabla \cdot (\mathbf{v}_{a_m} (1 - \Phi) c_{s_m} \rho_m T_m)$	general form	(5.31)
$+(\mathbf{v}_{a_w} S_w \rho_w \Phi) \cdot \nabla(c_{s_w} T)$	case 1a	(6.38)
$+(\mathbf{v}_{a_w} S_w \rho_w \Phi) \cdot \nabla(c_{s_w} T)$	case 1	(7.9)
$+(\mathbf{v}_{a_w} S_w \rho_w \Phi c_{s_w}) \cdot \nabla T$	case 2	(7.13)
$+(\mathbf{v}_{a_w} S_w \rho_w \Phi) \cdot \nabla(c_{s_w} T)$	case 3	(7.18)
$\rho c_s \mathbf{v} \cdot \nabla T$	COMSOL	(8.42)
Conductive term		
$+\nabla \cdot (\mathbf{J}_{h_w} + \mathbf{J}_{h_i} + \mathbf{J}_{h_m})$	general form	(5.31)
$-\nabla \cdot [(S_w \Phi \lambda_w + S_i \Phi \lambda_i + (1 - \Phi) \lambda_m + S_w \Phi c_{s_w} \rho_w \mathbf{D}_w) \cdot \nabla T]$	case 1a	(6.38)
$-\nabla \cdot [(S_w \Phi \lambda_w + S_i \Phi \lambda_i + (1 - \Phi) \lambda_m + S_w \Phi c_{s_w} \rho_w \mathbf{D}_w) \cdot \nabla T]$	case 1	(7.9)
$-\nabla \cdot [(S_w \Phi \lambda_w + S_i \Phi \lambda_i + (1 - \Phi) \lambda_m) \cdot \nabla T]$	case 2	(7.13)
$-\nabla \cdot [(S_w \Phi \lambda_w + S_i \Phi \lambda_i + (1 - \Phi) \lambda_m + S_w \Phi c_{s_w} \rho_w \mathbf{D}_w) \cdot \nabla T]$	case 3	(7.18)
$-\nabla \cdot [((1 - \Phi) \lambda_m + \Phi \lambda) \cdot \nabla T]$	COMSOL	(8.42)
Source term – direct heat source		
$r_{h_w} + r_{h_i} + r_{h_m}$	general form	(5.31)
r_{hQ}	case 1a	(6.38)
r_{hQ}	case 1	(7.9)
(-)	case 2	(7.13)
r_{hQ}	case 3	(7.18)
Q_0	COMSOL	(8.42)
Source term – inflowing heat		
$-c_{s_w} T_w \hat{r}_{f_w} - c_{s_i} T_i \hat{r}_{f_i}$	general form	(5.31)
$+c_{s_w} \rho_w q_w (T_w - \hat{T})$	case 1a	(6.38)
$+c_{s_w} \rho_w q_w (T_w - \hat{T})$	case 1	(7.9)
(-)	case 2	(7.13)
$+c_{s_w} \rho_w q_w (T_w - \hat{T})$	case 3	(7.18)
(-)	COMSOL	(8.42)
Source term – from storage term		
(-)	general form	(5.31)
$\left(S_w \Phi \rho_w T \frac{\partial c_{s_w}}{\partial p} + L \left[\rho_i S_i \frac{\partial \Phi}{\partial p} + \rho_i \Phi \frac{\partial S_i}{\partial p} \right] \right) \frac{\partial p}{\partial t}$	case 1a	(6.38)
$+S_w \Phi \rho_w T \frac{\partial c_{s_w}}{\partial p} \frac{\partial p}{\partial t}$	case 1	(7.9)
(-)	case 2	(7.13)
$+S_w \Phi \rho_w T \frac{\partial c_{s_w}}{\partial p} \frac{\partial p}{\partial t}$	case 3	(7.18)
(-)	COMSOL	(8.42)

8 Formulations from the literature

Presently, there exist already quite a number of approaches to groundwater flow under permafrost conditions that have eventually been cast into a numerical simulation code. Exemplarily, the work of /ZOT 12/, /BAR 16/, /SCH 17/, /FER 17/, and /GRE 18 as well as an own approach will be discussed more closely in the following, basically in chronological order.

8.1 Approaches in different versions of COMSOL Multiphysics

Several authors make use of the simulation code COMSOL Multiphysics which is a quite versatile tool that allows tackling the task of modelling groundwater flow under permafrost conditions. In the following, three examples of approaches by different authors are presented. Additionally, an own attempt to cover case 2 (see section 7.3) is described.

As COMSOL Multiphysics is continuously advanced, older models are obviously based on older versions of the code. While the balance equations appear to be the same for all models there are new features in the present version. Older models are therefore referred to /COM 16/ while the present version is referring to /COM 21/.

8.1.1 Approaches used in /COM 16/

COMSOL Multiphysics /COM 16/ contains pre-set formulations for groundwater flow and heat flow namely a balance equation for single-phase flow based on Darcy's law

$$\frac{\partial(\rho_w \Phi)}{\partial t} - \nabla \cdot \left(\rho_w \frac{\mathbf{k}}{\eta_w} \right) = \dot{m}_w \quad (8.1)$$

\dot{m}_w - production of water [kg/(s m³)]

as well as an alternative formulation for unsaturated flow based on Richards' equation (symbol explanation see section 8.1.3)

$$\rho_w \left(\frac{C_m}{\rho_w g} + S_w S \right) \frac{\partial p}{\partial t} + \nabla \cdot \left(-\rho_w \frac{k_{rw}(S_w)}{\eta_w} \mathbf{k} \cdot (\nabla p_w - \rho_w \mathbf{g}) \right) = \dot{m}_w \quad (8.2)$$

and the balance equation for heat flow in porous media

$$(\rho c_s)_b \frac{\partial T}{\partial t} + (\rho_w c_{s w} \mathbf{v}_{f w}) \cdot \nabla(T) - \nabla \cdot (\lambda_b \nabla T) = q_h \quad (8.3)$$

$(\rho c_s)_b$ - bulk parameter for the heat capacity [J/(s m³ K)]

$c_{s w}$ - specific heat capacity for water [J/(kg K)]

λ_b - bulk thermal conductivity [J/(s m K)]

where the bulk parameters (index b) are defined as

$$(\rho c_s)_b = (1 - \Phi) \rho_m c_{s m} + \Phi \rho c_s \quad (8.4)$$

ρ_m - matrix density [kg/m³]

$c_{s m}$ - specific heat capacity of the matrix [J/(kg K)]

ρ - fluid density [kg/m³]

c_s - specific heat capacity of the fluid [J/(kg K)]

and

$$\lambda_b = (1 - \Phi) \lambda_m + \Phi \lambda \quad (8.5)$$

λ_m - thermal conductivity of the matrix [J/(s m K)]

λ - thermal conductivity of the fluid [J/(s m K)]

Note that the second summand in (8.4) as well as in (8.5) is meant to represent the water properties.

The EOS' can either be chosen from the COMSOL material library from a quite large selection of different substances or they can be freely chosen to be either constants or user-defined functions where the latter can be dependent on primary variables or other functions. The same applies to the CEs except that there is no pre-set library for obvious reasons.

Unfortunately, the range of validity for the formulations in the material library is not obviously mentioned. Especially the lower temperature bound is not entirely clear. From comparison with relevant data (see appendix B) it appears, though, that the EOS' from the material library are valid only down to 0 °C. This has not been changed with the version discussed in the next subsection. As errors in the EOS are to be expected to grow increasingly when temperatures are falling below 0 °C, results from models using temperature-dependent EOS should therefore be looked at with particular care.

8.1.2 New features in /COM 21/

In comparison to the program version from 2016 the present version shows some relevant changes in the treatment of heat flow. While the balance equation remains basically the same referring to the matrix and a fluid (which may also be a gas), there is an additional section that accounts for phase changes of the fluid. Up to five phase change conditions can be defined here but only one change is described in the following. This particular section calculates bulk properties for the fluid in all phase states:

- fluid density according to

$$\rho = S_w \rho_w + S_i \rho_i \quad (8.6)$$

ρ - bulk parameter for the fluid density [kg/m³]

- fluid specific heat capacity c_s according to

$$c_s = \frac{S_w \rho_w c_{s w} - S_i \rho_i c_{s i}}{S_w \rho_w + S_i \rho_i} + L \frac{\partial \left(\frac{1}{2} \frac{S_w \rho_w - S_i \rho_i}{S_w \rho_w + S_i \rho_i} \right)}{\partial T} \quad (8.7)$$

c_s - bulk parameter for the fluid heat capacity [J/(kg K)]

- fluid thermal conductivity according to

$$\lambda = S_w \lambda_w + S_i \lambda_i \quad (8.8)$$

λ - bulk parameter for the fluid thermal conductivity [J/(s m K)]

The bulk expression $(\rho c_s)_b$ as given with (8.4) thus reads now

$$\begin{aligned} (\rho c_s)_b &= (1 - \Phi) \rho_m c_{s m} \\ &+ \Phi (S_w \rho_w + S_i \rho_i) \left[\frac{S_w \rho_w c_{s w} - S_i \rho_i c_{s i}}{S_w \rho_w + S_i \rho_i} + L \frac{\partial \left(\frac{1}{2} \frac{S_w \rho_w - S_i \rho_i}{S_w \rho_w + S_i \rho_i} \right)}{\partial T} \right] \end{aligned} \quad (8.9)$$

In the same way, the thermal conductivity for the water reads in the latest version

$$\lambda_b = (1 - \Phi) \lambda_m + \Phi (S_w \lambda_w + S_i \lambda_i) + \lambda_{disp} \quad (8.10)$$

λ_{disp} - tensor of thermal dispersion [J/(s m K)]

Note that the bulk thermal conductivity contains additionally the thermal dispersion term λ_{disp} . It is directly related to the expression $S_w \Phi c_{sw} \rho_w \mathbf{D}_w$ derived in section 5.3 for thermo-hydraulic dispersion in equation (6.38).

Finally, the condition

$$S_w + S_i = 1 \tag{ 8.11 }$$

is introduced. The saturations depend on the transition function $\theta_2(T)$ that is called “phase indicator for phase 2”²² and is formulated as a “smoothed heaviside function” /COM 16/. The Heaviside function is actually defined as being 0 for negative arguments and 1 for positive arguments. In the context discussed here, this function is obviously a function of temperature. However, in /COM 21/ it is modified in two ways. First, the point of transition from 0 to 1 is stretched to a finite length $\Delta T_{1 \rightarrow 2}$. Second, the reference point for the transition can be shifted to the temperature $T_{pc,1 \rightarrow 2}$ that is defined by $\theta_2(T_{pc,1 \rightarrow 2}) = 0.5$. The complement function $\theta_1(T)$ is then simply devised as the difference of $\theta_2(T)$ to 1.

$$\theta_1 + \theta_2 = 1 \tag{ 8.12 }$$

The actual formulation of the transition function is not easily found and could thus not be determined for this report. However, it is illustrated in /COM 21/ as depicted in Fig. 8.1.

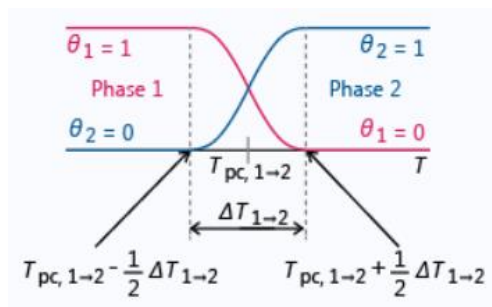


Fig. 8.1 Illustration of the transition functions $\theta_1(T)$ and $\theta_2(T)$; from /COM 21/

²² basically a soil freezing characteristic curve

8.1.3 Approach from /ZOT 12/

The work described in /ZOT 12/ points at the degradation of embankments below the Alaska Highway²³ by permafrost. Primarily the contribution of convective heat transport with the flowing groundwater was investigated. The authors chose to use Richards' equation for the groundwater flow:

$$\rho_w \left(\frac{C_m}{\rho_w g} + S_w S \right) \frac{\partial p}{\partial t} + \nabla \cdot \left(-\rho_w \frac{k_{rw}(\epsilon_p)}{\eta_w} \mathbf{k} \cdot (\nabla p_w - \rho_w \mathbf{g}) \right) = \rho_w q_w \quad (8.13)$$

- C_m - specific moisture capacity [1/m]
- S - storage coefficient, accounting for fluid and matrix compressibility [1/Pa]
- ϵ_p - volumetric weighting factor[-]²⁴

using a van Genuchten formulation to represent the soil water retention characteristic in the Richard's equation:

$$\theta = \left(\frac{1}{1 + (\alpha \Psi)^n} \right)^m \quad (8.14)$$

- θ - volumetric water content [m³/m³]
- Ψ - capillary pressure head [m]
- α, m, n - parameters according to /VGN 80/ [1/m], [-], [-]

There is no hint in the text whether porosity, density or viscosity are handled as variables or constants. While this seems to indicate that constants were used, there is a possibility, that density and viscosity formulations from the COMSOL material library have been used. In this case, density is a function of temperature but not pressure /BAR 16/.

Heat flow was apparently considered in the fluid only. Where bulk parameters (index b) are expected by COMSOL, just constant fluid parameters were used. However, thermal conductivity, heat capacity and hydraulic conductivity for frozen and unfrozen conditions

²³ located in the Yukon Territory, Canada

²⁴ It is assumed here, that the volumetric weighing factor is basically a phase saturation. This speculation could not be substantiated, though.

were discriminated as constants in the data table. It is thus not entirely clear, if and how heat flow in the ice has been taken into account.

$$(\rho c_s)_w \frac{\partial T}{\partial t} + (\rho_w c_{s w} \mathbf{v}_{f w}) \cdot \nabla(T) - \nabla \cdot (\lambda_b \nabla T) = q_h \quad (8.15)$$

λ_b - bulk thermal conductivity (COMSOL); here: $\lambda_b = \lambda_w$ [J/(s m K)]

q_h - heat source [J/(s m³)]

A pressure dependence of thermal parameters was not considered. The formulations for the relative permeability and the temperature-dependent saturation were unfortunately not disclosed.

8.1.4 Approach from /BAR 16/

With respect to safety analyses for Deep Geological Repositories, /BAR 16/ used the codes FRAC3DVS-OPG and COMSOL Multiphysics for paleo-climate modelling involving permafrost and glaciations. The code FRAC3DVS-OPG is skipped in the discussion here, since it was not able at that time to solve heat transport equation.

Other than the modelling of /ZOT 12/, the COMSOL-models from /BAR 16/ are based on the Darcy's Law interface that combines Darcy's law with the continuity equation:

$$\frac{\partial(\rho_w \Phi)}{\partial t} + \nabla \cdot \left(-\rho_w \frac{k_{r w} \mathbf{k}}{\eta_w} \cdot (\nabla p_w - \rho_w \mathbf{g}) \right) = \rho_w q_w \quad (8.16)$$

The relative permeability $k_{r w}$ has been added to the COMSOL formulation. It reduces the absolute permeability \mathbf{k} in a given temperature range between T_0 and T_1 by 6 orders of magnitude:

$$k_{r w} = 10^{-6} \quad \text{for } T < T_0$$

$$k_{r w} = 10^{(6 * \left[\frac{T - T_0}{T_1 - T_0} - 1 \right])} \quad \text{for } T_0 < T < T_1 \quad (8.17)$$

$$k_{r w} = 1 \quad \text{for } T_1 < T$$

The density ρ_w in equation (8.16) is a linear function of pressure and of temperature (down to -10 °C)

$$\rho_w = \rho_{ref} \left(1 + \beta_p (p - p_{ref}) + \beta_T (T - T_{ref}) \right) \quad (8.18)$$

- ρ_{ref} - reference density [kg/m³]
- p_{ref} - reference pressure [Pa]
- T_{ref} - reference temperature [K]
- β_p - compressibility of water; $\beta_p = 4.4 * 10^{-10}$ according to /BAR 16/ [1/Pa]
- β_T - thermal expansion coefficient; $\beta_T = 5 * 10^{-4}$ according to /BAR 16/ [1/K]

and the viscosity is approximated by an approach presented by /TAN 11/ that allows for calculation of the viscosity at temperatures below 0 °C²⁵:

$$\eta_w = 0.6612 (T - 229)^{-1.562} \quad (8.19)$$

The temperature is calculated by the “Heat Transfer in Porous Media”-interface as in /ZOT 12/:

$$(\rho c_s)_b \frac{\partial T}{\partial t} + (\rho_w c_{s_w} \mathbf{v}_{f_w}) \cdot \nabla T - \nabla \cdot (\lambda_b \nabla T) = q_h \quad (8.20)$$

but the bulk parameters are explained here by

$$(\rho c_s)_b = S_w \rho_w c_{s_w} + S_m \rho_m c_{s_m} \quad (8.21)$$

$$\lambda_b = S_w \lambda_w + S_m \lambda_m$$

While, apparently, standard formulations provided by COMSOL were used for water at temperatures above 0 °C, special formulations were introduced to describe the material properties of ice. It is not explicitly explained in the text, but it seems that a transition from water to ice properties at decreasing temperature was applied. The thermal conductivity of ice is fitted to data from /CRC 13/ by

$$\lambda_w = -0.0151 * T + 2.0785 \quad (8.22)$$

where temperature T is to be inserted in [°C] and the specific heat capacity of ice is approximated according to /MUR 05/

$$c_{s_w} = -2.0572 + 0.14644 * T + 0.06163 * T \left[-\left(\frac{T}{125.1} \right)^2 \right] \quad (8.23)$$

²⁵ Note that the units on the left-hand side and the right-hand side of approaches (8.19), as well as (8.22) and (8.23) later on, are not compatible

Additionally, a function H_{lh} is defined that is equivalent to a predefined saturation function $S_w(T)$ - a SFCC - with explicitly given temperatures T_0 and T_1 denoting the end values for ice $S_w(T_0) = 0$ and for water $S_w(T_1) = 1$ (see above). The function H_{lh} is called “a step function” in /BAR 16/ but from the graphs it can be concluded that the curve connecting $S_w(T_0)$ and $S_w(T_1)$ is actually smoothed. Using a third order polynomial for that purpose would result in

$$S_w = -\frac{2}{(T_1-T_0)^3}(T-T_0)^3 + \frac{3}{(T_1-T_0)^2}(T-T_0)^2 \quad \text{for } T_0 < T < T_1 \quad (8.24)$$

The derivative of H_{lh} or $S_w(T)$ with respect to temperature is denoted as $D(T)$ and interpreted as “a normalized pulse in the phase change temperature range T_0 and T_1 “. Multiplied with the latent heat L , it serves as a modification of the specific heat capacity of the water in equation (8.20)

$$c_{s w} \rightarrow c_{s w} + D(T)L \quad (8.25)$$

It is noted by /BAR 16/ that this modification affects not only the storage term but also the advection term which should not undergo such a modification. It is held, though, that the modification in the advection term is negligible “... because (of) the low porosity and low permeability of the rock...“. The balance equation (8.20) writes after insertion of the bulk parameters (8.21)

$$\begin{aligned} (S_w \rho_w c_{s w} + S_m \rho_m c_{s m}) \frac{\partial T}{\partial t} + (\rho_w c_{s w} \mathbf{v}_{f w}) \cdot \nabla T \\ - \nabla \cdot ((S_w \lambda_w + S_m \lambda_m) \nabla T) = q_h \end{aligned} \quad (8.26)$$

8.1.5 Approach from /SCH 17/

The flow equation used by /SCH 17/ reads

$$S_w S_s \frac{\partial h}{\partial t} - \nabla \cdot (k_{r w} \mathbf{K} \cdot \nabla h) + \Phi \frac{\rho_w - \rho_i}{\rho_w} \frac{\partial S_w}{\partial t} = 0 \quad (8.27)$$

S_s - specific storage coefficient [1/m]

where the specific storage coefficient S_s is defined as

$$S_s = \Phi \beta_p \rho g \quad (8.28)$$

β_p - compressibility of the water [1/Pa]

The dependencies of the density and viscosity on temperature and salinity are expressly neglected. The chosen formulation implies furthermore that also no influence of the hydraulic pressure is considered.

Several approaches for the relative permeability are presented in /SCH 17/:

from /MCK 07/

$$k_r = \min \left(\max \left(k_{r \text{ res}}, \frac{S_{w \text{ res}} - 1}{T_{\text{res}}} (T - 273.15) + 1 \right), 1 \right) \quad (8.29)$$

also from /MCK 07/

$$k_r = \max (10^{-S_i \Phi \Omega}, k_{r \text{ res}}) \quad (8.30)$$

Ω - empirical "impedance factor"²⁶

while the formulation used by /SCH 17/²⁷ is based on an approach from /HAN 04/

$$k_r = \min (\max (10^{-S_i \Omega}, k_{r \text{ res}}), 1) \quad (8.31)$$

and the one from /KLE 05/ on measurements

$$k_r = \frac{\left(\frac{S_w}{\Phi}\right)^4}{\left(1 + \sqrt{1 - \frac{S_w}{\Phi}}\right)^2} \quad (8.32)$$

Actually used was apparently formulation (8.31).

The related heat flow equation is given as

$$C_p \frac{\partial T}{\partial t} + (C_w \mathbf{v}_{f w}) \cdot \nabla T - \nabla \cdot (\lambda_a \nabla T) - L_f \frac{\partial \theta_w}{\partial t} = 0 \quad (8.33)$$

C_p - effective heat capacity of the rock/water/ice composite [J/(m³ K)]

C_w - heat capacity of the water [J/(m³ K)]

λ_a - effective thermal conductivity the rock/water/ice mixture [J/(s m³ K)]

²⁶ $\Omega=50$ was chosen for in the framework of the INTERFROST benchmark /GRE 18/.

²⁷ $\Omega=6$

- L_f - volume-specific latent heat of fusion [J/m³]
 θ_w - volume fraction of water-filled space of the bulk volume [-]

which is based on the following definitions:

$$C_p = (1 - \Phi)C_m + \Phi(S_w C_w + S_i C_i)$$

$$\lambda_a = \lambda_m^{(1-\Phi)} \lambda_w^{S_w \Phi} \lambda_i^{S_i \Phi} \quad (8.34)$$

$$L_f = \rho_w L$$

$$\theta_w = S_w \Phi$$

To fit the contribution of the latent heat into the pre-set formulation frame of COMSOL, the effective heat capacity C_p is combined with the respective term to an apparent heat capacity C_a :

$$C_a = C_p - L_f \frac{\partial \theta_w}{\partial T} \quad (8.35)$$

The relation between the water saturation and temperature is called “soil freezing curve” by /SCH 17/. Again, several approaches are presented by the authors:

from /MCK 07/

$$S_w = S_{w\ res} + (1 - S_{w\ res}) e^{-\left(\frac{T-273.15}{W}\right)^2} \quad (8.36)$$

$S_{w\ res}$ - residual water saturation [-]

W - fitting parameter [K]

from /BEN 09/

$$S_w = erf\left(2.1 + \frac{T - 273.15}{0.25}\right) + 1 \quad (8.37)$$

and used by /SCH 17/

$$S_w = S_{wres} \quad \text{for } T \leq -d$$

$$S_w = 0.5 + \frac{S_{wres}}{2} + (1 - S_{wres}) \left(0.9375 \left[\frac{T+d}{d} \right] - \frac{5}{8} \left[\frac{T+d}{d} \right]^3 + \frac{3}{16} \left[\frac{T+d}{d} \right]^5 \right) \quad (8.38)$$

$$\text{for } -d < T < 0$$

$$S_w = 1 \quad \text{for } T \geq 0$$

d - half of the transition interval²⁸ between freezing point and residual water saturation [K]

Interestingly, also a reference from /BUR 76/ with actual measurements of the soil freezing curve is cited (see also subsections 9.4.3 and 9.4.4).

8.1.6 Own attempt on case 2

While setting up a new model on case 2 is beyond the scope of this report, the theoretical background based on the possibilities of the COMSOL code in its latest version is developed here. It will be referenced further on as “own attempt”. For simulating groundwater flow, the Darcy’s Law interface is chosen that combines the generalized Darcy’s law with the continuity equation:

$$\frac{\partial(\rho_w \Phi)}{\partial t} + \nabla \cdot \left(-\rho_w \frac{k_{rw} \mathbf{k}}{\eta_w} \cdot (\nabla p_w - \rho_w \mathbf{g}) \right) = \dot{m}_w \quad (8.39)$$

Since density and porosity are assumed to be constant in case 2, equation (8.39) can be simplified to

$$-\rho_w \nabla \cdot \left(\frac{k_{rw} \mathbf{k}}{\eta_w} \cdot \nabla p_w \right) = \dot{m}_w \quad (8.40)$$

²⁸ The parameter d is actually given in /SCH 17/ as the whole transition interval. However, plotting the function and comparing it with a related figure given in /SCH 17/ showed that only half of the transition zone must be meant.

where the source term reads

$$\dot{m}_w = -\Phi(\rho_w - \rho_i) \frac{\partial S_w}{\partial T} \frac{\partial T}{\partial t} \quad (8.41)$$

This adaption has been rather easily derived as it concerns only migration of the water phase. While more finesse had been required for models based on /COM 16/ as the ice-phase was not taken into account in the older version, the elaborate workarounds are now replaced by a formulation in /COM 21/ that includes the required physics. Still unaltered compared to earlier versions, the following heat balance equation is used

$$(\rho c_s)_b \frac{\partial T}{\partial t} + (\rho c_s \mathbf{v}) \cdot \nabla T - \nabla \cdot (\lambda_b \nabla T) = q_h \quad (8.42)$$

The SFCC has been realized in COMSOL as a modified Heaviside-function that provides a smooth 2nd derivative and has a transition range of $\Delta T_{1 \rightarrow 2} = 1$ °C. The value of 0.5 is assigned to the temperature $T_{pc,1 \rightarrow 2} = -0.5$ °C. Relative permeability of the water is then assumed to follow another such function that is also defined by a transition range of $\Delta T_{1 \rightarrow 2} = 1$ °C but centered at $T_{pc,1 \rightarrow 2} = 0$ °C and only evaluated for negative temperatures. Since the function provides a value of 0.5 at 0°C, it is additionally multiplied by 2 so that the relative permeability of water equals 1 for $T \geq 0$ °C. Both functions are visualized in Fig. 9.1 and Fig. 9.3. While the curves provided by COMSOL have no direct relation to the physics in question, they appear to fit other approaches nevertheless quite nicely (cp. section 9.4.3).

8.2 Approach from /FER 17/

An addendum for the reference manual of the code DarcyTools /SVE 14/ relating to the extension that deals with the so-called “Ice Model” is presented in /FER 17/. Here, the flow equation is given as

$$\frac{\partial(\Phi \rho_w)}{\partial t} + \frac{\partial(S_i \Phi [\rho_i - \rho_w])}{\partial t} - \nabla \cdot \left(\frac{k_r \mathbf{k}}{\eta_w} \cdot (\nabla p_w - \rho_w \mathbf{g}) \rho_w \right) = \rho_w q_w \quad (8.43)$$

where the porosity is a linear function of pressure. Water and ice density as well as water viscosity are quadratic functions of temperature. The ice saturation S_i is given by an equivalent so-called “ Φ -function” being defined as

$$S_i = S_{i \max} \left[1 - e^{\left\{ -\left(\frac{\min(T, T_L) - T_L}{w} \right)^2 \right\}} \right] \quad (8.44)$$

- $S_{i \max}$ - maximum ice saturation [-]
 T_L - thawing temperature [°C]
 w - thawing interval²⁹ [°C]

Alternatively, a linearized form is also provided

$$S_i = S_{i \max} \left[\max \left\{ 0, \min \left(1, \frac{T_L - T}{2w} \right) \right\} \right] \quad (8.45)$$

Furthermore, the permeability tensor is apparently just the diagonal matrix. The components of the permeability matrix are reduced according to a factor α if $S_i < 0^\circ\text{C}$ holds. The factor α is thus essentially the relative permeability k_r which is why k_r appears in equation (8.43) instead of α . The relative permeability is defined by /FER 17/ as

$$k_r = \max(k_{r \min}, (1 - S_i)^a) \quad (8.46)$$

and means that a minimum of water flow is always allowed for, even under completely frozen conditions. No suggestions are made in /FER 17/, though, as to a quantification of the parameters $k_{r \min}$ and a .

The heat equation is given as

$$\begin{aligned} \rho_w \Phi \frac{\partial(c_{s_w} T)}{\partial t} + \frac{\partial((1 - \Phi)c_{s_m} T)}{\partial t} + \frac{\partial(\Phi \rho_i (c_{s_i} - c_{s_w}) S_i T)}{\partial t} - \rho_i \Phi L \frac{\partial S_i}{\partial t} \\ + \nabla \cdot (\rho_w \mathbf{v} c_{s_w} T) - \nabla \cdot (\rho_w \mathbf{v}) c_{s_w} T - \nabla \cdot (\lambda_b \nabla T) = q_h \end{aligned} \quad (8.47)$$

Note that equation (8.47) has apparently been subject to a substitution with the mass balance equation (8.43). While this has led in the present work to a term $\rho_w \mathbf{v} \cdot \nabla(c_{s_w} T)$ (see section 5.3.1), the substitution in /FER 17/ results in the equivalent two terms $+\nabla \cdot (\rho_w \mathbf{v} c_{s_w} T)$ and $-\nabla \cdot (\rho_w \mathbf{v}) c_{s_w} T$.

²⁹ range of temperatures over which the ice saturation varies with temperature.

Heat capacity and thermal conductivity of the pure phases are handled as quadratic functions of the temperature. The related parameters are not explained explicitly. The bulk thermal conductivity λ_b is either calculated by

$$\lambda_b = \left(\sqrt{\lambda_{ref}} + \left(\sqrt{\lambda_i} - \sqrt{\lambda_f} \right) S_i \Phi \right)^2 \quad (8.48)$$

or by the simpler formulation

$$\lambda_b = \lambda_{ref} + (\lambda_i - \lambda_f) S_i \Phi \quad (8.49)$$

8.3 Approach from /GRE 18/

Among the publications about permafrost hydrology, the work of /GRE 18/ is somewhat special as it summarizes the combined effort of a large international group of modelling teams using all in all thirteen different codes in the framework of the benchmark exercise INTERFROST. The underlying balance equations that are presented in /GRE 18/ were agreed upon by the group thus suggesting a sound basis for capturing the essential effects and phenomena of groundwater flow under permafrost conditions.

The flow equation is written in terms of a hydraulic conductivity and reads

$$(S_w \Phi \rho_w g \beta) \frac{\partial h}{\partial t} + \Phi \frac{\rho_w - \rho_i}{\rho_w} \frac{\partial S_w}{\partial t} - \nabla \cdot (\mathbf{K} \cdot (\nabla h + \nabla z)) = 0 \quad (8.50)$$

β - water³⁰ compressibility [1/Pa]

h - piezometric head [m]

\mathbf{K} - hydraulic conductivity [m/s]

where the hydraulic conductivity is given as

$$\mathbf{K} = k_r(T) \mathbf{k} \frac{\rho_w g}{\eta_w} \quad (8.51)$$

³⁰ Probably by mistake, the parameter β is labelled "Porous medium compressibility" among the parameters listed in /GRE 18/. Its meaning is clearly defined in the text.

and the hydraulic head as

$$h = \frac{p}{\rho_w g} \quad (8.52)$$

Thermal expansion is assumed to be negligible “in the ranges considered”. Water viscosity and ice density are assumed to be constants. Sources (and sinks) of water are explicitly excluded from consideration. Only compressibility of the water is considered. It is contradictory, though, that the density of water is given /GRE 18/ as a constant in the list of parameters.

Like in /FER 17/, there is a reduction of the hydraulic conductivity by what is called “impedance factor” $k_r(T)$ but which is again equivalent to a relative permeability.

$$k_r = \max(10^{-6}, 10^{-\Phi\Omega[1-S_w]}) \quad (8.53)$$

Ω - parameter; $\Omega=50$ [-]

Water saturation S_w is defined here as

$$S_w = (1 - S_{w\ res})e^{\left\{-\left[\frac{(T-273.15)}{W}\right]^2\right\}} + S_{w\ res} \quad (8.54)$$

$S_{w\ res}$ - residual water saturation [-]

W - temperature parameter; $W=0.5$ [K]

For further comparison with other mass balance equations (see section 9.2.2), piezometric head and hydraulic conductivity are replaced in formulation (8.50) by pressure and hydraulic permeability using equations (8.51) and (8.52). Equation (8.50) gets also multiplied by the water density ρ_w reaching finally the form

$$(S_w\Phi\ \rho_w\ \beta)\frac{\partial p}{\partial t} + \Phi(\rho_w - \rho_i)\frac{\partial S_w}{\partial t} - \nabla \cdot \left(\rho_w \mathbf{k} \frac{k_r(T)}{\eta_w} \cdot (\nabla p + \rho_w g \nabla z) \right) = 0 \quad (8.55)$$

The heat flow equation is given as follows

$$\left[S_w\Phi\rho_w c_{s\ w} + S_i\Phi\rho_i c_{s\ i} + (1 - \Phi)\rho_m c_{s\ m} - L\rho_i\Phi\frac{\partial S_i}{\partial T} \right] \frac{\partial T}{\partial t} \quad (8.56)$$

$$-\nabla \cdot [(\rho_w c_{s\ w} \mathbf{K} T) \cdot \nabla h + (\rho_w c_{s\ w} \mathbf{K} T) \cdot \nabla z] - \nabla \cdot (\lambda_b \nabla T) = 0$$

where the bulk thermal conductivity λ_b is explained by

$$\lambda_b = \Phi S_w \lambda_w + \Phi S_i \lambda_i + (1 - \Phi)\lambda_m \quad (8.57)$$

Thermal conductivity and specific heat for the pure phases are taken to be constants.

9 Comparison of approaches

9.1 Introductory remark

The numerical models simulating groundwater and heat flow under permafrost conditions are controlled

- by the choice of processes that are accounted for in the balance equations,
- by the constitutive equations (CEs) that cover the properties of the porous matrix, and
- by the equations of state (EOS) that describe the state variables for the pure substances.

These three categories will be discussed in the following with reference to

- the work presented in this report, i.e. the general case represented by the reified balance equations (RBE, section 6.5),
- the seven numerical models shortly described in section 8, and
- a specific suggestion concerning freezing phenomena in soils from /AUK 16/ as described in detail in appendix C.

9.2 Balance equations

9.2.1 General observations

The balance equations for groundwater flow and for heat flow that are compiled in section 8 are given in quite different forms. As a consequence, it is often difficult to identify all processes that are taken into account if they are not explained in detail. By means of comparison of equations and in some cases backtracking the derivation, differences in the set of applied assumptions can be pointed out.

In principle, two types of balance equations for groundwater flow have been found. The work of /ZOT 12/ is based on unsaturated flow in the form of the Richards equation. All others rather use a modified form of saturated single-phase flow equation. Darcy's law has been incorporated in its original form based on hydraulic conductivity, but also in the more generalized form using hydraulic permeability. This formal difference does not lead

to differences in the underlying physical models, though. As a general rule, not all conceivable effects were considered in all formulations.

In terms of the underlying conceptual models, the formulations for heat flow were more similar among each other. There are differences in the handling of the three-phase porous medium, though. Where existing formulations for heat flow in porous media were used, only two materials, namely water and solid matrix, are often accounted for. However, this problem can be circumvented by formulating appropriate bulk parameters for the thermal properties.

9.2.2 Groundwater flow equations

The different formulations of the mass balance equation are compiled in Tab. 9.1. To facilitate a comparison, the table is arranged by the type of terms that come with the general balance equation (5.12). As a convention, source terms are assigned to the right-hand side of the balance equation.

Storage term

The storage term used in /ZOT 12/ is quite different from all other formulations since it is related to the Richards equation. Finding a relation to the other storage terms is therefore rather difficult and thus not pursued to greater depth here.

In principle, up to four mechanisms are described by the different storage terms:

- compressibility of the water,
- compressibility of ice,
- compressibility of the matrix, and
- storage by phase changes where the phases have different densities.

These properties and effects can be identified by the time derivative of the density of water ρ_w , the density of ice ρ_i the porosity Φ , and/or the water saturation S_w (or alternatively the volumetric fraction of ice S_i)³¹, respectively. Three categories of storage terms

³¹ It has to be kept in mind, though, that using the ice saturation instead of the water saturation in the time derivative leads to a change of sign.

can be defined according to this observation. The first category includes the terms from /ZOT 12/, /BAR 16/, /COM 16/ and /COM 21/ where only compressibility of any kind is addressed. The second category concerns just the term from the own attempt (section 8.1.6), where only the phase change is taken into account while the terms from /SCH 17/, /FER 17/, /GRE 18/ as well as the RBE from this work (section 6.5) account for both mechanisms.

The formulations based on /COM 16/ or /COM 21/ as well as those in /FER 17/ agree in that the storage term consists of the time derivative of the product of porosity and water density³². The selection of effects that drive these changes is decided by the choice of CEs and EOS. They are discussed in sections 7 and 9.4.

Also, the storage terms given by /SCH 17/ and /GRE 18/ are identical after replacing the storage coefficient in the formulation from /SCH 17/ with the definition (8.28). They are formulated in terms of a derivative of the hydraulic head with respect to time, though. Note that by using the coefficient for the water compressibility β in the storage terms given by /SCH 17/ and /GRE 18/, a certain simplification of the state equation for water density has already been adopted.

The storage terms from /SCH 17/ and /GRE 18/ can be derived from the storage term from the RBE by neglecting matrix compressibility as well as variations of the ice density and allowing the water density to respond only to changes in the hydraulic pressure. Note that introduction of the coefficient of water compressibility β required dividing the mass balance equation by the water density. The subsequent cancelling of the density in the advective term while still being subject to a differential operator is inconsistent even if it might be justified by allowing only negligible variations of the density.

The storage term in the RBE derived in this work comprises obviously all four types of storage listed above. Less obvious is, however, that they stem from the general form $\partial/\partial t (\Phi[S_w \rho_w + S_i \rho_i])$ in equation (6.5). Interestingly, the same starting point leads also to the terms in the formulation from /FER 17/.

³² The density in /COM 16/ is also assigned to the water density as there is no pre-set option to include another water phase.

Tab. 9.1 Groundwater flow equations from section 8

Groundwater flow equation			Source	Equation
Storage term / time derivatives ³³	Advective term	Source term		
$\frac{\partial(\Phi\rho)}{\partial t}$	$-\nabla \cdot \left(\rho \frac{\mathbf{k}}{\eta} \cdot (\nabla p + \rho \mathbf{g}) \right)^{34}$	Q_m	/COM 16/ /COM 21/	(8.1)
$\rho_w \left(\frac{C_m}{\rho_w g} + S_w S \right) \frac{\partial p}{\partial t}$	$+\nabla \cdot \left(-\rho_w \frac{k_{rw}(\epsilon_p)}{\eta_w} \mathbf{k} \cdot (\nabla p_w - \rho_w \mathbf{g}) \right)$	$\rho_w q_w$	/ZOT 12/	(8.13)
$\frac{\partial(\rho_w \Phi)}{\partial t}$	$+\nabla \cdot \left(-\rho_w \frac{k_{rw} \mathbf{k}}{\eta_w} \cdot (\nabla p_w - \rho_w \mathbf{g}) \right)$	$\rho_w q_w$	/BAR 16/	(8.16)
$S_w S_s \frac{\partial h}{\partial t} + \Phi \frac{\rho_w - \rho_i}{\rho_w} \frac{\partial S_w}{\partial t}$	$-\nabla \cdot (k_{rw} \mathbf{K} \cdot \nabla h)$	(-)	/SCH 17/	(8.27)
$\Phi(\rho_w - \rho_i) \frac{\partial S_w}{\partial t}$	$-\rho_w \nabla \cdot \left(\frac{k_{rw} \mathbf{k}}{\eta_w} \cdot \nabla p_w \right)$	(-)	own attempt	(8.39)
$\frac{\partial(\Phi \rho_w)}{\partial t} + \frac{\partial(S_i \Phi [\rho_i - \rho_w])}{\partial t}$	$-\nabla \cdot \left(\rho_w \frac{k_{rw} \mathbf{k}}{\eta_w} \cdot (\nabla p_w - \rho_w \mathbf{g}) \right)$	$\rho_w q_w$	/FER 17/	(8.43)
$(S_w \Phi \rho_w \mathbf{g} \beta) \frac{\partial h}{\partial t} + \Phi \frac{\rho_w - \rho_i}{\rho_w} \frac{\partial S_w}{\partial t}$	$-\nabla \cdot (\mathbf{K} \cdot (\nabla h + \nabla z))$	(-)	/GRE 18/	(8.50)
$(S_i \rho_i + S_w \rho_w) \frac{\partial \Phi}{\partial t} + S_w \Phi \frac{\partial \rho_w}{\partial t} + S_i \Phi \frac{\partial \rho_i}{\partial t} + \Phi(\rho_w - \rho_i) \frac{\partial S_w}{\partial t}$	$-\nabla \cdot \left(\rho_w \frac{k_{rw} \mathbf{k}}{\eta_w} \cdot (\nabla p_w - \rho_w \mathbf{g}) \right)$	$\rho_w q_w$	RBE	(6.33)

8

³³ Note that the storage term in Tab. 9.1 is presented as derivatives with respect to time while it is given with respect to the primary variables p_w and T in Tab. 7.1.

³⁴ The vector \mathbf{g} of gravitational acceleration is defined as vector \mathbf{g} with an opposite sign.

Advective term

In most formulations, the advective term is based one way or the other on Darcy's law where hydraulic conductivity/permeability is subject to a saturation-dependent reduction for subzero temperatures. Only in /ZOT 12/, the reduction is a function of a "volumetric weighing factor" that is formally handled similar to a saturation. In /SCH 17/, density and viscosity are treated as constants allowing for a simple formulation in terms of hydraulic conductivity and piezometric heads. A formulation similar to that of /SCH 17/ is given by /GRE 18/. But here the compressibility of water is taken into account which calls for the additional buoyancy term.

Where the pressure-dependence of the density is neglected as in case 2 (section 7.3), the advection term can be simplified by removing the density from under the gradient operator (see Tab. 7.1). Note that equation (8.50) from /GRE 18/ has been transformed to the equivalent pressure-dependent formulation (8.55) in section 8.3. As mentioned above, dividing by the density has been executed to introduce the compressibility coefficient β despite the density being a variable and subject to a differential operator. While this is probably of little consequence like neglecting its variability in the first place, it is nevertheless inconsistent.

Non-advective term

Generally, no non-advective term was found in the investigated mass balance equations.

Source term

A source term accounting for fluid mass entering or leaving the domain was included in all formulations except in /SCH 17/, /GRE 18/, and the own attempt where it was explicitly excluded.

Key results from the comparison of the mass balance equations

- Storage term
 - The highest diversity of approaches from the literature for the mass balance equation can be found in the storage term.

- The storage terms in the selection of models investigated here may comprise compressibility of water, ice, and/or matrix as well as the volumetric changes of different densities of water and ice during freezing or melting. All four properties/effects have been found by derivation of the mass balance equation in section 5.
 - In the terms from /BAR 16/, /SCH 17/, /GRE 18/, and the own attempt some simplifications have apparently been applied one way or the other.
 - The terms from /FER 17/ and from the present work show the highest degree of generality.
- Advective term
 - Darcy's flow law is at the core of all advective terms.
 - All formulations include a reduction of hydraulic permeability/conductivity due to saturation or a related quantity.
 - Not all formulations allow for density-dependent flow.
 - Non-advective term
 - No non-advective term has been found among the surveyed literature.
 - Source term
 - Where considered at all, a simple mass sink/source term for water has been implemented.

9.2.3 Heat flow equations

Analogously to the mass balance equations discussed in the previous subsection, the heat energy balance equations investigated here are compiled in tables. However, they are split up into Tab. 9.2 to Tab. 9.5.

according to the type of terms that come with the general balance equation (5.31). Again, source terms are assigned to the right-hand side.

Storage term

At the first glance, the formulations for the storage term in Tab. 9.2 look quite diverse. This includes the first four entries, which are all based on pre-set formulations provided by the COMSOL code /COM 16/, /COM 21/. The formulation from /ZOT 12/ looks like a

quite general form of the storage term but is restricted exclusively to water properties. If a formulation for the water density from the COMSOL material library has been used, this would have introduced a dependence on temperature. This does unfortunately not become clear from the reference, though.

The storage terms from /BAR 16/, /SCH 17/, and /COM 16/ relate to the fluid phase, that is water, as well as the solid phase constituting the matrix. Other than the formulation in /COM 21/, /COM 16/ does not address ice as a separate phase explicitly. The formulations from /BAR 16/ and /SCH 17/ thus include workarounds in terms of user-defined modifications of parameters and user-defined functions to acknowledge ice properties as well. In /BAR 16/, the properties of ice are thus included as a user-defined extension of the properties of water for temperatures below 0 °C. In /SCH 17/, the effective heat capacity of the rock/water/ice composite C_p is modified according to (8.34) to include all three phases. In the own attempt, these workarounds could be avoided by using /COM 21/.

Tab. 9.2 Heat flow equation – storage terms (relates to Tab. 7.2)

Storage term	Source	Equation
$(\rho c_s)_b \frac{\partial T}{\partial t}$	/COM 16/ /COM 21/	(8.3)
$(\rho c_s)_w \frac{\partial T}{\partial t}$	/ZOT 12/	(8.15)
$(S_w \rho_w c_{s_w} + S_m \rho_m c_{s_m}) \frac{\partial T}{\partial t}$	/BAR 16/	(8.26)
$C_p \frac{\partial T}{\partial t} - L_f \frac{\partial S_w}{\partial t}$	/SCH 17/	(8.33)
$(\rho c_s)_b \frac{\partial T}{\partial t}$	own attempt	(8.42)
$\rho_w \Phi \frac{\partial(c_{s_w} T)}{\partial t} + \frac{\partial((1 - \Phi)c_{s_m} T)}{\partial t} + \frac{\partial(\Phi \rho_i (c_{s_i} - c_{s_w}) S_i T)}{\partial t} - \rho_i \Phi L \frac{\partial S_i}{\partial t}$	/FER 17/	(8.47)
$\left[S_w \Phi \rho_w c_{s_w} + S_i \Phi \rho_i c_{s_i} + (1 - \Phi) \rho_m c_{s_m} - L \rho_i \Phi \frac{\partial S_i}{\partial T} \right] \frac{\partial T}{\partial t}$	/GRE 18/	(8.56)
$S_w \Phi \rho_w \frac{\partial(c_{s_w} T)}{\partial t} + S_i \Phi \rho_i \frac{\partial(c_{s_i} T)}{\partial t} + (1 - \Phi) \rho_m \frac{\partial(c_{s_m} T)}{\partial t} - L \frac{\partial(\rho_i S_i \Phi)}{\partial t}$	RBE	(6.34)9.1

By contrast, the remaining three entries appear to be closer related to each other. Contributions from water, ice and the solid matrix to the storage term as well as from the latent heat from phase changes are clearly identifiable in /FER 17/, /GRE 18/ and in the present work. There are some differences, among them, though. The heat capacities as well as the ice density are assumed to be constant in the formulation from /GRE 18/, allowing for removing these quantities from the time derivative and treating them as mere factors.

The term accounting for the latent heat is slightly more general in the formulation of /FER 17/ than in /GRE 18/ in that it leaves open whether the ice saturation might be dependent on other quantities besides temperature. The porosity, however, is apparently treated as a constant in both formulations which is in contradiction to the definition in /FER 17/ stating that the porosity is a function of the hydraulic pressure. Indeed, the derivation in this work indicates that also a time dependence of the ice density and the porosity may have also to be accounted for.

The stringent derivation of the heat flow equation resulting in the RBE has revealed that including groundwater sources is on the one hand not trivial but allows on the other hand for certain simplifications without losing validity.

They are also included in the approach by /FER 17/, but here they are differently formulated. Generally, the water properties are assigned here to the whole pore space. But where ice is present, the difference to the ice properties is added according to the ice content S_i . Therefore, the first storage term $\rho_w \Phi \partial(c_{s_w} T) / \partial t$ refers only to water while the third term accounts for the possible difference to the ice properties. Temperature-dependence of saturation and water density introduce non-linearities in this term.

A term acknowledging the contribution of latent heat in case of phase changes is included in all formulations but the one from /ZOT 12/. Again, particular care is required when using /COM 16/ since the ice phase and therefore the latent heat due to phase changes is not accounted for in the pre-set formulations. In /BAR 16/, a user-defined function representing gain or loss of energy is added to the specific heat of water (cp. (8.25)). Further modification of the specific heat according to (8.35) includes also the contribution of the latent heat.

Convective term

The convective term contains basically the same quantities in all eight formulations (see Tab. 9.3) but they are formulated in different ways. Only the RBE as well as /COM 21/ include additionally heat convection by hydraulic dispersion that is formally attributed to the conductive term.

In the term from /FER 17/ and from /GRE 18/ all quantities are subject to the gradient operator $\nabla \cdot [\rho_w c_{s w} \mathbf{v} T]$. Derivation of the heat energy balance in subsection 5.3.1 shows that the gradient over all four quantities is an early form of the convective term (see (5.21)) before it gets simplified by inserting the mass balance equation. Simplification with the mass balance equation reduces this expression to $\rho_w \mathbf{v} \cdot \nabla [c_{s w} T]$ but also introduces an additional source term (see (5.23)). The same simplification has apparently also been done in /FER 17/, resulting in a different form of the convective term and the source term, though.

Tab. 9.3 Heat flow equation – convective terms (relates to Tab. 7.3)

Convective term	Source	Equation
$\rho c_s \mathbf{v} \cdot \nabla T$	/COM 16/ /COM 21/	(8.3)
$+\rho_w c_{s w} \mathbf{v}_{f w} \cdot \nabla T$	/ZOT 12/	(8.15)
$+\rho_w c_{s w} \mathbf{v}_{f w} \cdot \nabla T$	/BAR 16/	(8.26)
$C_w \mathbf{v}_{f w} \cdot \nabla T$	/SCH 17/	(8.33)
$\rho c_{s w} \mathbf{v}_{f w} \cdot \nabla T$	own attempt	(8.42)
$+\nabla \cdot (\rho_w \mathbf{v} c_{s w} T)$	/FER 17/	(8.47)
$-\nabla \cdot [\rho_w c_{s w} \mathbf{K} T \cdot \nabla h + \rho_w c_{s w} \mathbf{K} T \cdot \nabla z]$	/GRE 18/	(8.56)
$+(\mathbf{v}_{a w} S_w \rho_w \Phi) \cdot \nabla (c_{s w} T)$	RBE	(6.38)

For the balance equation based on /COM 21/, the specific heat has obviously been assumed to be constant, allowing for removing it from under the gradient operator and lining it up with the other two factors $\rho_w c_{s w} \mathbf{v}_{f w} \cdot \nabla T$. It thus appears to be somewhat inconsistent to assign a function to this quantity as in /BAR 16/ where the specific heat is directly temperature-dependent function or in /SCH 17/ where it is introduced as a bulk parameter that depends on the saturation and therefore on temperature again. It might only be acceptable if variations in the heat capacity are small.

Conductive term

Up to four mechanisms for conductive heat flow can be found in the selection of models investigated here as shown in Tab. 9.4. They include heat conduction by water, by ice and by the matrix as well as, formally, spreading of heat by hydraulic dispersion. These can either be expressed separately as in the stringent derivation of the RBE or in the general form $-\nabla \cdot (\lambda_b \nabla T)$ as in the formulation of /COM 21/. The latter expression clarifies that the basic difference between the approaches lies in the bulk thermal conductivity λ_b that has indeed been defined quite differently:

- In principle, the conductive term in the formulation provided by /COM 21/ is a general formulation that includes all conceivable influences on the bulk thermal conductivity λ_b .
- While in /ZOT 12/ only one single conductivity value is included for the simulation, /BAR 16/ takes also the solid phase into account. In both cases, the transition from water to ice, and vice versa, is not clearly defined in terms of the state variables.
- All other formulations include the thermal conductivity for all three phases separately. However,
 - in /SCH 17/ the effective/bulk thermal conductivity is defined as a weighted geometric mean from the thermal conductivities of rock, water and ice without further justification.
 - a reason for the weighting methods presented by /FER 17/ of the pure phase variables, in particular the mean square-root weighting (see equation (8.48)) is also not given.
 - the bulk thermal conductivity presented in /GRE 18/ is a volumetric weighted mean. The same mean was arrived at in this work which leads naturally also to the referring implementation in the own attempt.

Tab. 9.4 Heat flow equation – conductive terms ((relates to Tab. 7.3)

Conductive term	Source	Equation
$-\nabla \cdot (\lambda_b \nabla T)$	/COM 16/	(8.3)
$-\nabla \cdot (\lambda_b \nabla T)$	/COM 21/	(8.10)
$-\nabla \cdot (\lambda_w \nabla T)$	/ZOT 12/	(8.15)
$-\nabla \cdot ((S_w \lambda_w + S_m \lambda_m) \nabla T)$	/BAR 16/	(8.26)
$-\nabla \cdot (\lambda_m^{(1-\Phi)} \lambda_w^{S_w \Phi} \lambda_i^{S_i \Phi} \nabla T)$	/SCH 17/	(8.33)
$-\nabla \cdot [((1 - \Phi) \lambda_m + \Phi(S_w \lambda_w + S_i \lambda_i)) \nabla T]$	own attempt	(8.42)
$-\nabla \cdot \left(\left(\sqrt{\lambda_{ref}} + \left(\sqrt{\lambda_i} - \sqrt{\lambda_f} \right) S_i \Phi \right)^2 \nabla T \right)$	/FER 17/	(8.47)
$-\nabla \cdot (\lambda_{ref} + (\lambda_i - \lambda_f) S_i \Phi \nabla T)$		
$-\nabla \cdot [(\Phi S_w \lambda_w + \Phi S_i \lambda_i + (1 - \Phi) \lambda_m) \nabla T]$	/GRE 18/	(8.56)
$-\nabla \cdot [(S_w \Phi \lambda_w + S_w \Phi c_{sw} \rho_w \mathbf{D}_w + S_i \Phi \lambda_i + (1 - \Phi) \lambda_m) \nabla T]$	RBE	(6.38)

Source term

The source terms considered here are compiled in Tab. 9.5. The only formulations that do entirely without source terms stem from /SCH 17/ and /GRE 18/. Because of following the INTERFROST benchmark specifications, the same applies to the own attempt. All others include at least a heat source from outside the solution domain. Heat energy that is tied to an inflow of groundwater is additionally included in /FER 17/ and the RBE.

Tab. 9.5 Heat flow equation – source terms (relates to Tab. 7.3)

Source term	Source	Equation
Q_0	/COM 16/ /COM 21/	(8.3)
$+q_h$	/ZOT 12/	(8.15)
$+q_h$	/BAR 16/	(8.26)
(-)	/SCH 17/	(8.33)
(-)	own attempt	(8.42)
$+\nabla \cdot (\rho_w \mathbf{v}) c_{sw} T + q_h$	/FER 17/	(8.47)
(-)	/GRE 18/	(8.56)
$r_{hQ} + c_{sw} \rho_w q_w (T - \hat{T})$	RBE	(6.38)

Key results from the comparison of heat balance equations

- Storage term
 - In the models investigated here, heat may be stored by water, ice and the solid matrix. An additional contributor is the latent heat from phase changes.
 - All four mechanisms are accounted for in the approaches from /FER 17/, /GRE 18/ and in the RBE.
 - The storage terms based on the COMSOL formulations are quite diverse since the older version of this simulator does not account for the ice phase. Different workarounds have been formulated in /BAR 16/ and /SCH 17/ when using the older version while this problem has been resolved in /COM 21/.
 - Some of the EOS are treated differently, either as constants or as functions.
 - A minor inconsistency has been detected concerning the porosity in the formulations in /FER 17/. It is introduced as a function of the hydraulic pressure but later apparently treated as a constant.

- Convective term
 - Based on fluid flow, the convective term contains essentially the same quantities in all eight formulations.
 - Only the RBE as well as /COM 21/ include additionally heat convection by thermo-hydraulic dispersion. For formal reasons, this contribution is assigned to the conductive term.
 - In the heat flow equation in /COM 21/, the specific heat has obviously been assumed to be constant without saying so. This led to a probably involuntary inconsistency in the formulation from /BAR 16/ where the specific heat is treated as a temperature-dependent function or in /SCH 17/ where it is introduced as a bulk parameter that depends on the saturation and therefore on temperature again.
 - Simplifications in the EOS in /GRE 18/ have induced simplifications in the convective term as well.

- Conductive term
 - Heat conduction by water, by ice and by the matrix has been identified as well as, formally, spreading of heat by thermo-hydraulic dispersion.
 - Apart from the contribution from thermo-hydraulic dispersion, the general form of the conductive term is the same in all eight formulations.

- The basic difference lies in the bulk thermal conductivity λ_b that has been defined quite differently in different sources.
 - Not all three phases are considered in all approaches.
 - The bulk thermal conductivity of water, ice and matrix, where applicable, is calculated either by geometric averaging or by mean square-root weighting or as a volumetric weighted mean. While the first two methods are not justified in the literature, the latter is confirmed by the stringent derivation of the RBE.
- Source term
 - Some formulations do entirely without source terms. All others include at least a heat source from outside the solution domain.
 - Heat energy that is tied to an inflow of groundwater is only included in /FER 17/ and the RBE.

9.3 Equations of state

Four state variables control groundwater and heat flow under permafrost conditions. These are density and viscosity, where applicable, as well as thermal conductivity and specific heat. From Tab. 9.6 it becomes clear that these state variables are formally treated quite differently in different approaches for the balance equations, ranging from constant values over abstract polynomials to analytical functions that are fitted to measured data. The wide variety of combinations shows that there is no set of relevant effects generally agreed upon. Depending on the purpose of a specific model, a specific selection of effects may be relevant. Relevance for specific problems seems not to be the main motivation for any of the selections found in the literature, though, as such motivations are nowhere stated.

Except for the implementations by /BAR 16/ and the present work, rather little effort at choosing realistic and appropriate formulations for the related equations of state (EOS) is discernible in the approaches discussed here. This is quite unfortunate as the true EOS in question are invariably the same for any foreseeable problem. Moreover, where simplifications of the EOS are introduced, the range of validity should be declared but such a declaration is generally missing.

Tab. 9.6 State variables as used in the investigated approaches ¹⁾

Index	Density ρ	Viscosity η	Thermal conduct. λ	Specific heat c_s	Source	Eq.s
w	II)	II)	II)	II)	/COM 21/	(8.2)
i	II)	-	II)	II)		(8.3)
m	II)	-	II)	II)		
w	unclear	unclear	const.	const.	/ZOT 12/	(8.13)
i	-	-	const.	const.		(8.15)
m	const.	-	-	-		
w	$\rho(p, T)^{III)}$ -10<T<+90 0<p<0.001	$\eta(T)^{IIIa)}$ -20<T<280	$\lambda(T)^{IIIa)}$ -20<T<0	$c_s(T)^{IIIa)}$ -5<T<0 [°C]	/BAR 16/	(8.16)
i	-	-	$\lambda(T)^{IIIa)}$ -100<T<0	$c_s(T)^{IIIa)}$ -100<T<0 [°C]		(8.26)
m	const.	-	-	-		
w	const.	const.	const. ^{IV)}	const. ^{IV)}	/SCH 17/	(8.27)
i	const.	-	const. ^{IV)}	const. ^{IV)}		(8.33)
m	const.	-	const. ^{IV)}	const. ^{IV)}		
w	const.	$\eta(T)$ -20<T<+20 [°C]	const.	const.	own attempt	(8.39)
i	const.	-	const.	const.		(8.42)
m	const.	-	const.	const.		
w	$\rho(p, T)^V)$	$\eta(T)^V)$	$\lambda(T)^V)$	$c_s(T)^V)$	/FER 17/	(8.43)
i	$\rho(T)^V)$	-	$\lambda(T)^V)$	$c_s(T)^V)$		(8.47)
m	const.	-	$\lambda(T)^V)$	$c_s(T)^V)$		
w	$\rho(p)^{III)}$	const.	const.	const.	/GRE 18/	(8.50)
i	const.	-	const.	const.		(8.56)
m	const.	-	const.	const.		
w	$\rho(p_w, T)^{IIIa)}$ -40<T<200 0.1<p<5	$\eta(T)^{IIIa)}$ -20<T<200	$\lambda(T)^{IIIa)}$ -20<T<200	$c_s(p_w, T)^{IIIa)}$ -20<T<200 0.1<p<5	RBE	(6.33)
i	$\rho(T)^{IIIa)}$ -40<T<0	-	$\lambda(T)^{IIIa)}$ 20<T<0	$c_s(T)^{IIIa)}$ -20<T<0		(6.38)
m	const.	-	$\lambda(T)$ -20<T<200	$c_s(T)^{IIIa)}$ -20<T<200		

I) w: water; i: ice; m: matrix; temperatures in [°C]; pressures in [MPa]

II) either user-defined or from the material library; validity of formulations from the material library: $T \geq 0$ °C

III) linear function

IIIa) analytic function fitted to data

IV) unclear

V) general quadratic function

9.4 Constitutive equations

9.4.1 General observations

Constitutive equations (CEs) concern basically material properties, in particular porosity, water/ice saturation and relative permeability for the water. The balance equations discussed in section 9.2 are therefore more or less derived on general principles, leaving the task of choosing appropriate material parameters to the user. A sound basis for this choice in a concrete case is presently very hard to come by without the results of specific measurements.

Against this background, the publication of /AUK 16/ appears to be particularly helpful as it presents an analytical approximation to the thermal soil properties under freezing conditions, based on fractionated grain size distributions. This work is described shortly in appendix C and is included in the following comparison.

Where there is one of the scarce concrete applications, the (supposedly) realistic data can be matched by the more abstract constitutive equations. Such a comparison has been performed for the ice saturation in section 9.4.3 and the relative permeability of water in section 9.4.4, revealing principal differences in the chosen CEs.

9.4.2 Porosity

The porosity can change due to forces on the porous matrix which may be macroscopic mechanical forces from outside the domain in question or forces from inside the pore space like hydraulic pressure. In those cases, the pressure must be related to the strength of the porous matrix. A phenomenon particularly difficult to describe in a mathematical model is that of frost heave as it relates to a change in porosity that influences also the effect of freezing on the groundwater flow. It will not be discussed here any further. Changes of the porosity are not considered in the formulations of /ZOT 12/, /BAR 16/, /SCH 17/, the own attempt, and /GRE 18/. Only /FER 17/ and the RBE include the theoretical basis for a pressure-dependent porosity in the balance equations.

9.4.3 Water/ice saturation

The approaches for the SFCC as compiled in Tab. 9.7 are rather different among each other. As a general rule there are two variants of these transition functions. The first variant is characterized by changes in saturation from full ice saturation ($S_i = 1$) to full water saturation ($S_i = 0$) /COM 21/, /BAR 16/, the own attempt, and /FER 17/. The other variant allows for acknowledging a residual water saturation S_{wres} for temperatures falling below the temperatures in the transition zone /MCK 07/, /SCH 17/, and /GRE 18/.

An exception from these two variants is constituted by the approaches from /BEN 09/ and /AUK 16/ as the resulting curves converge towards $S_i = 1$ but not within a given transition interval. The approach from /AUK 16/ provides SFCCs for granular soils based on fractionated grain size distributions. In order to show the range that is covered by this formulation, four different artificial soils are defined here: sand, silt and clay composed of grains with a uniform size and a mixture of these three soil types in equal shares.

All formulations for the SFCC – except those from /AUK 16/ – are kind of abstract. It was thus tried to match the resulting curves to a high degree to the formulation from /BEN 09/ as this approach does not contain any parameters at all. The parameters used are listed in Tab. 9.8. The parameters used to evaluate the SFCC from /AUK 16/ for the four types of soil are compiled in Tab. 9.9.

The resulting curves are depicted in Fig. 9.1. This plot brings up several noteworthy facts. Firstly, the abstract formulations for the SFCC can be matched rather well to each other. Quite some properties of such a curve have to be known beforehand, though. By contrast, the curves based on /AUK 16/ describe some lowering of the freezing temperature due to the different grain size distributions. Also, a rather slow convergence of the ice saturation towards full saturation becomes obvious. While the more abstract formulations from the other literature should be able to fit the saturation curve from /AUK 16/ for sand, it appears to be impossible to fit the curves for silt, clay, or the mixture.

Checking the match between the curves resulting from the approach in /AUK 16/ and actual measurements would be enlightening but is still pending. A first impression can be given by the work of /BUR 76/, though, who have measured the unfrozen water content at subzero temperatures for silt, illite and clay (see Fig. 9.2). These measurements cor-

roborate the approach from /AUK 16/ in that (a) the soil freezing curves appear to converge with decreasing temperature very slowly to a water content of zero and (b) in that it relates the rate of convergence of the ice saturation to $S_i = 1$ to the particle size of the soil in question. However, much more laboratory work is advisable to substantiate the suggested formulations.

Tab. 9.7 Approaches for the SFCC

Formula	Source	Equation
(unspecified modification of a Heaviside function)	/COM 21/	(-) ³⁵
$S_w = -\frac{2}{(T_1 - T_0)^3} (T - T_0)^3 + \frac{3}{(T_1 - T_0)^2} (T - T_0)^2$	/BAR 16/	(8.24)
$S_w = \frac{1}{2} \left[\operatorname{erf} \left(2.1 + \frac{T - 273.15}{0.25} \right) + 1 \right]$	/BEN 09/	(8.37) ³⁶
$S_w = 0.5 + \frac{S_{wres}}{2} + (1 - S_{wres})$ $\left(0.9375 \left[\frac{T + d}{d} \right] - \frac{5}{8} \left[\frac{T + d}{d} \right]^3 + \frac{3}{16} \left[\frac{T + d}{d} \right]^5 \right)$	/SCH 17/	(8.38)
(modified Heaviside function)	own attempt	(-) ³⁷
$S_i = S_{i \max} \left[1 - e^{\left\{ -\left(\frac{\min(T, T_L) - T_L}{w} \right)^2 \right\}} \right]$	/FER 17/ (exponential)	(8.44)
$S_i = S_{i \max} \left[\max \left\{ 0, \min \left(1, \frac{T_L - T}{2w} \right) \right\} \right]$	/FER 17/ (linear)	(8.45)
$S_w = (1 - S_{wres}) e^{\left\{ -\left[\frac{(T - 273.15)}{w} \right]^2 \right\}} + S_{wres}$	/MCK 07/ (8.36) /GRE 18/ (8.54)	
$S_w = \frac{1}{\Phi} \frac{\rho_w}{\rho_b} e^{(0.2618 + 0.5519 \ln(A_{spec}) - 1.4495(A_{spec})^{-0.2640} \ln T_c)}$	/AUK 16/	(C.14)
(not specified)	RBE	

³⁵ see section 8.1.2.

³⁶ This function is modified compared to (8.37), as the function in square brackets does obviously not fit.

³⁷ see section 8.1.6.

Tab. 9.8 Parameters used to evaluate the SFCC in Tab. 9.7 except equation (C.14)

Source(s)	Equation	Parameters		
/BAR 16/	(8.24)	T_0 [°C]	T_1 [°C]	
		-1	0	
/SCH 17/	(8.38)	$S_{w\ res}$ [-]	d [°C]	
		0.05	0.5	
own attempt	(see section 8.1.6)	$\Delta T_{1 \rightarrow 2}$ [°C]	$T_{pc,1 \rightarrow 2}$ [°C]	
		1	-0.5	
/FER 17/ (exponential)	(8.44)	$S_{i\ max}$ [-]	T_L [°C]	w [°C]
		1	0	0.5
/FER 17/ (linear)	(8.45)	$S_{i\ max}$ [-]	T_L [°C]	w [°C]
		1	0	0.5
/MCK 07/ /GRE 18/	(8.36)	$S_{w\ res}$ [-]	W	
	(8.54)			0.05

Tab. 9.9 Parameters used to evaluate equation (C.14) in Tab. 9.7

Material	d_i [mm]	d_g [mm]	σ_g [-]	A_{spec} [m ² /g]	ρ_b [kg/m ³] ³⁸	Φ [%] ³⁹
Sand	1.000	1.000	1	3.9	2500	40
Silt	0.010	0.010	1	252	2600	40
Clay	0.001	0.001	1	2032	2800	40
Mixture in equal shares	1.0/0.01/0.001	0.022	17.67	126	2633	20

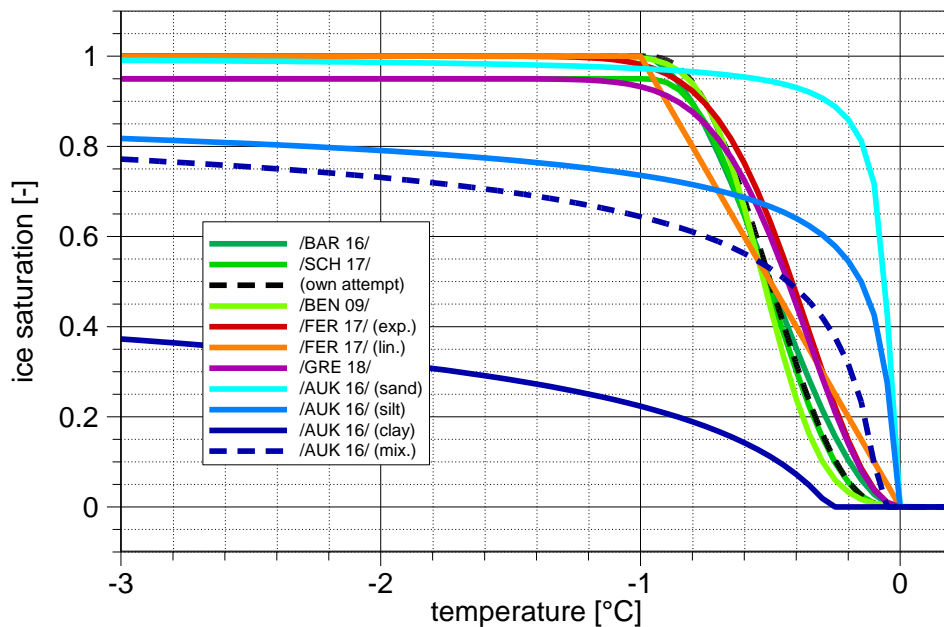


Fig. 9.1 Approaches for the SFCC

³⁸ These are density values in the range of the main constituents.

³⁹ Yet another educated guess based on maximum porosity of a sphere packing and practical knowledge.

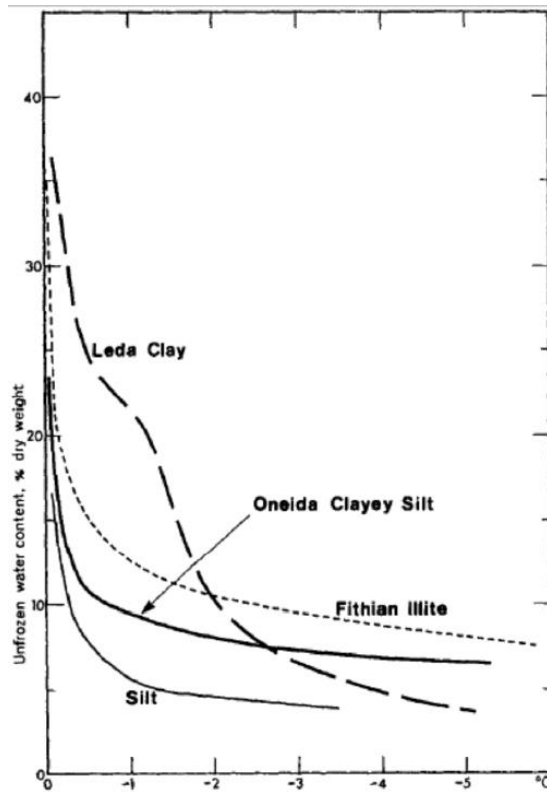


Fig. 9.2 Measured unfrozen water content for silt, illite and clay; from /BUR 76/

9.4.4 Relative permeability for water

The principle of the reduction of the single-phase water permeability with decreasing subzero temperatures appears to be applied in all cases. However, the approaches for the relative permeability of water are quite diverse. It may depend on

- a “volumetric weighing factor ϵ_p ” as in /ZOT 12/,
- temperature only as in /BAR 16/ and /MCK 07/a,
- the temperature-dependent water or ice saturation only as in /KLE 05/, /FER 17/, and /AUK 16/, or
- saturation and an “impedance factor” Ω as in /MCK 07/b/, /SCH 17/, and /GRE 18/.

In /COM 16/, /COM 21/ and this work, the choice of the relative permeability is left with the user. All other approaches are arranged in Tab. 9.10. Not surprising, there are also differences in the general characteristics of the resulting curves. According to /BAR 16/ and the formulations from COMSOL as used in the own attempt, the relative permeability goes down to zero at the lower end of the transition interval. By contrast, the formula-

tions from /MCK 07/a, /MCK 07/b, /KLE 05/, /SCH 17/, /FER 17/ and /GRE 18/ include a user-defined residual permeability while the formula from /AUK 16/ provides a quick but never complete convergence towards zero. Additionally, the decrease of the freezing temperature according to the grain size distribution is acknowledged here.

Tab. 9.10 Approaches for the relative permeability for water

Formula	Source	Equation
(not specified)	/COM 21/	
(unclear; see section 8.1.3)	/ZOT 12/	
$k_r = 10^{(6 * \frac{T-T_0}{T_1-T_0} - 1)}$ for $T_0 < T < T_1$	/BAR 16/	(8.17)
$k_r = \min \left(\max \left(k_{r \text{ res}}, \frac{S_w \text{ res} - 1}{T_{\text{res}}} (T - 273.15) + 1 \right), 1 \right)$	/MCK 07/a	(8.29)
$k_r = \max (10^{-S_i \Phi \Omega}, k_{r \text{ res}})$	/MCK 07/b	(8.30)
$k_r = \frac{\left(\frac{S_w}{\Phi} \right)^4}{\left(1 + \sqrt{1 - \frac{S_w}{\Phi}} \right)^2}$	/KLE 05/	(8.32)
$k_r = \min (\max (10^{-S_i \Omega}, k_{r \text{ res}}), 1)$	/SCH 17/	(8.31)
(modified Heaviside function; see section 8.1.6)	own attempt	
$k_r = \max (k_{r \text{ min}}, (1 - S_i)^a)$	/FER 17/	(8.46)
$k_r = \max (10^{-6}, 10^{-\Phi \Omega [1 - S_w]})$	/GRE 18/	(8.53)
$k_r = S_w^{2b+3}$ with $b = d_g^{-0.5} + 0.2 \sigma_g$	/AUK 16/	(C.7)
(not specified)	RBE	

A plot for comparison of an artificial case is given in Fig. 9.3. The parameters used to plot the relative permeability curves are compiled in Tab. 9.11 and Tab. 9.12. The curves plotted in Fig. 9.3 are not matching each other as well as all the ice saturation curves in Fig. 9.1. However, they seem to suggest that a match of all curves could be achieved after some fitting, except those from /AUK 16/ and the linear function from /MCK 07/a.

Ultimately, this is not entirely satisfying, since the data for fitting the relative-permeability function to real data are by and large very scarce. However, there are the data from /BUR 76/ as shown in Fig. 9.5. They seem to indicate that the relative permeability as a general rule falls below 10^{-8} within the first half degree Celsius below 0 °C, see Fig. 9.4. It would be highly valuable to substantiate this impression by further laboratory tests.

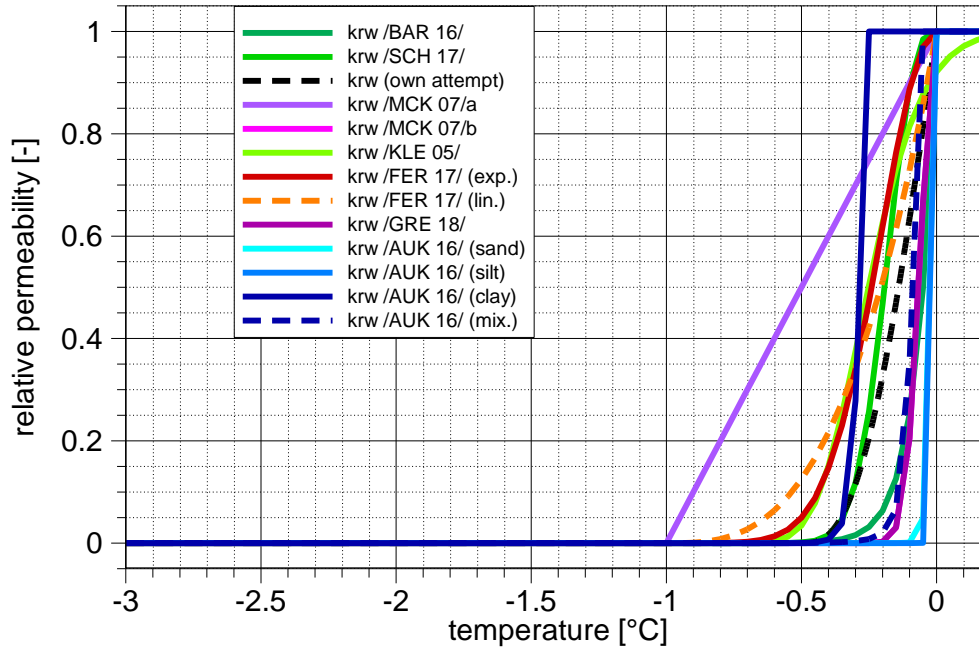


Fig. 9.3 Approaches for the relative permeability for water

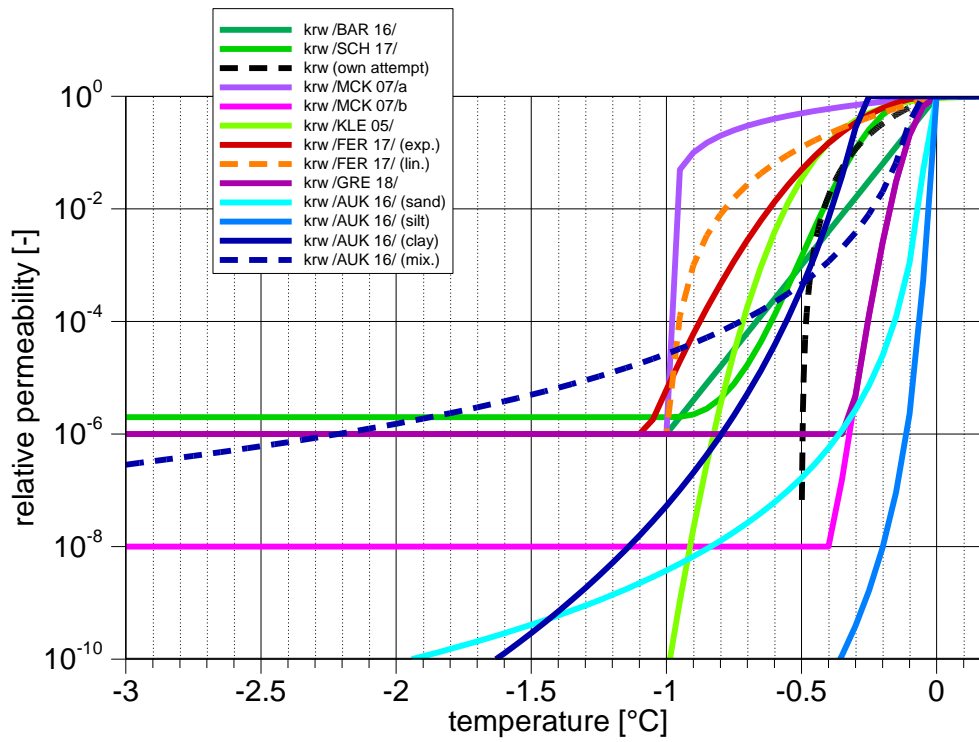


Fig. 9.4 Approaches for the relative permeability for water, log-scale

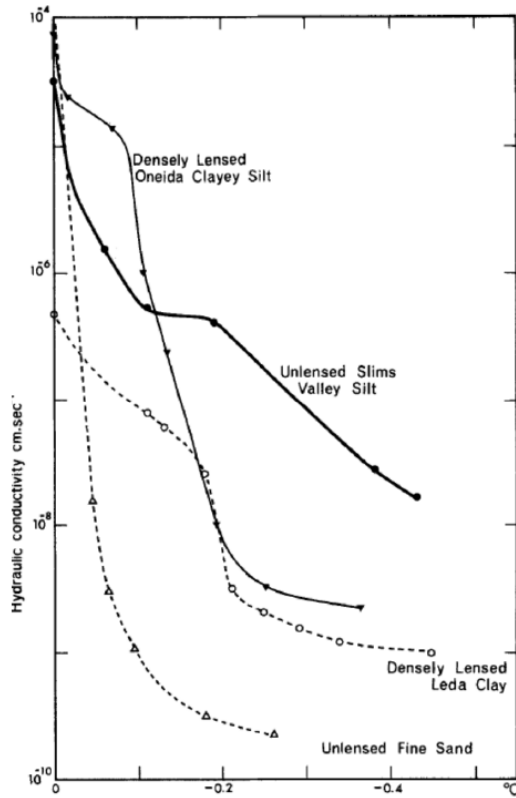


Fig. 9.5 Measured relative permeability for sand, silt and clay; from /BUR 76/

Tab. 9.11 Parameters used to evaluate the equations in Tab. 9.10 (except (C.7)

Source	Equation	Parameters	
/BAR 16/	(8.17)	T_0 [°C]	T_1 [°C]
		-1	0
/MKC 07/a	(8.29)	T_{res} [°C]	$k_{r,res}$ [°C]
		-1	10^{-6}
/MKC 07/b	(8.30)	Ω	Φ
		50	0.37
/KLE 05/	(8.32)	-	Φ
		-	1
/SCH 17/	(8.31)	Ω	-
		6	-
own attempt	(with modifications; see section 8.1.6)	$\Delta T_{1 \rightarrow 2}$ [°C]	$T_{pc,1 \rightarrow 2}$ [°C]
		1	0
/FER 17/	(8.46) (S_i exp. & lin.)	$k_{r,min}$ [-]	a [-]
		10^{-6}	3
/GRE 18/	(8.53)	Φ [-]	Ω [-]
		0.37	50

Tab. 9.12 Parameters used to evaluate equation (C.7) in Tab. 9.10

Material	d_i [mm]	d_g [mm]	σ_g [-]	b	$2b + 3$
Sand	1.000	1.000	1	1.2	5.4
Silt	0.010	0.010	1	10.2	23.4
Clay	0.001	0.001	1	31.6	66.2
Mixture in equal shares	1.0/0.01/0.001	0.022	17.67	3.6	10.2

10 Summary, conclusions and recommendations

10.1 Summary

Some basic definitions concerning the various aspects of a landscape under permafrost conditions are given in section 1 of this report. Furthermore, it is demonstrated that any conceivable geological repository for radioactive waste in Germany will be subject to permafrost during its lifetime. Permafrost has a considerable impact on a groundwater flow system and thereby on the hypothetical migration path of radionuclides in the geosphere in case of a canister breach. A key feature in the groundwater system under such conditions is posed by open taliki (singular: talik) that are unfrozen zones in the otherwise frozen ground connecting surface waters to deep and otherwise isolated aquifers. However, not too much is known about development and stability of taliki.

The problem addressed by the work presented here is defined in section 2. The present report intends to lay the groundwork for a modelling exercise aiming at understanding of the mechanisms about talik forming and its persistence. Descriptions of the underlying physics are compiled for setting up a suitable conceptual framework. The focus of this report is restricted, though, to a sound comprehension of an ensuing mathematical model including the physics-based parameters and functions that form the basis for numerical simulations.

Subsequently, the physical particularities of freezing water are discussed in section 3 and in section 4, the conceptual understanding of groundwater flow under freezing conditions is built up.

The next step consists of illustrating two methodologies for deriving balance equations in subsection 5.1. General balance equations for flow and heat transport are derived in subsections 5.2 and 5.3 that are expressively developed without prematurely introducing assumptions and restrictions.

Thereby, a metaphorical “game board” for simulations is set up that is supplemented in section 6 by a figurative “book of rules” that defines (a) the choice of processes that are to be taken into account, (b) the principles behind the constitutive relations, and (c) the

related state variables. The game board in combination with this book of rules lead to reified balance equations (RBE) as given at the end of section 6.

From that point on the game board remains basically the same. The book of rules, however, also requires some “amendments”. These amendments declare the intended range of validity for the numerical model with respect to the primary variables, in the present case: pressure and temperature. These ranges control eventually the degree of complexity that is required for the mathematical formulation of the constitutive equations (CEs) and the equations of state (EOS).

The book of rules including the amendments thus defines a particular game i.e. a particular modelling framework. As a model is principally designed for a specific purpose, rules may be altered in any aspect (choice of processes, principle of the CEs, required state variables, ranges of validity) to serve different purposes. Depending on the nature of such alterations, the ensuing modifications in the numerical framework may be of differing complexity, though.

In section 7 of this report, three possible amendments are defined. The first case is intended to provide the most general frame for work in the region around a radioactive waste repository. The second case being tailored to the international INTERFROST benchmark exercise (see appendix A) is strongly restricting the variability of case 1 and the third case aims at the investigation concerning development and stability of taliki, presumably requiring particular attention to the EOS’ and CEs. These three amendments lead to three games/cases where first of all the ranges of validity for the referring model concerning temperature and pressure vary.

In parallel, data from the literature concerning the EOS for water, ice and rock are compiled for the subzero temperature range down to $-40\text{ }^{\circ}\text{C}$ (see appendix B). Analytical formulations are derived for temperatures below $0\text{ }^{\circ}\text{C}$ and combined with known formulations for temperatures above $0\text{ }^{\circ}\text{C}$. As the latter are rather general and thus quite complex, a set of simpler analytical functions valid for temperatures between $-20\text{ }^{\circ}\text{C}$ and $+20\text{ }^{\circ}\text{C}$ ($0\text{ }^{\circ}\text{C}$ in case of ice) as well as for pressures of up to 10 MPa are developed as well.

Since the ranges of validity limit the variation of an EOS within the given bounds, simplifications particularly of the EOS may be introduced. Based on the idea that an EOS varying by less than 1 % might reasonably well be approximated by a constant value, different sets of EOS are suggested for the three cases. The reified balance equations are then adapted to the three cases and compared among each other.

With a clear picture of the balance equations, the equations of state and the principles behind the constitutive equations, a (rather arbitrary) choice of models from the literature has been compiled and described in section 8. Finally, all these approaches are compared with the own RBE in section 9 including the CEs and EOS'.

10.2 Conclusions

10.2.1 General remarks

Two important findings are reflected in the conceptual model. First, any conceivable geological radioactive waste repository will sooner or later be affected by permafrost but not necessarily by glaciations. Second, groundwater flow under permafrost conditions should be understood well enough before increasing the physical complexity e.g. by considering the hydrological situation in the presence of an ice shield.

Finding an adequate set of equations in the literature proved to be difficult, though, due to the fact that the referring formulations are quite diverse but often only loosely justified. It thus appears that setting up an appropriate and defensible set of equations requires establishing all formulations including the balance equations from scratch.

On the one hand, this has proved to be a tedious task. On the other hand, having accomplished this task does not only provide a deep insight into the nature of the balance equations but also allows rather easily for incorporating additional terms or even additional balance equations describing further processes if need arises. It helps furthermore considerably to backtrace certain terms in the formulations from the literature to their origin which is particularly helpful if the original term has been transformed into several equivalent but differently looking terms.

Quite naturally, only a problem-specific range of the primary variables out of the full spectrum of possible values is relevant and needs to be considered in the balance equations, in the CEs and particularly in the EOS'. This limits the variability of the EOS' according to the range adopted to a degree that suggests in some cases replacing a function by a constant. However, as any such simplification requires a certain tolerance against the accompanying errors, criteria for simplifications are somewhat problem dependent as different models may show different degrees of sensitivity to such errors. The decision about tolerable errors in the EOS depends therefore on the robustness of a particular model and is thus ultimately in the responsibility of the modeler.

10.2.2 Comparison of the balance equations

In principle, two types of balance equations for groundwater flow have been found. The work of /ZOT 12/ is based on unsaturated flow in the form of Richards' equation. All others rather use a modified form of the saturated single-phase flow equation. It has to be mentioned, though, that in some formulations the hydraulic pressure has been exchanged for the hydraulic head.

In any case, there is a certain resemblance between the Richards equation and the conventional continuity equations. The absolute permeability, a measure for flow resistance, is corrected in all models by a saturation dependent relative permeability.

In terms of the underlying conceptual models, the formulations for heat flow are more similar among each other than for groundwater flow. There are differences in the handling of the three-phase porous medium, though. Where existing formulations for heat flow in porous media are used, only two materials, namely water and solid matrix, are often accounted for. However, this problem can be circumvented by formulating appropriate bulk parameters for the thermal properties.

Not unexpected is the observation that different formulations of the balance equations in the literature were just the consequence of different simplifications or definitions. These could all be traced back to the general formulation derived in this report. Among them are:

- Not all formulations allow for density-dependent flow.
- No storage of water is accounted for in cases 1 and 2 of the present derivation.

- The formulation in /GRE 18/ does not include a mass sink/source term.
- By introducing the coefficient β for the water compressibility as in /SCH 17/ and /GRE 18/, the state equation for water density has been preset without saying so.

Also noteworthy is the fact that several inconsistencies have been found in the balance equations:

- Cancelling the water density under a differential operator by dividing the mass balance equation by the water density as in /SCH 17/ and /GRE 18/ is only possible if the water density is a constant. However, the density is later nevertheless defined in /GRE 18/ to be pressure dependent.
- The porosity in the flow equation from /FER 17/ is introduced as a function of the hydraulic pressure but later apparently treated as a constant.
- For the energy balance equation as formulated in /COM 16/ and /COM 21/, the specific heat has obviously been assumed to be constant, allowing for removing it from under the gradient operator. It is therefore not consistent to assign a temperature-dependent function to this quantity as in /BAR 16/ or in /SCH 17/.

However, the relevance of these inconsistencies for concrete problems is an open question yet. The comments given above are therefore strictly non-judgmental remarks.

It appears that earlier attempts on simulation of groundwater flow under permafrost conditions have been living with more severe simplifications than later ones:

- The formulation of the heat flow equation from /ZOT 12/ looks quite general but is actually restricted exclusively to water properties.
- A term acknowledging the contribution of latent heat in case of phase changes is included in all formulations but the one from /ZOT 12/.
- While in /ZOT 12/ only one single heat conductivity value is included for the simulation, /BAR 16/ takes also the solid phase into account. In both cases, the transition from water to ice, and vice versa, is not clearly defined in terms of the state variables.
- In the formulation from /BAR 16/ the density change during melting or freezing is apparently not taken into account.
- The storage terms for heat flow based on the COMSOL formulations are quite diverse. One reason is that the older version of this simulator does not account for the

ice phase. Different workarounds have therefore been formulated in /BAR 16/ and /SCH 17/. In the meantime, this problem has been resolved in /COM 21/.

- Only the present work as well as /COM 21/ include additionally heat convection by thermo-hydraulic dispersion. Note that it has been described earlier in the literature e.g. in /KRÖ 91/. It is thus somewhat astonishing that it has only been found in the equations from /COM 21/. However, the selection of codes for this report is not really representative. Furthermore, it cannot be ruled out that the effect from this term has somewhere already been identified to be of secondary importance.

The stringent derivation of the heat flow equation performed in this report has revealed that including heat sources is not trivial. Heat energy may be added to the underground by heaters, by phase changes of water or by inflowing water. In the context of permafrost, it is a necessity to include the effect of freezing. This is why all heat balance equations (except one) take a term containing the latent heat into consideration that is related to sinks/sources of heat in water and ice. However, heat energy that is tied to an inflow of groundwater is only considered in /FER 17/ and the present work.

Additional right-hand side terms found in the literature are quite different when looked up closely. However, they are by-products of expanding a general storage term and can thus be seen as a part of the original storage term instead as an independent production term.

All in all, the formulations from /FER 17/, /COM 21/ and from the present work show the highest degree of generality in the investigated selection of formulations.

10.2.3 Comparison of the EOS

Four state variables control groundwater and heat flow under permafrost conditions. These are density and viscosity, where applicable, as well as thermal conductivity and specific heat. Depending on the literature and thus probably on the purpose of a specific model, they may be represented by constant values, abstract polynomials or by analytical functions matching measured data. The wide variety of presented combinations shows that there is no generally agreed upon set of EOS. Relevance for specific problems seems not to be the main motivation for any of the selections, though, as such a motivation is nowhere stated.

In the pre-set formulations of older versions of COMSOL, it is quite difficult to find adequate formulations for the EOS that take all three phases into account. This applies in particular to the bulk thermal conductivity λ_b that has been introduced quite differently by different authors to circumvent this problem. There is no need for this, though, when using the latest versions that allow for including up to 5 optional phase changes in one fluid.

Except for the implementations by /BAR 16/ and the present work, rather little effort has been expended for choosing realistic and appropriate formulations for the EOS. Moreover, where specific formulations or simplifications of the EOS are introduced, the range of validity is generally missing. The complete set of EOS' as presented in appendix B that cover reasonable temperature and pressure ranges should therefore be useful for any new model developments.

10.2.4 Comparison of the CEs

As the CEs concern basically material properties which are in the present case porosity, water/ice saturation and relative permeability for the water, they cannot be given as clearly defined relations as in case of the EOS. Notably for the water/ice saturation and the relative permeability for the water there is hardly any basis for a sound choice in a concrete case. If no specific measurements are available, the choice of appropriate material parameters is left solely to the experience of the user, i.e. his/her gut feeling.

A variable porosity is not considered in many formulations. Only /FER 17/ and this work have been found to include the theoretical basis for a pressure-dependent porosity in the balance equations.

The approaches used for the soil freezing characteristic curve (SFCC) can be ascribed to three categories. The first class of SFCCs represents a transition from full water saturation to full ice saturation in a temperature range from the melting point of water down to a user-defined lower bound temperature $T_{trans\ low}$. The second class of SFCCs describes a similar transition but below $T_{trans\ low}$ a residual water saturation remains regardless of the temperature. Finally, SFCCs were found where the resulting curves converge mathematically towards $S_i = 1$ but not within a given transition interval.

Except for the approach by /AUK 16/, all SFCCs investigated here were abstract and rather derived on general principles. It thus appears to be of marginal benefit that generic data as used in the INTERFROST benchmark can nevertheless be matched. The only mitigation of this situation would be that the modelling results are not overly sensitive to variations in the SFCC. This is still to be confirmed, though.

The principle of reducing the single-phase water permeability according to the local temperature appears to be applied in all cases. However, the approaches for the relative permeability of water are quite diverse.

In some cases, the choice of the relative permeability function is left with the user. The pre-set functions of the remaining approaches can again be arranged in three classes according to general characteristics. First, the relative permeability goes down to zero at the lower end of the transition interval. Second, a user-defined constant residual permeability remains at low temperatures. Third, the relative permeability converges quickly but never completely towards zero.

A general observation concerning the formulations for the relative permeability appears to be kind of strange. On the one hand there are quite sophisticated approaches for the relative water permeability. But on the other hand, it seems that very little effort has gone into acquisition of data and fitting the related curves. At that, the contribution from /AUK 16/ is apparently a rare exception.

10.3 Recommendations

Concerning modelling in general, documenting the “game board” and writing up a book of rules certainly helps to make a model transparent and to facilitate comparisons with other codes. One way or the other, it should become part of any code documentation. Furthermore, every formulation of CEs and EOS’ introduces restrictions to the applicability of a model due to its range of validity in terms of the primary variables. These should also be part of a model documentation.

Left to clarify with respect to the balance equations examined here, is the relevance of hydro-thermal dispersion as a physical aspect of the heat flow problem. Maybe also the

impact of inconsistencies in some numerical models by handling certain state variables at one point as constants and at another point as variables should be determined.

Another set of advisable actions concerns the data underlying the physical model concept. These are specifically and without priority:

- Since the approaches for the SFCC and the relative permeability are mostly quite weakly substantiated it would be quite interesting to evaluate the impact of uncertainties in this respect on model results. A related sensitivity analysis appears therefore to be generally advisable.
- If the results of such a sensitivity analysis indicate the necessity of more accurate application of these CEs, an attempt should be made to compile a conclusive set of referring data from the literature. Failing that, the known data should be supplemented by specific laboratory measurements.
- A check based on these data might be illuminating in showing the predictive capability of the approaches from /AUK 16/.
- CEs for freezing conditions basically relate to the porous media formed by common soils. It would be quite enlightening to broaden the field of applications to fractures in crystalline rock.

Note finally, if these recommendations are already outdated by the literature or ongoing work, the author would deeply appreciate any sort of hints in this regard.

References

- /AUK 16/ Aukenthaler, M., Brinkgreve, R., & Haxaire, A.: A practical approach to obtain the soil freezing characteristic curve and the freezing/melting point of a soil-water system. In Proceedings of the GeoVancouver 2016: the 69th Canadian Geotechnical Conference, Vancouver, Canada (pp. 1-8), 2016.
- /BAR 16/ Barnard, M.: The Impact of Glaciation and Permafrost on Groundwater Flow. Thesis, University of Waterloo, Ontario, Canada, 2016. UWSpace: <http://hdl.handle.net/10012/10332>.
- /BEA 72/ Bear, J.: Dynamics of fluids in Porous Media. Dover Publications, New York 1972.
- /BGE 20/ Bundesanstalt für Endlagerung mbH (BGE): Zwischenbericht Teilgebiete gemäß §13 StandAG. Geschäftszeichen: SG01101/16-1/2-2019#3 – Objekt-ID: 755925 – Revision: 000, BGE, Peine, 2020.
- /BEN 09/ Bense, V.F., Ferguson, G., Kooi, H.: Evolution of shallow groundwater flow systems in areas of degrading permafrost. Geophysical Research Letters, 36, 2009. doi:10.1029/2009gl039225
- /BGR 12/ BGR: Karte der untersuchungswürdigen Wirtsgesteinsformationen - Ergebnisse der regionalen BGR-Studien. Webpages of BGR, 2012. https://www.bgr.bund.de/DE/Themen/Endlagerung/Downloads/Charakterisierung_Wirtsgesteine_geotech_Barrieren/4_Wirtsgesteinsuebergreifend/Karte_Wirtsgesteinsformationen_Dtl.html (as of 15.06.2021)
- /BRO 97/ Brown, J., Ferrians, O. J., Jr, Heginbottom, J. A., & Melnikov, E. S.: Circum-Arctic map of permafrost and ground-ice conditions. Circum-Pacific Map 45, US Geological Survey Reston, 1997.
- /BUR 76/ Burt, T.P. and Williams, P.J.: Hydraulic conductivity in frozen soils, Earth Surface Processes and Landforms, 1(4), 349-360, 1976.
- /COM 16/ COMSOL: Documentation. 2016.

- /COM 21/ COMSOL: Documentation. 2021. <https://www.comsol.com/documentation>
- /CRC 86/ Weast, R.C., Astle, M.J., Beyer, W.H. (eds.): CRC Handbook of Chemistry and Physics. Chemical Rubber Company (CRC), Second printing, CRC Press, Inc., Boca Raton, Florida, 1986.
- /CRC 13/ Haynes, W.M. (ed.): CRC Handbook of Chemistry and Physics. Chemical Rubber Company (CRC), 94th Edition, Cleveland, Ohio: CRC Press, 2013. (cited in /BAR 16/)
- /DAN 67/ D'Ans, J., Lax, E.: Taschenbuch für Chemiker und Physiker, Band I, Makroskopische physikalisch-chemische Eigenschaften. 3. Auflage, Springer-Verlag Berlin · Heidelberg · New York, 1967.
- /DEL 98/ Delisle, G.: Numerical simulation of permafrost growth and decay. Journal of Quaternary Science 13 (4), 325-333, 1998.
- /EAR 19/ Earle, S.: Physical Geology. BCcampus OpenEd, Victoria, B.C., Canada, 2019. <https://opentextbc.ca/geology/chapter/9-2-the-temperature-of-earths-interior/>
- /ETB 21/ The Engineering Toolbox: Resources, Tools and Basic Information for Engineering and Design of Technical Applications. www.engineeringtoolbox.com, as of 2021.
- /FER 17/ Ferry, M.: Darcy Tools, Ice Model. Report TR 16114, MFRDC, 6 rue de la Perche, 44700 Orvault, France, 2017.
- /FIN 20/ Finsterle, S., Cooper, C., Muller, R.A., Grimsich, J., Apps, J.: Sealing of a deep horizontal borehole repository for nuclear waste. Energies, 14, 91, 2021. <https://dx.doi.org/10.3390/en14010091>
- /GÄR 87/ Gärtner, S.: Zur diskreten Approximation kontinuumsmechanischer Bilanzgleichungen. Bericht Nr. 24/1987, Institut für Strömungsmechanik und Elektronisches Rechnen im Bauwesen, Universität Hannover, 1987.

- /GRE 18/ Grenier, C., Anbergen, H., Bense, V., Chanzy, Q., Coon, E., Collier, N., Costard, F., Ferry, M., Frampton, A., Frederick, J., Gonçalves, J., Holmén, J., Jost, A., Kokh, S., Kurylyk, B., McKenzie, J., Molson, J., Mouche, E., Or-gogozo, L., Pannetier, R., Rivière, A., Roux, N., Rühaak, W., Scheidegger, J., Selroos, J.-O., Therrien, R., Vidstrand, P., Voss, C.: Groundwater flow and heat transport for systems undergoing freeze-thaw: Intercomparison of numerical simulators for 2D test cases. *Advances in Water Resources* 114 (2018) 196–218, Elsevier, 2018.
- /HAN 04/ Hansson, K., Simunek, J., Mizoguchi, M., Lundin, L.C., van Genuchten, M.T.: Water flow and heat transport in frozen soil: Numerical solution and freeze-thaw applications. *Vadose Zone Journal*, 3(2), 693-704, 2004.
- /HEG 09/ Heginbottom, J.A., Brown, J., Humlum, O. and Svensson, H.: State of the Earth's Cryosphere at the Beginning of the 21st Century: Glaciers, Global Snow Cover, Floating Ice, and Permafrost and Periglacial Environments: Chapter A in *Satellite image atlas of glaciers of the world*. U.S. Geological Survey, Reston, VA, 2009.
- /IAP97/ International Association for Properties of Water and Steam: Release on the IAPWS Industrial Formulation 1997 for the Thermodynamic Properties of Water and Steam. 1997. Homepage: <http://www.iapws.org>.
- /IAP 03/ The International Association for the Properties of Water and Steam: Re-vised Release on the IAPS Formulation 1985 for the Viscosity of Ordinary Water Substance. 2003. Homepage: <http://www.iapws.org>.
- /IAP 08/ The International Association for the Properties of Water and Steam: Re-vised Release on the IAPWS Formulation 2008 for the Viscosity of Ordinary Water Substance. 2008. Homepage: <http://www.iapws.org>.
- /IAP 11/ The International Association for the Properties of Water and Steam: Re-vised Release on the IAPWS Formulation 2011 for the Thermal Conductivity of Ordinary Water Substance. 2011. Homepage: <http://www.iapws.org>.

- /IAP 15/ The International Association for the Properties of Water and Steam: Revised Guideline on Thermodynamic Properties of Supercooled Water. 2015. Homepage: <http://www.iapws.org>.
- /IAP 18/ The International Association for the Properties of Water and Steam: Revised Release on the IAPWS Formulation 1995 for the Thermodynamic Properties of Ordinary Water Substance for General and Scientific Use. IAPWS R6-95, 2018. Homepage: <http://www.iapws.org>.
- /IPA 21/ International Permafrost Association (IPA): What is permafrost? Online article, as of October 2021. <https://ipa.arcticportal.org/publications/occasional-publications/what-is-permafrost>
- /JNC 00/ Japan Nuclear Cycle Development Institute (JNC): H12: Project to Establish the Scientific and Technical Basis for HLW Disposal in Japan, Supporting Report 1: Geological Environment in Japan. Report JNC TN 1410 2000-002, JNC, Tokai-mura, 2000.
- /JOH 16/ Johansson, E.: The influence of climate and permafrost on catchment hydrology. Thesis, Department of Physical Geography, Stockholm University, 2016.
- /KEL 98/ Keller, S.: Permafrost in der Weichsel-Kaltzeit und Langzeitprognose der hydrogeologischen Entwicklung der Umgebung von Gorleben / NW-Deutschland. Z. Angew. Geol. 48, 111-119, 1998.
- /KLE 05/ Kleinberg, R.L. and Griffin, D.D.: NMR measurements of permafrost: unfrozen water assay, pore-scale distribution of ice, and hydraulic permeability of sediments, Cold Regions Science and Technology, 42(1), 63-77, 2005, doi:10.1016/j.coldregions.2004.12.002.
- /KRÖ 91/ Kröhn, K.-P.: Simulation von Transportvorgängen im klüftigen Gestein mit der Methode der Finiten Elemente. Report 29/1991, Institut für Strömungsmechanik und Elektronisches Rechnen im Bauwesen, University of Hannover, 1991.

- /KRÖ 08/ Kröhn, K.-P.: Values required for the simulation of CO₂-storage in deep aquifers. FKZ 03 G 0622 B (BMWi), Bericht GRS-236, GRS Braunschweig, 2008.
- /KRÖ 10/ Kröhn, K.-P.: State Variables for Modelling Thermohaline Flow in Rocks. FKZ 02 E 10336 (BMWi), Gesellschaft für Anlagen- und Reaktorsicherheit (GRS) mbH, GRS-268, Köln, 2010.
- /KRÖ 11/ Kröhn, K.-P.: Code VIPER - Theory and Current Status. Statusreport, FKZ 02 E 10548 (BMWi), Gesellschaft für Anlagen- und Reaktorsicherheit (GRS) mbH, GRS-269, Köln, 2011.
- /LAN 61/ Landolt-Börnstein: Zahlenwerte und Funktionen aus Physik, Chemie, Astronomie Geophysik und Technik; Zweiter Band: Eigenschaften der Materie in ihren Aggregatzuständen, 4. Teil; Kalorische Zustandsgrößen. Springer-Verlag, 1961.
- LAN 69/ Landolt-Börnstein: Zahlenwerte und Funktionen aus Physik, Chemie, Astronomie, Geophysik und Technik; Zweiter Band: Eigenschaften der Materie in ihren Aggregatzuständen, 5. Teil, Bandteil a: Transportphänomene I (Viskosität und Diffusion). Springer-Verlag, 1969.
- /LAN 71/ Landolt-Börnstein: Zahlenwerte und Funktionen aus Physik, Chemie, Astronomie Geophysik und Technik; Zweiter Band: Eigenschaften der Materie in ihren Aggregatzuständen, 1. Teil; Mechanisch-thermische Zustandsgrößen. Springer-Verlag, 1971.
- /LAN 72/ Landolt-Börnstein: Zahlenwerte und Funktionen aus Physik * Chemie * Astronomie * Geophysik und Technik; IV. Band Technik; Bandteil b Thermodynamische Eigenschaften von Gemischen; Verbrennung; Wärmeübertragung. Springer-Verlag, 1972.
- /LAN 82a/ Landolt-Börnstein: Zahlenwerte und Funktionen aus Naturwissenschaften und Technik; Neue Serie; Group V, Volume 1; Physical Properties of Rocks; Subvolume a. Springer-Verlag, 1982.

- /LAN 82b/ Landolt-Börnstein: Zahlenwerte und Funktionen aus Naturwissenschaften und Technik; Neue Serie; Group V, Volume 1; Physical Properties of Rocks; Subvolume b. Springer-Verlag, 1982.
- /MAL 20/ Mallants D., Travis K., Chapman N., Brady P.V., Griffiths, H.: The State of the Science and Technology in Deep Borehole Disposal of Nuclear Waste Energies, 13, 833, 2020. doi:10.3390/en13040833
- /MIK 14/ Miklovicz, T.: Investigation on the potential of combined heat, power and metal extraction in Hungary. BSc Thesis, University of Miskolc, Faculty of Earth Science and Engineering, Institute of Mineralogy and Geology, Miskolc, Hungary, 2014.
- /MCK 07/ McKenzie, J.M., Voss, C.I., Siegel, D.I.: Groundwater flow with energy transport and water–ice phase change: Numerical simulations, benchmarks, and application to freezing in peat bogs. *Advances in Water Resources*, Volume 30, Issue 4, Pages 966-983, April 2007.
- /MOO 11/ Moore, E. and Molinero, V.: *Structural transformation in supercooled water controls the crystallization rate of ice. Nature. 479 (7374): 506–508, 2011.*doi:10.1038/nature10586
- /MOT 06/ Mottaghy, D., Rath, V.: Latent heat effects in subsurface heat transport modelling and their impact on paleotemperature reconstructions. *Geophysical Journal International*, 164, p 236-245, 2006.(cited in /BAR 16/)
- /MÜL 19/ Müller, M. and Ludwig, H.-M.: Impact of different liquid uptake processes on salt frost scaling mechanism. Conference on Concrete in arctic conditions, Trondheim, Norway, 2019.
- /MUR 05/ Murphy, D. M., Koop, T.: Review of the vapour pressures of ice and supercooled water for atmospheric applications. *Quaternary Journal of the Royal Meteorological Society*, 131, p 1539-1565, 2005. (cited in /BAR 16/)

- /NOS 22/ Noseck, U., Becker, D., Fahrenholz, C., Flügge, J., Hagemann, S., Hor-
mann, V., Kröhn, K.-P., Kröhn, M., Meleshyn, A., Mönig, J., Moog, H.,
Rübel, A., Spießl, S., Wolf, J.: Scientific Basis for a Safety Case of Deep
Geological Repositories. FKZ 02E11647 (BMW), Report GRS-643, Gesell-
schaft für Anlagen- und Reaktorsicherheit (GRS) gGmbH, Braunschweig,
2022.
- /OBU 21/ Obu, J.: How much of the Earth's surface is underlain by permafrost? Jour-
nal of Geophysical Research: Earth Surface, 126, 2021.
<https://doi.org/10.1029/2021JF006123>
- /PAB 12/ de Pablo, M.Á., Ramos, M., Viaira, G., Molina, A.: Revealing the secrets of
permafrost. Science in School, The European journal for science teachers,
issue 22, 2012, <https://www.scienceinschool.org/2012/issue22/permafrost>
(as of 9th June 2021)
- /PAR 18/ Parazoo, N.C., Koven, C.D., Lawrence, D.M., Romanovsky, V., and Miller,
C.E.: Detecting the permafrost carbon feedback: talik formation and in-
creased cold-season respiration as precursors to sink-to-source transitions.
The Cryosphere, 12, 123–144, 2018, <https://doi.org/10.5194/tc-12-123-2018>.
- /RAT 62/ Ratcliffe, E. H.: The thermal conductivity of ice, new data on the temperature
coefficient. *Philosophical Magazine*, 7:79, p 1197-1203, 1962. (cited in
/BAR 16/)
- /REN 03/ Renssen, H. and Vandenberghe, J.: Investigation of the relationship be-
tween permafrost distribution in NW Europe and extensive winter sea-ice
cover in the North Atlantic Ocean during the cold phases of the Last Glacia-
tion. *Quaternary Science Reviews* 22, 209-223, 2003.
- /SCH 61/ Scheidegger, A.E.: General Theory of Dispersion in Porous Media. *Journal*
of Geophysical Research, Vol. 66, No.10, 1961.

- /SCH 17/ Scheidegger, J., Busby, J.P., Jackson, C.R., McEvoy, F.M., Shaw, R.P.: Coupled modelling of permafrost and groundwater, A case study approach. British Geological Survey, Contractor Report no. BGS/CR/16/053, Keyworth, Nottinghamshire, UK, 2017.
- /SDW 21/ Spektrum der Wissenschaften: Lexikon der Geowissenschaften: geothermischer Gradient. Online-article, as of October 2021. <https://www.spektrum.de/lexikon/geowissenschaften/geothermischer-gradient/5754>
- /SKB 06/ Svensk Kärnbränslehantering AB (SKB): Climate and climate-related issues for the safety assessment SR-Can. Technical report TR-06-23, Svensk Kärnbränslehantering AB, Stockholm, 2006.
- /STA 17/ Deutscher Bundestag: Gesetz zur Suche und Auswahl eines Standortes für ein Endlager für hochradioaktive Abfälle (Standortauswahlgesetz - StandortAG). Decision of the Deutscher Bundestag, 2017.
- /SVE 14/ Svensson, U., Ferry, M.: Darcytools: A computer code for hydrogeological analysis of nuclear waste repositories in fractured rock. *Journal of Applied Mathematics and Physics* 2 (06), 365, 2014.
- /TAN 11/ Tan, X., Chen, W., Tian, H., Cao, J.: Water flow and heat transport including ice/water phase change in porous media: Numerical simulation and application. *Cold Regions Science and Technology*, 68, p 74-84, 2011. (cited in /BAR 16/)
- /TFL 21/ The Free Library: Arctic area of the tundra and Antarctic dominion. Online article, retrieved Oct 20, 2021 from <https://www.thefreelibrary.com/Arctic+area+of+the+tundra+and+Antarctic+dominion.-a0237305901>
- /VAN 93/ Vandenberghe, J. and Pissart, A.: Permafrost changes in Europe during the Last Glacial. *Permafrost and Periglacial Processes* 4, 121–135, 1993.

- /VEV 05/ van Everdingen, R.O. (ed.): Multi-language Glossary of Permafrost and Related Ground-ice Terms. International Permafrost Association, Terminology Working Group, 1998 (revised 2005)
- /VGN 80/ van Genuchten, M.T.: A closed-form equation for predicting the hydraulic conductivity of unsaturated soils. Soil Sci. Soc. Am. J., 1980.
- /WIK 21/a Wikipedia: Geothermische Tiefenstufe. Online article as of October 2021. https://de.wikipedia.org/wiki/Geothermische_Tiefenstufe
- /WIK 21/b Wikipedia: Permafrost. Online article as of October 2021. https://en.wikipedia.org/wiki/Permafrost#cite_note-16
- /ZOT 12/ Zottola J., Darrow M., Daanen R., Fortier D., de Grandpré I.: Investigating the Effects of Groundwater Flow on the Thermal Stability of Embankments over Permafrost. 15th International Conference on Cold Regions Engineering, Quebec, Canada, 2012. DOI: 10.1061/9780784412473.060

References from /AUK 16/

- /AND 72/ Anderson, D.M. and Tice, A.R.: Predicting unfrozen water content in frozen soils from surface area measurements, *Highway Research Record*, Volume 393, 12–18, 1972.
- /CAM 85/ Campbell, G. S.: *Soil Physics with Basic*, Elsevier, 1985.
- /REM 04/ Rempel, A.W., Wettlaufer, J.S. and GraeWorster, M.: Premelting dynamics in a continuum model of frost heave, *J. Fluid Mech.* 498, 227–244, 2004.
- /SEP 10/ Sepaskhah, A.R., Tabarzad, A. and Fooladmand, H.R.: Physical and empirical models for estimation of specific surface area of soils. *Archives of Agronomy and Soil Science* 56(3), 325–335, 2010.
- /SHA 88/ Sharp, R. P.: *Living Ice: Understanding Glaciers and Glaciation*. Cambridge University Press, 1988.
- /SHI 84/ Shirazi, M.A. and Boersma, L.: A unifying quantitative analysis of soil texture. Cited in /AUK 16/, *Soil ci. Soc. Am. J.* 48, 142–147, 1984.
- /TAR 96/ Tarnawski, V.R. and Wagner, B.: On the prediction of hydraulic conductivity of frozen soils, *Canadian Geotechnical Journal* 33(1), 176–180, 1996.
- /THO 09/ Thomas, H., Cleall, P., LI, Y.-C., Harris, C. and Kern-Luetschg, M.: Modelling of cryogenic processes in permafrost and seasonally frozen soils, *Géotechnique* 59(3), 173–184, 2009.
- /WAG 11/ Wagner, W., Riethmann, T., Feistel, R. and Harvey, A.H.: New equations for the sublimation pressure and melting pressure of H₂O Ice Ih, *Journal of Physical and Chemical Reference Data* 40(4), 2011.
- /WET 06/ Wettlaufer, J. and Worster, M.G.: Premelting dynamics. *Annual Review of Fluid mechanics* 38(1), 427– 452, 2006.

/ZHO 14/ Zhou, M.M.: Computational simulation of freezing: Multiphase modelling and strength upscaling, Ph. D. thesis, Ruhr University Bochum, 2014.

Table of figures

Fig. 1.1	Ground conditions in relation to temperature and depth	2
Fig. 1.2	Types of permafrost and taliki	5
Fig. 1.3	Radial temperature profiles for the earth	6
Fig. 1.4	Multi-barrier system envisaged for a deep geological repository	8
Fig. 1.5	Potential sites for a deep geological repository (left) and permafrost conditions during the latest ice age (right)	8
Fig. 1.6	Potential sites for a deep geological repository; present state of the site selection process in Germany.....	9
Fig. 1.7	Impact of permafrost on radionuclide migration.....	10
Fig. 4.1	Relevant processes for groundwater flow under permafrost conditions	15
Fig. 4.2	Principle sketch illustrating porosity Φ and saturations S	16
Fig. 5.1	Infinitesimal volume element	19
Fig. 5.2	Macroscopic control volume being carried with the flux.....	21
Fig. 6.1	Density (top left), viscosity (top right), thermal conductivity (bottom left), and heat capacity (bottom right) for water and ice, where applicable.....	41
Fig. 6.2	Volumetric changes in water and ice during freezing.....	43
Fig. 7.1	Permafrost thickness over surface temperature	54
Fig. 8.1	Illustration of the transition functions $\theta_1(T)$ and $\theta_2(T)$	64
Fig. 9.1	Approaches for the SFCC	94
Fig. 9.2	Measured unfrozen water content for silt, illite and clay.....	95
Fig. 9.3	Approaches for the relative permeability for water	97
Fig. 9.4	Approaches for the relative permeability for water, log-scale.....	97
Fig. 9.5	Measured relative permeability for sand, silt and clay.....	98
Fig. B.1	Data and formulations for water density at atmospheric pressure	135
Fig. B.2	Density of water as a function of temperature and pressure	136
Fig. B.3	Data and ad hoc formulation for the ice density.....	137
Fig. B.4	Data and formulations for water viscosity at atmospheric pressure	138
Fig. B.5	Viscosity of water as a function of temperature and pressure.....	139
Fig. B.6	Data and formulations for thermal conductivity of water	140
Fig. B.7	Thermal conductivity of water as a function of temperature and pressure .	141
Fig. B.8	Data and formulation for thermal conductivity of ice	142

Fig. B.9	Thermal conductivity of granite.....	143
Fig. B.10	Data and formulations for heat capacity of water.....	144
Fig. B.11	Heat capacity of water as a function of temperature and pressure	145
Fig. B.12	Data and formulation for heat capacity of ice.....	146
Fig. B.13	Heat capacity of igneous rock	147
Fig. B.14	Density of water and ice in the whole considered temperature range	148
Fig. B.15	Viscosity of water in the whole considered temperature range	149
Fig. B.16	Thermal conductivity of water and ice in the whole temperature range.....	150
Fig. B.17	Thermal conductivity of the rock.....	151
Fig. B.18	Heat capacity of water and ice in the whole considered temperature range.....	152
Fig. B.19	Heat capacity of the rock.....	152

List of tables

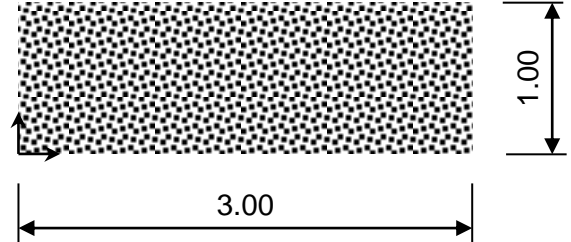
Tab. 7.1	Groundwater flow equations from this work.....	57
Tab. 7.2	Heat flow equations – storage term	59
Tab. 7.3	Heat flow equations – convective, conductive, and source terms	60
Tab. 9.1	Groundwater flow equations from section 8.....	80
Tab. 9.2	Heat flow equation – storage terms (relates to Tab. 7.2)	83
Tab. 9.3	Heat flow equation – convective terms (relates to Tab. 7.3)	85
Tab. 9.4	Heat flow equation – conductive terms (relates to Tab. 7.3)	87
Tab. 9.5	Heat flow equation – source terms (relates to Tab. 7.3)	87
Tab. 9.6	State variables as used in the investigated approaches	90
Tab. 9.7	Approaches for the SFCC	93
Tab. 9.8	Parameters used to evaluate the SFCC in Tab. 9.7	94
Tab. 9.9	Parameters used to evaluate equation (C.14) in Tab. 9.7.....	94
Tab. 9.10	Approaches for the relative permeability for water.....	96
Tab. 9.11	Parameters used to evaluate the equations in Tab. 9.10.....	98
Tab. 9.12	Parameters used to evaluate equation (C.7) in Tab. 9.10.....	99
Tab. B.1	Compilation of formulations for the EOS.....	153
Tab. B.2	Data for calculation of variability of state variables in case 1	155
Tab. B.3	Data for calculation of variability of state variables in case 2	156
Tab. B.4	Data for calculation of variability of state variables in case 3	157
Tab. B.5	Data for calculation of variability of state variables	158
Tab. B.6	Chosen expressions for the state variables in cases 1 to 3	159
Tab. C.1	Ranges of grain sizes characterizing clay, silt and sand.....	161
Tab. C.2	Parameters for eq. (C.10).....	163

A Appendix: Formalized test case descriptions

A.1 Test case TH2 “Frozen inclusion thaw”

Model geometry

- Dimensions: Two-dimensional
- Orientation: Horizontal
- Structure: Homogeneous
- Shape: Rectangular
 - Length (in x-direction): 3.00 m
 - Width (in y-direction): 1.00 m



General physical parameters

- Gravitational acceleration⁴⁰ g : 9.81 m/s²

Matrix parameters

- Porosity Φ : 0.37
- Water saturation curve (after /MCK 07/):

$$S_w = \begin{cases} \text{for } T > 273.15 \text{ K} & S_w = 1 \\ \text{for } T < 273.15 \text{ K} & S_w = (1 - S_{w \text{ res}}) \cdot e^{\left\{-\left[\frac{T-273.15}{W}\right]^2\right\}} + S_{w \text{ res}} \end{cases}$$

with $S_{w \text{ res}} = 0.05$, $W = 0.5$

- Absolute permeability k : $1.3 \cdot 10^{-10} \text{ m}^2$
- Absolute hydraulic conductivity K : $K = (k \rho_w g) / \eta$
- Relative hydraulic conductivity (after /MCK 07/):
 $K_r = \max(10^{-6}, 10^{-\Phi \Omega (1 - S_w)})$ with $\Omega = 50$
- Thermal conductivity of the solid matrix λ_s : 9.0 W/(m K)
- Specific heat capacity of the solid matrix $c_{s \text{ s}}$: 835 J/(kg K)
- Compressibility β : $10^{-8} \text{ (m s}^2\text{)/kg}$ (matrix plus water)
- Density of solid grains ρ_s : 2650 kg/m³

⁴⁰ This declaration is given in /GRE 18/ but appears to be rather pointless since the 2D-model is horizontal.

Fluid parameters

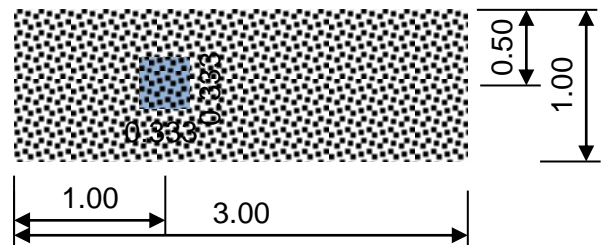
- Water
 - Thermal conductivity λ_w : 0.6 W/(m K)
 - Specific heat capacity $c_{s,w}$: 4182 J/(kg K)
 - Density ρ_w : 1000 kg/m³
 - Viscosity η_w : $1.793 \cdot 10^{-3}$ kg/(m s)
 - Latent heat of fusion L : 340 J/kg
- Ice
 - Thermal conductivity λ_i : 2.14 W/(m K)
 - Specific heat capacity $c_{s,i}$: 2060 J/(kg K)
 - Density ρ_i : 920 kg/m³

Bulk properties

- Bulk thermal conductivity: $\lambda_b = \Phi S_w \lambda_w + \Phi (1-S_w) \lambda_i + (1-\Phi) \lambda_m$

Initial conditions

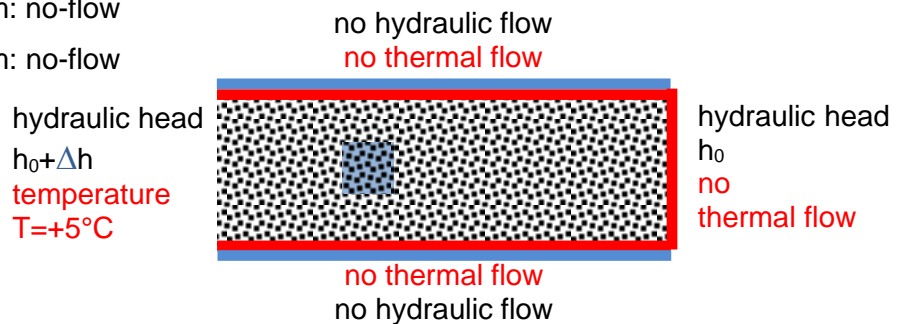
- Steady-state flow
- Two domains of constant temperature
 - All over the model: $T = +5$ °C
 - Except in a square area: $T = -5$ °C
 - Geometry of the square area
 - Side length: 0.333 m
 - Centre at: $x = 1.00$ m
 $y = 0.50$ m



Boundary conditions

- Hydraulic boundary conditions
 - Dirichlet-boundaries
 - at $x=0.00$ m: constant hydraulic head $h_0 + \Delta h$
 h_0 is arbitrary
 $\Delta h = 0.00$ m and 0.27 m, respectively
 - at $x = 3.00$ m: constant hydraulic head h_0

- Neumann-boundaries
 - at $y = 0.00$ m: no-flow
 - at $y = 1.00$ m: no-flow
- Thermal boundary conditions
 - Dirichlet-boundaries
 - at $x = 0.00$ m: constant temperature $T = +5$ °C
 - Neumann-boundaries
 - at $x = 3.00$ m: no-flow
 - at $y = 0.00$ m: no-flow
 - at $y = 1.00$ m: no-flow



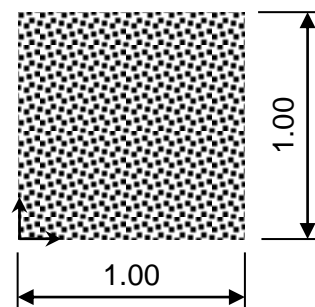
Expected results

- Contour plots: Hydraulic head and temperature at time 22,860 s (6.4 h); this should be shortly before the threshold time when the minimum temperature rises above 0 °C.
- Line plots along $y=0.50$ m:
 - Without advection: at $t=0$ s, $t=1260$ s, and $t= 5.9$ days
 - With advection ($\Delta h=0.27$ m; gradient 9%): at $t=0$ s, $t= 930$ s, and $t= 16.6$ h

A.2 Test case TH3 “Talík Opening/Closure”

Model geometry

- Dimensions: Two-dimensional
- Orientation: Horizontal
- Structure: Homogeneous
- Shape: Quadratic, side length: 1.00 m



General physical parameters

- Gravitational acceleration g : 9.81 m/s²

Matrix parameters

- Porosity Φ : 0.37
- Water saturation curve (after /MCK 07/):

$$S_w = \begin{cases} \text{for } T > 273.15 \text{ K} & S_w = 1 \\ \text{for } T < 273.15 \text{ K} & S_w = (1 - S_{w \text{ res}}) \cdot e^{\left\{-\left[\frac{T-273.15}{W}\right]^2\right\}} + S_{w \text{ res}} \end{cases}$$
- with $S_{w \text{ res}} = 0.05, W = 0.5$
- Absolute permeability k : $1.3 \cdot 10^{-10} \text{ m}^2$
- Absolute hydraulic conductivity K : $K = (k \rho_w g) / \eta$
- Relative hydraulic conductivity (after /MCK 07/):

$$k_r = \max(10^{-6}, 10^{-\Phi \Omega (1 - S_w)}) \text{ with } \Omega = 50$$
- Thermal conductivity of the solid matrix λ_s : 9.0 W/(m K)
- Specific heat capacity of the solid matrix $c_{s \text{ m}}$: 835 J/(kg K)
- Compressibility β : $10^{-8} \text{ (m s}^2\text{)/kg}$ (matrix plus water)
- Density of the solid grains ρ_s : 2650 kg/m³

Fluid parameters

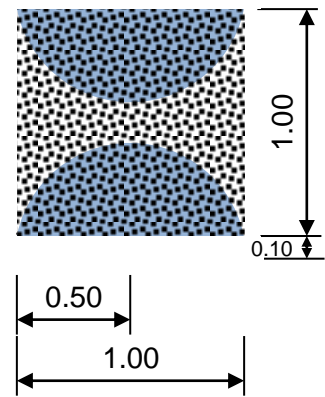
- Water
 - Thermal conductivity λ_w : 0.6 W/(m K)
 - Specific heat capacity $c_{s \text{ w}}$: 4182 J/(kg K)
 - Density ρ_w : 1000 kg/m³
 - Viscosity η_w : $1.793 \cdot 10^{-3} \text{ kg/(m s)}$
 - Latent heat of fusion L : 340 J/kg
- Ice
 - Thermal conductivity λ_i : 2.14 W/(m K)
 - Specific heat capacity $c_{s \text{ i}}$: 2060 J/(kg K)
 - Density ρ_i : 920 kg/m³

Bulk properties

- Bulk thermal conductivity: $\lambda_b = \Phi S_w \lambda_w + \Phi (1 - S_w) \lambda_i + (1 - \Phi) \lambda_m$

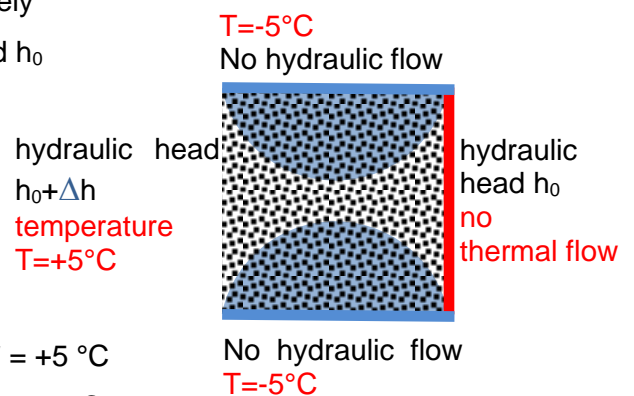
Initial conditions

- Steady-state flow
- Two domains of constant temperature
 - All over the model: $T = +5\text{ }^\circ\text{C}$
 - Except in two almost semi-circular areas: $T = -5\text{ }^\circ\text{C}$
 - Geometry of these semi-circular areas
 - radius: 0.5099 m
 - centres at: $x = 0.50\text{ m}, y = -0.10\text{ m}$
 $x = 0.50\text{ m}, y = 1.10\text{ m}$



Boundary conditions

- Hydraulic boundary conditions
 - Dirichlet-boundaries
 - at $x = 0.00\text{ m}$: constant hydraulic head $h_0 + \Delta h$;
 h_0 is arbitrary
 $\Delta h = 0.00\text{ m}$ and 0.09 m , respectively
 - at $x = 1.00\text{ m}$: constant hydraulic head h_0
 - Neumann-boundaries
 - at $y = 0.00\text{ m}$: no-flow
 - at $y = 1.00\text{ m}$: no-flow
- Thermal boundary conditions
 - Dirichlet-boundaries
 - at $x = 0.00\text{ m}$: constant temperature $T = +5\text{ }^\circ\text{C}$
 - at $y = 0.00\text{ m}$: constant temperature $T = -5\text{ }^\circ\text{C}$
 - at $y = 1.00\text{ m}$: constant temperature $T = -5\text{ }^\circ\text{C}$
 - Neumann-boundaries
 - at $x = 1.00\text{ m}$: no-flow



Expected results

- Contour plots: Hydraulic head and temperature at time 19,860 s (5.5 h)
- Line plots along $x = 0.50\text{ m}$:
 - Without advection: at $t = 0$, $t = 120\text{ s}$, and $t = 2.71\text{ d}$
 - With advection ($\Delta h = 0.09\text{ m}$; gradient 9%): at $t = 0\text{ s}$, $t = 765\text{ s}$, and $t = 2.07\text{ d}$

B Appendix: State variables including subzero temperatures

B.1 Data and formulations

In the context of CO₂-sequestration and when the groundwater flow code d^{3f}++ has been extended to include non-isothermal problems, two relating reports were written to compile formulations for the state variables: /KRÖ 08/ and /KRÖ 10/. While all state variables that are of interest here were covered, the lowest temperature considered had been 0 °C. Additional data has therefore been collected in the present work to supplement the already existing formulations.

In general, there are not many sources providing data for state variables of water⁴¹ in the subzero temperature domain, particularly where pressure-dependencies are concerned. However, also analytical formulations can be found in the literature. Their complexity increases with the range of validity for temperatures and pressures that are covered as well as with the desired degree of accuracy. In a considerable number of cases, quite some computational effort for evaluation of these formulations is thus required.

In the light of the rather limited temperature and pressure ranges that are of interest here, more straightforward simple approaches are therefore derived in the following for $-20\text{ °C} < T < +20\text{ °C}$ and $0.1\text{ MPa} < p < 10\text{ MPa}$. Basis of these approaches are the available data that are basically representing the conditions under atmospheric pressure as well as already established formulations providing pressure dependencies. In a first step, data for state variables at atmospheric pressure are compiled from which the new approaches are derived. In the second step, these new approaches are modified to cover also the pressure-dependency as guided by the existing formulations. In all functions presented in this subsection, the temperature has the dimension [°C] and pressure the dimension [MPa].

⁴¹ Note that a dependence on pressure is assumed here to apply to water only.

Remarks on rock characteristics as used further on:

(1) The term “rock” is used in the sense of granite, an igneous rock, further on. Data for “rock” derived in the following are thus strictly speaking applicable for granite only.

(2) With respect to thermal conductivity and heat capacity, water in the pore space of granite is hardly noticeable even if a porosity of 1 % is considered /KRÖ 10/. The data provided in the following represent therefore basically dry rock.

(3) Data for rock below 0 °C were not explicitly sought. There is no reason to suspect sudden changes in the EOS for the pure rock material at the freezing point of water. Instead, it is assumed here that the known EOS for rock can be extrapolated based on the known trends for temperatures above 0 °C as only a rather narrow additional subzero temperature range is required for the purpose at hand.

B.1.1 Density

Water⁴²

The water density has been measured for each full degree Celsius down to -10 °C and then in steps of 5 °C down to -30 °C /CRC 86/. Further data has been found in /LAN 72/. As should be expected, the subzero data fit matches the quite precise data from /IAP 97/ at 0 °C very well. A formulation for subzero temperatures is presented in /IAP 15/. In the pressure range of interest here, the uncertainty is stated to be less than 0.04 % down to 239 K. The accuracy of an analytical formulation fitted to the formulation from /IAP 15/ can thus safely be assumed to be high. Proposed for subzero temperatures at atmospheric pressure is formulation (B.1) which is restricted to temperatures in the range -20 °C < T < +20 °C but much easier to evaluate. The match of data points and analytical formulation (B.1) is depicted in Fig. B.1.

$$\rho_w(T) = 999.974 - (0.0075 + 0.001 * a) * (T - 4)^2 \tag{ B.1 }$$
$$+ (1.5 * 10^{-4} - 5 * 10^{-5} * a * (T - 4)^3 \quad ; a = (\text{sign}(T - 4) + 1) / 2)$$

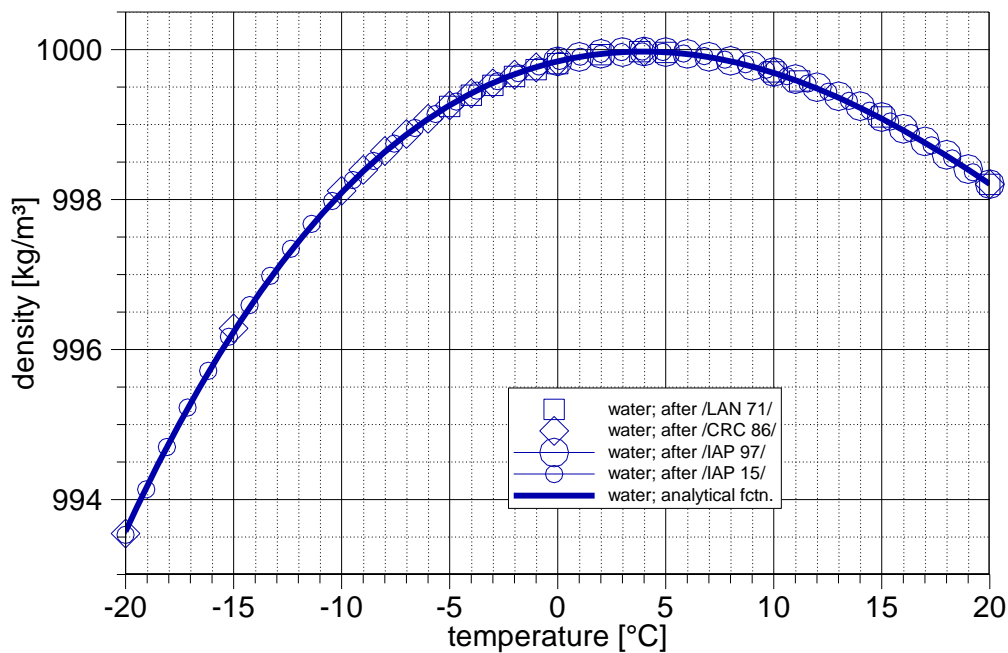


Fig. B.1 Data and formulations for water density at atmospheric pressure

⁴² Data sources: /CRC 86/, /LAN 72/, /IAP 97/, /IAP 15/

The formulations from /IAP 15/ are assumed to represent the dependence of the water density on pressure sufficiently accurate to use them as a reference for the new approach (B.2) based on equation (B.1). The curves from /IAP 15/ and the results from equation (B.2) are compared in Fig. B.2.

$$\rho_w(p, T) = \rho_w(T) + (0.0025 * \rho_w(T) - 0.0205 * T + 5 * 10^{-4} * T^2) * \frac{p - 0.1}{4.9} - \left(\frac{p}{20}\right)^4 \quad (\text{B.2})$$

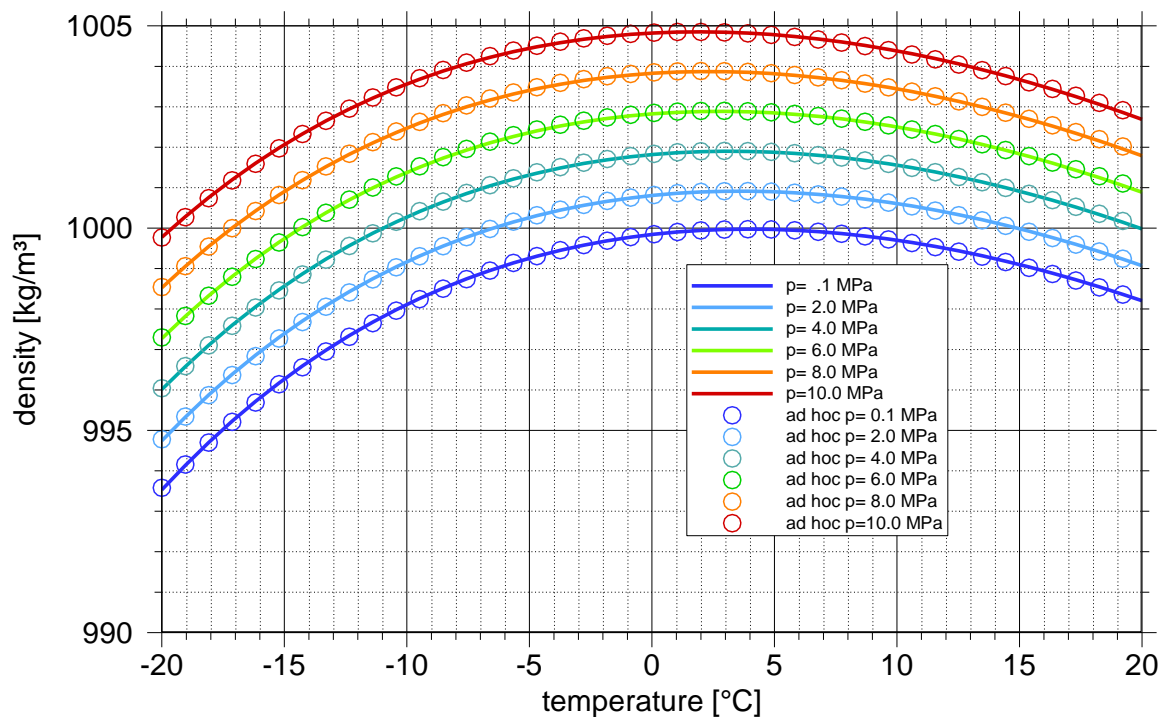


Fig. B.2 Density of water as a function of temperature and pressure

Ice⁴³

For the density of ice, only four data points between -40 °C and 0 °C could be identified. They appear to relate rather stringently to a straight line. At that, the data point at -40 °C is particularly helpful. Adopted is therefore the analytical formulation (B.3) whose match with the data can be checked in Fig. B.3.

⁴³ Data sources: /LAN 82/, /LAN 72/

$$\rho = -0.15 * T + 917$$

(B.3)

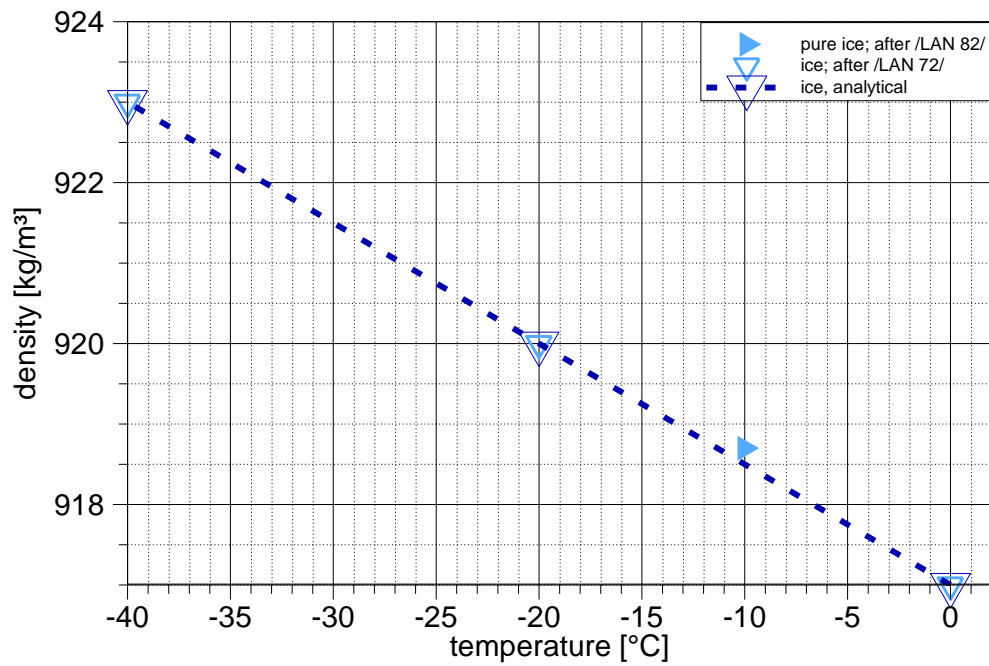


Fig. B.3 Data and ad hoc formulation for the ice density

Rock⁴⁴

The density of rock appears to be more or less independent of temperature and pressure for all practical purposes /KRÖ 10/.

⁴⁴ From /KRÖ 10/, based on /LAN 82/

B.1.2 Viscosity

Water⁴⁵

Data for the viscosity of water below 0 °C are available from different sources compiled in /LAN 69/ at a distance of 1 °C down to -20 °C meaning that the data density is quite high. Furthermore, there are formulations from /IAP 03/ and /IAP 08/ that can be considered to be highly reliable⁴⁶. Based on these data, the analytical formulation (B.4) has been derived which is compared to the data in Fig. B.4:

$$\begin{aligned} \eta_w(T) = & 0.00439 - 8.475 \cdot 10^{-5} \cdot (T + 20) + 2.25 \cdot 10^{-6} \cdot (T - 20) \\ & * (T + 20) - 6 \cdot 10^{-8} \cdot (T - 20) * (T + 20) * T \\ & + 1.45 \cdot 10^{-9} \cdot (T - 20) * (T + 20) * T^2 \end{aligned} \quad (\text{B.4})$$

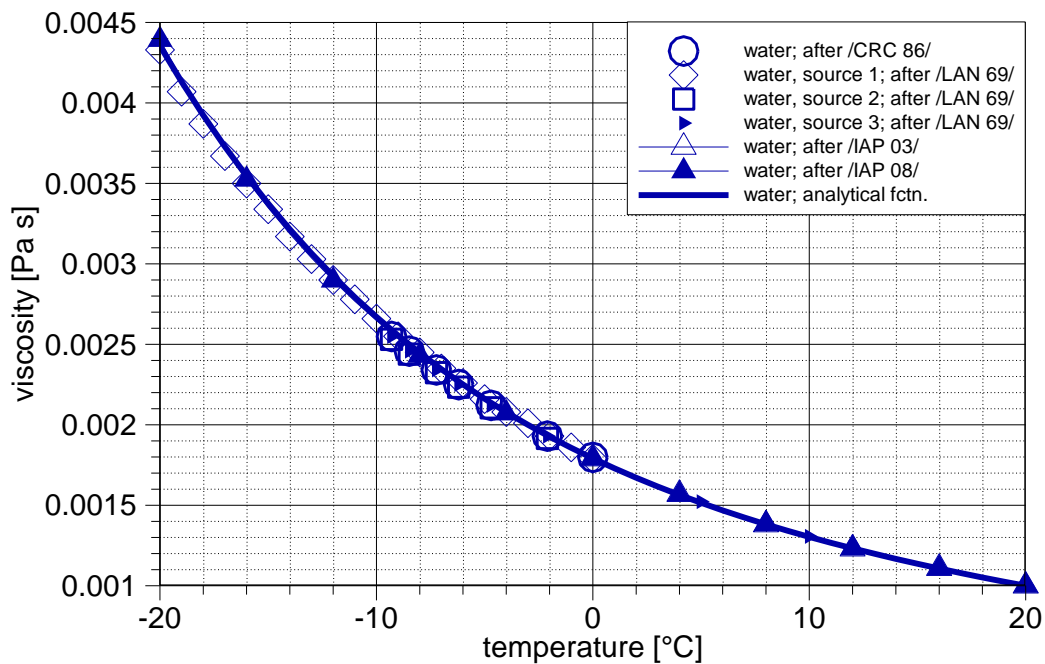


Fig. B.4 Data and formulations for water viscosity at atmospheric pressure

⁴⁵ Data sources: /CRC 86/, /LAN 69/, /IAP 03/, /IAP 08/

⁴⁶ "For the metastable subcooled liquid at atmospheric pressure, Eq. (10)..." (the formulation for viscosity) "...is in fair agreement (within 5 %) with available data down to 250 K." /IAP 08/.

The formulations from /IAP 08/ are assumed to represent the dependence of the water viscosity on pressure sufficiently accurate to use them as a reference for a new approach (B.5) are compared in Fig. B.5.

$$\eta_w(p, T) = \eta_w(T) * \left[1 + (3.4 * 10^{-4} * (T + 20) - 0.017) * \frac{p - 0.1}{4.9} \right] \quad (B.5)$$

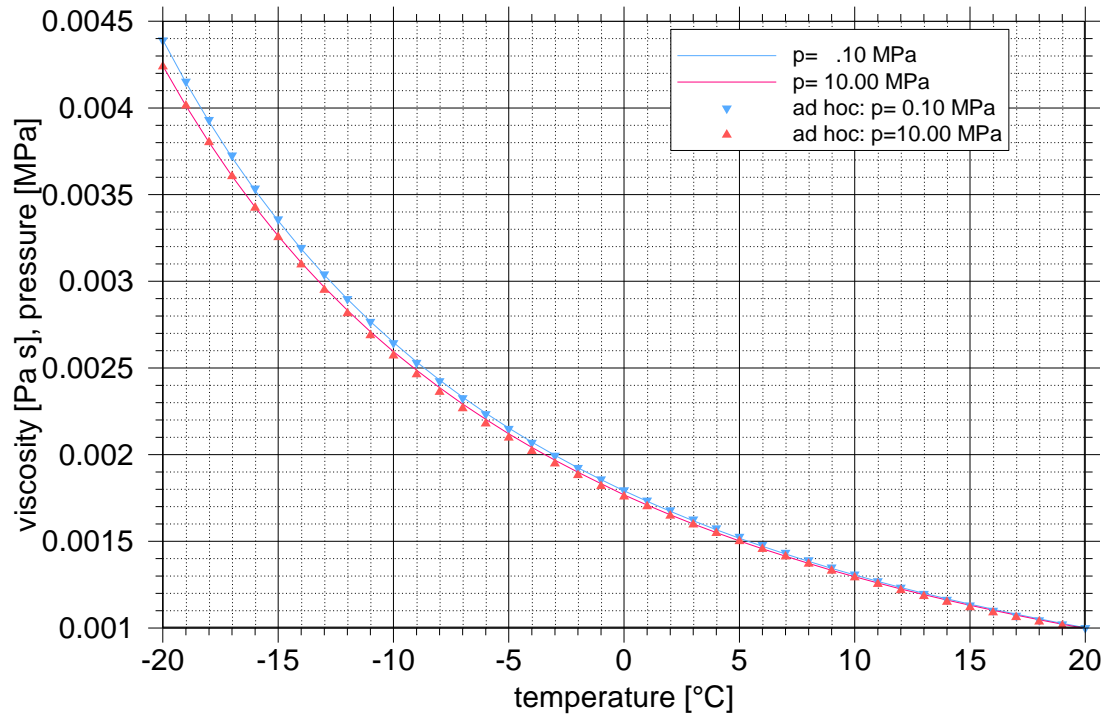


Fig. B.5 Viscosity of water as a function of temperature and pressure

Ice and rock

Viscosity of ice and rock is considered to be negligible.

B.1.3 Thermal conductivity

Water⁴⁷

Not that many data are apparently known to represent the thermal conductivity of water below the freezing point. Some could be found in /LAN 72/ and /CRC 86/. They reach down to -23 °C, show a slight scatter and appear to follow a straight line. However, there is also a formulation from /IAP 11/ that has a curvature not only above 0 °C (as the data from /CRC 86/) but also below. Concerning accuracy, the statement in the footnote to subzero temperature viscosity applies here as well. As the IAPWS has scrutinized the available data from the literature to a much higher degree than could possibly be done in the framework of the present work, highest confidence is given to the formulation from /IAP 11/. A referring analytical formulation that is restricted to the temperature range between -20 °C and +20 °C may read as in (B.6). This ad hoc formulation is compared graphically in Fig. B.6 to the data and other formulation.

$$\lambda_w(T) = 0.55559 + 0.0027 * T - 3 * 10^{-5} * (T + 1.5)^2 - 4 * 10^{-7} * (T - 0.5)^3 \quad (\text{B.6})$$

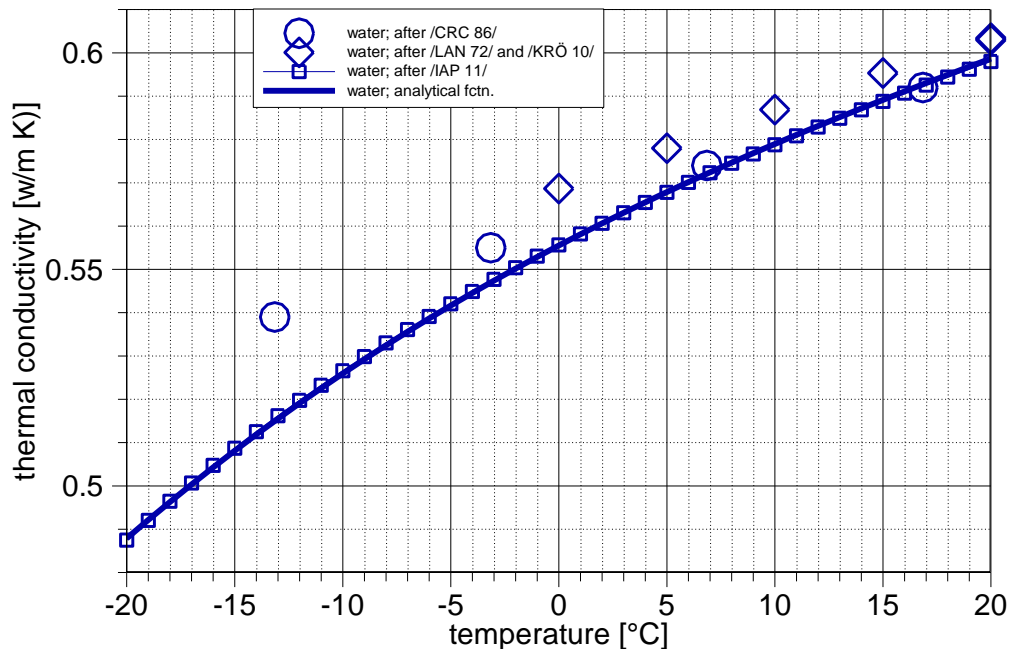


Fig. B.6 Data and formulations for thermal conductivity of water

⁴⁷ Data sources: /CRC 86/, /LAN 72/, /KRÖ 10/, /IAP 11/

The formulations from /IAP 11/ are assumed to represent the dependence of the water thermal conductivity on pressure sufficiently accurate to use them as a reference for a new approach (B.7) based on equation (B.6). The curves from /IAP 11/ and the resulting equation (B.7) are compared in Fig. B.7.

$$\lambda_w(p, T) = \lambda_w(T) * \left[1 + (7 * 10^{-3} - 1.8 * 10^{-4} * T) * \frac{p - 0.1}{4.9} + \left(\frac{p}{20} \right)^2 \right] \quad (B.7)$$

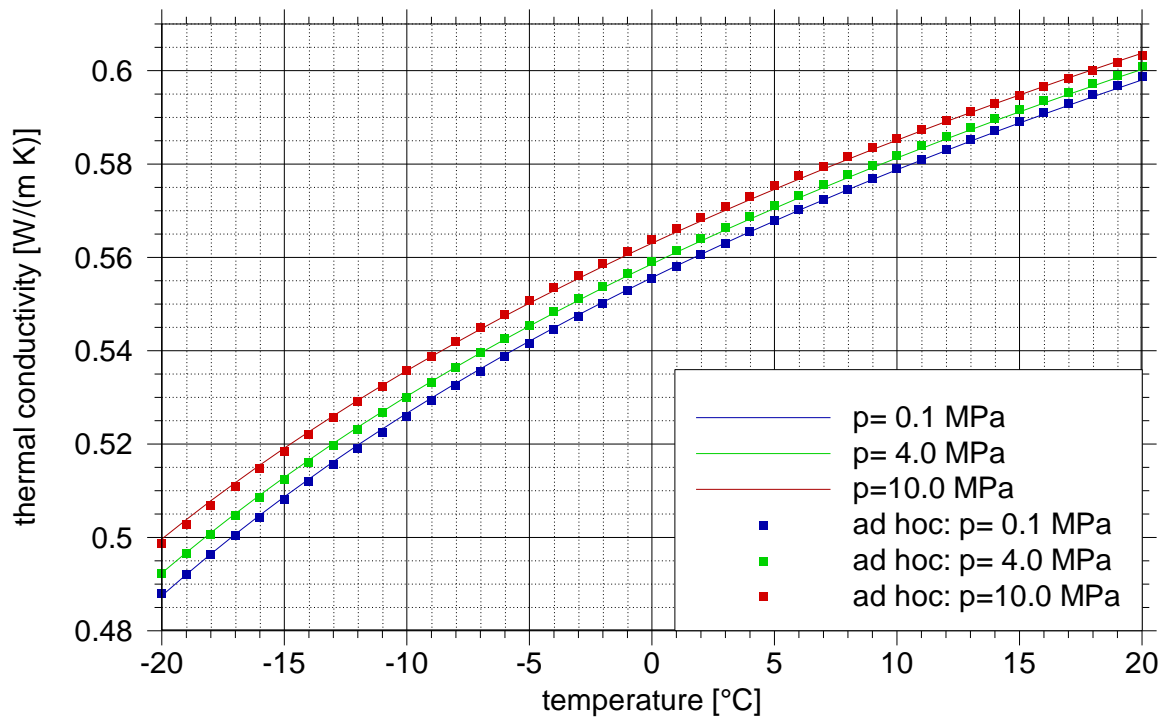


Fig. B.7 Thermal conductivity of water as a function of temperature and pressure

Ice⁴⁸

The data for the thermal conductivity of ice are rather scarce adding up to only 4 data points between -40 °C and 0 °C. /LAN 82/ nevertheless presents a formula to describe this as an EOS. However, it contradicts earlier data from /LAN 72/ even if not so much in the trend than in the absolute values. Analytical formulation (B.8) has therefore been derived and is graphically compared with data from the literature in Fig. B.8.

$$\lambda = -0.009 * T + 2.2558 \quad (B.8)$$

⁴⁸ Data sources: /LAN 72/, /LAN 82/

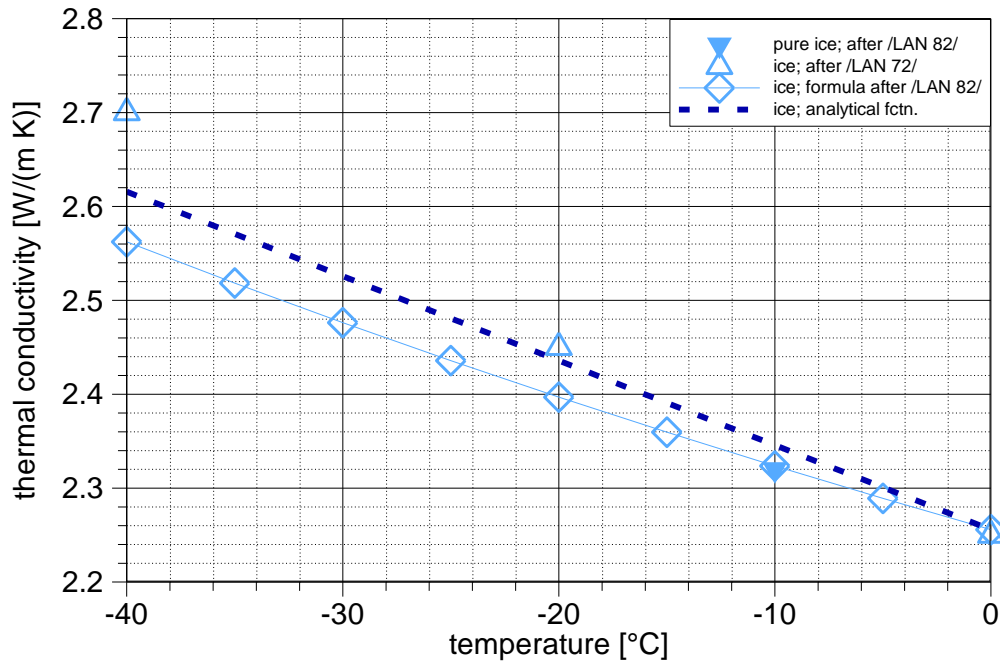


Fig. B.8 Data and formulation for thermal conductivity of ice

Rock⁴⁹

Since “rock” may be of different type (igneous, metamorphic, sedimentary) and be differently composed at that, it cannot be defined as a pure substance like water. The thermal conductivity of dry rock has been found to be varying between 2 and 6 W/(m K) at 25 °C leading to bounding curves as described in /KRÖ 10/. As a first approximation following /LAN 82/, equation (B.9) is thus proposed for cases where this property is not known from measurements. As this formulation is valid for temperatures between 0 °C up to 1200 °C is assumed that the range of validity can safely be extended to -20 °C.

$$\lambda(T) = 3.6 - 0.49 \cdot 10^{-2} T + 0.61 \cdot 10^{-5} T^2 - 2.58 \cdot 10^{-9} T^3 \quad \text{with } T \text{ in } [^{\circ}\text{C}] \quad (\text{B.9})$$

Equation (B.9) is visualized in Fig. B.9 together with the bounding cases from /KRÖ 10/. As indicated, the actual thermal conductivity might differ from formulation (B.9) by a factor of about 1.8 in both directions.

⁴⁹ After discussion in /KRÖ 10/, based on data from /LAN 82/ and /VOS03/

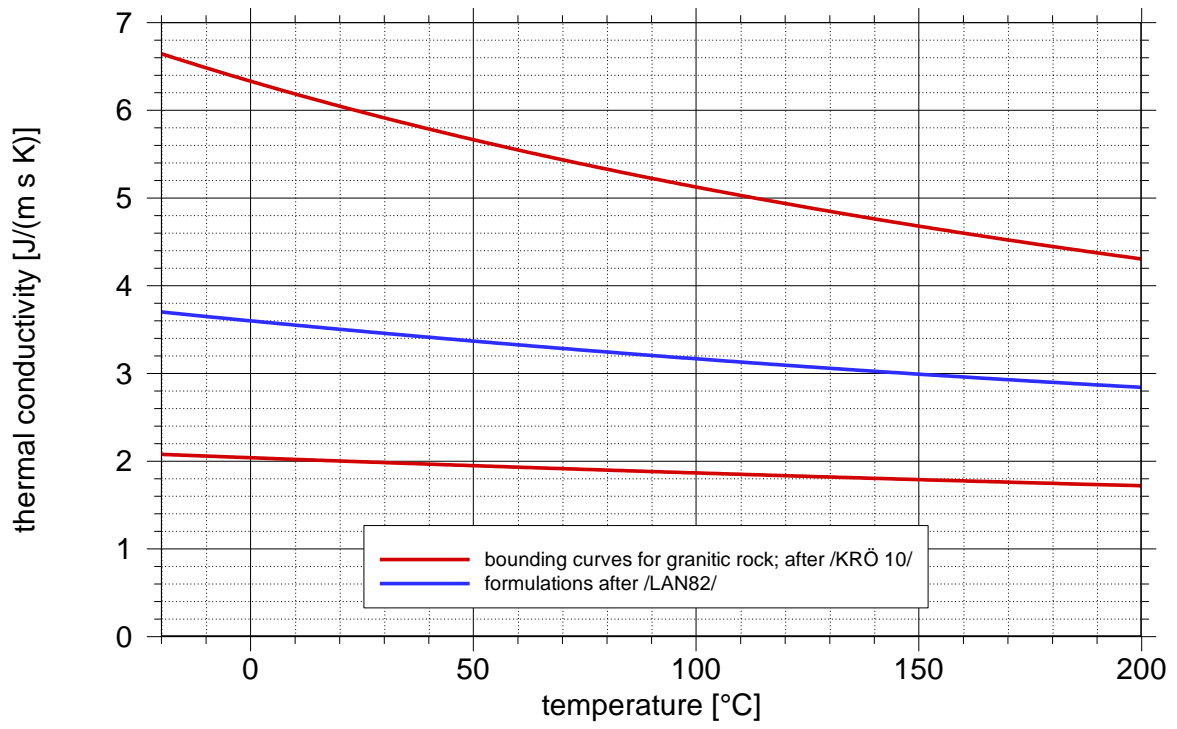


Fig. B.9 Thermal conductivity of granite according to /LAN 82/

B.1.5 Heat capacity

Water⁵⁰

Data for heat capacity of water for temperatures below 0 °C seem to be particularly hard to come by. Only data down to -3 °C have been found. However, there is a formulation from /IAP 15/ for supercooled water that is consistent with the approach from /IAP 97/ for the much better-known data above 0 °C. The formulation from /IAP 15/ is thus taken to be a reference here. The analytical formulation (B.10) for the temperature range between -20 °C and +20 °C has been developed for easier application. All cited data and formulations are shown in Fig. B.10 for graphic comparison.

$$c_{s,w}(T) = \left[4.179 + 3 \cdot 10^{-5} \cdot (0.5 \cdot \hat{T})^2 - 3 \cdot 10^{-7} \cdot \hat{T}^3 - 6 \cdot 10^{-11} \cdot (0.95 \cdot \hat{T})^5 - 2 \cdot 10^{-14} \cdot \hat{T}^7 - 4.5 \cdot 10^{-18} \cdot \hat{T}^9 \right] \cdot 1000 \left[\frac{\text{J}}{\text{kg K}} \right] \quad (\text{B.10})$$

with $\hat{T} = T - 40$

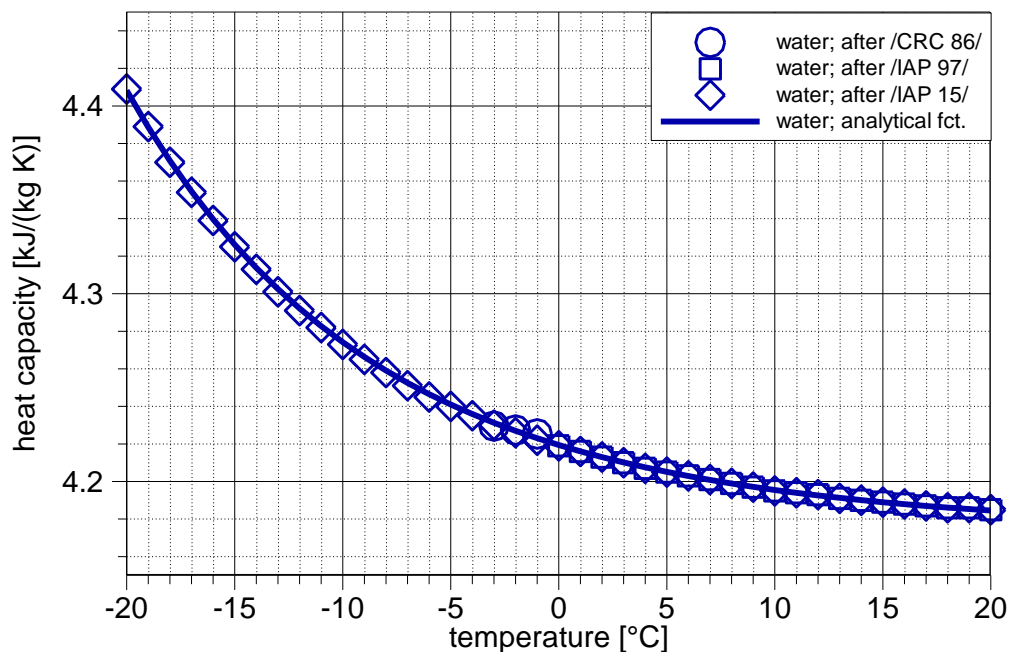


Fig. B.10 Data and formulations for heat capacity of water

⁵⁰ Data sources: /CRC 86/, /IAP 97/, /IAP 15/

The formulations from /IAP 15/ are assumed to represent the dependence of the water thermal conductivity on pressure sufficiently accurate to use them as a reference for a new approach (B.11) based on equation (B.10). The curves from /IAP 15/ and the resulting equation (B.11) are compared in Fig. B.11.

$$c_{s,w}(p,T) = c_{s,w}(T) - 0.03 * p^* * \left[\frac{1 - 0.4 * T^* + 0.15(T^*)^2}{+0.10 * (T^*)^3 + 0.015 * (T^*)^5} \right] \quad (\text{B.11})$$

with $p^* = \frac{p - 0.1}{9.9}$ and $T^* = \frac{T - 20}{20}$

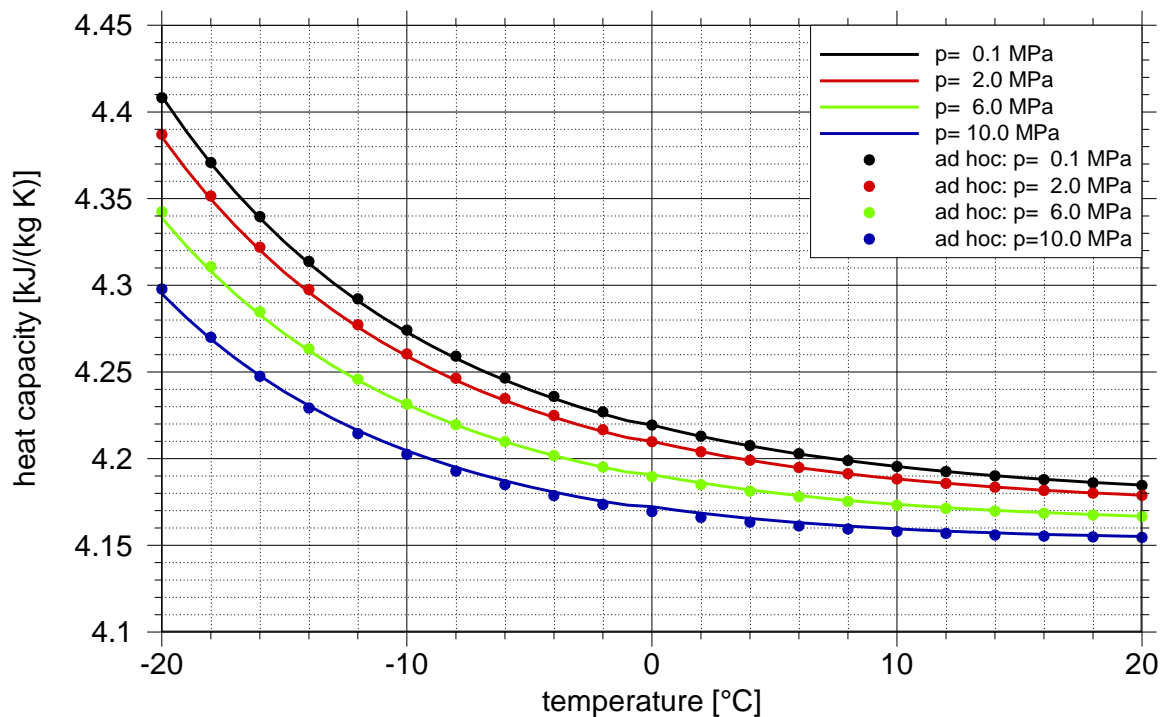


Fig. B.11 Heat capacity of water as a function of temperature and pressure

Ice⁵¹

The data from /LAN 82/ covers a temperature range down to -22 °C but are seemingly suffering from an insufficient number of digits after the decimal point (see Fig. B.12). There are enough data, though, to find an analytical formulation that follows the resulting

⁵¹ Data source: /LAN 82/

stepwise data curve continuously in a reasonably matching way. This function has been found with (B.12) and is compared with the data in Fig. B.12.

$$c_s = [2.1 + 0.0085 * (T + 2) - (T + 2) * (T + 22) * 0.00015] * 1000 \left[\frac{\text{J}}{\text{kg K}} \right] \quad (\text{ B.12 })$$

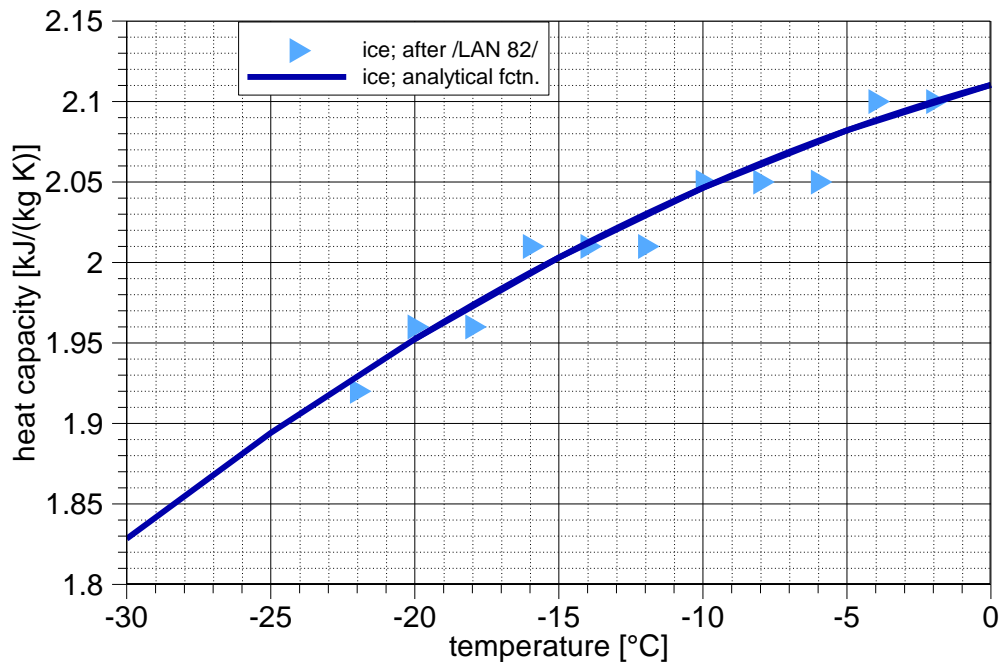


Fig. B.12 Data and formulation for heat capacity of ice

Rock⁵²

For igneous rock, there exists data for the heat capacity from /VOS 03/ for the temperature range between 10 °C and 300 °C. An ad hoc analytical formulation for this range is given in /KRÖ 10/:

$$c_s(T) = \frac{110}{300} * T - 130 * e^{-\frac{T}{70}} + 860 \quad \text{with } T \text{ in } [^{\circ}\text{C}] \quad (\text{ B.13 })$$

However, it is not entirely clear, if this formulation can safely be extrapolated into the subzero temperature range. A hint about the trend might be drawn from the “general formulation” provided by /LAN 82/ that indicates the trend probably more reliable:

⁵² After discussion in /KRÖ 10/ based on /VOS 03/

$$c_s(T) = 754 * \left(1 + 6.14 \cdot 10^{-4} * T - 19280 / T^2 \right) \text{ with } T \text{ in [K], } c \text{ in [J/(kg K)]} \quad (\text{B.14})$$

Function (B.14) is therefore extended into the subzero temperature range and depicted in Fig. B.13 together with formulation (B.15), a modification of function (B.13), that is adopted here for application to temperatures down to -20 °C:

$$c_s(T) = \frac{110}{300} * T - 130 * e^{-\frac{T}{90}} + 870 \text{ with } T \text{ in [}^\circ\text{C]} \quad (\text{B.15})$$

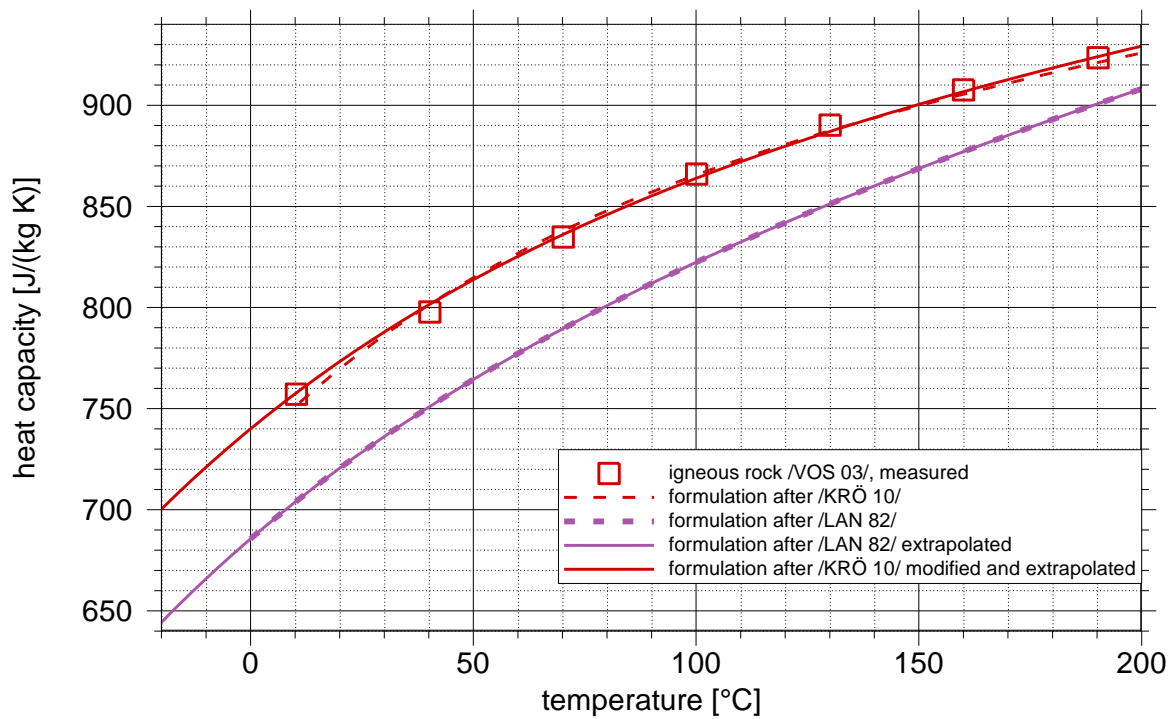


Fig. B.13 Heat capacity of igneous rock

B.2 Full range of primary variables T and p as considered in case 1

B.2.1 Density

Water and ice

The analytical formulations from /IAP 15/ for water (see appendix D.1) as well as the approach (B.3) for ice are shown together in Fig. B.14. A phase change between liquid and solid phase is accompanied by a considerable jump in density. Note that water boils above 100 °C at atmospheric pressure and close to 180 °C at 1 MPa. The jump between liquid and vapour phase is even higher than between water and ice and therefore outside the plot scale.

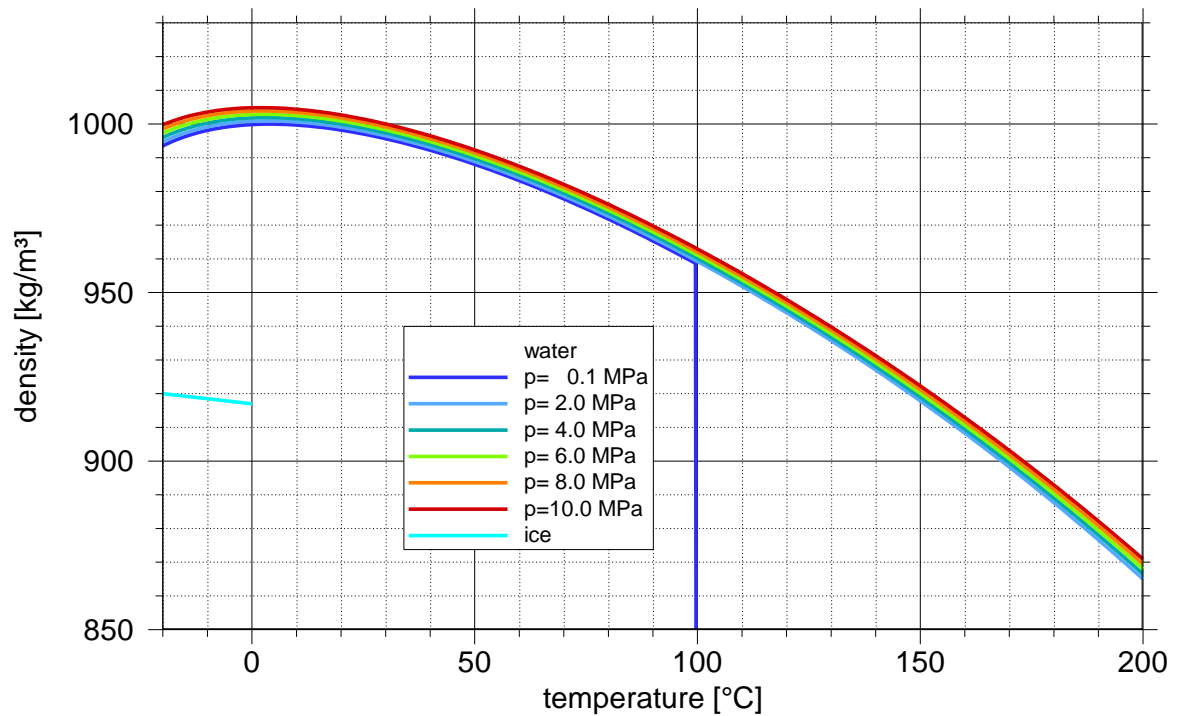


Fig. B.14 Density of water and ice in the whole considered temperature range

Rock

The density of rock is more or less independent of temperature and pressure /KRÖ 10/.

B.2.2 Viscosity

Since ice and rock are assumed to be immobile as already defined in section 6.2.1, viscosity is only relevant for water. Consequently, Fig. B.15 depicts only an evaluation of the formulations from /IAP 08/ (see appendix D.2). Note that the variability of the viscosity with pressure while present cannot be resolved with the chosen line thickness in this figure.

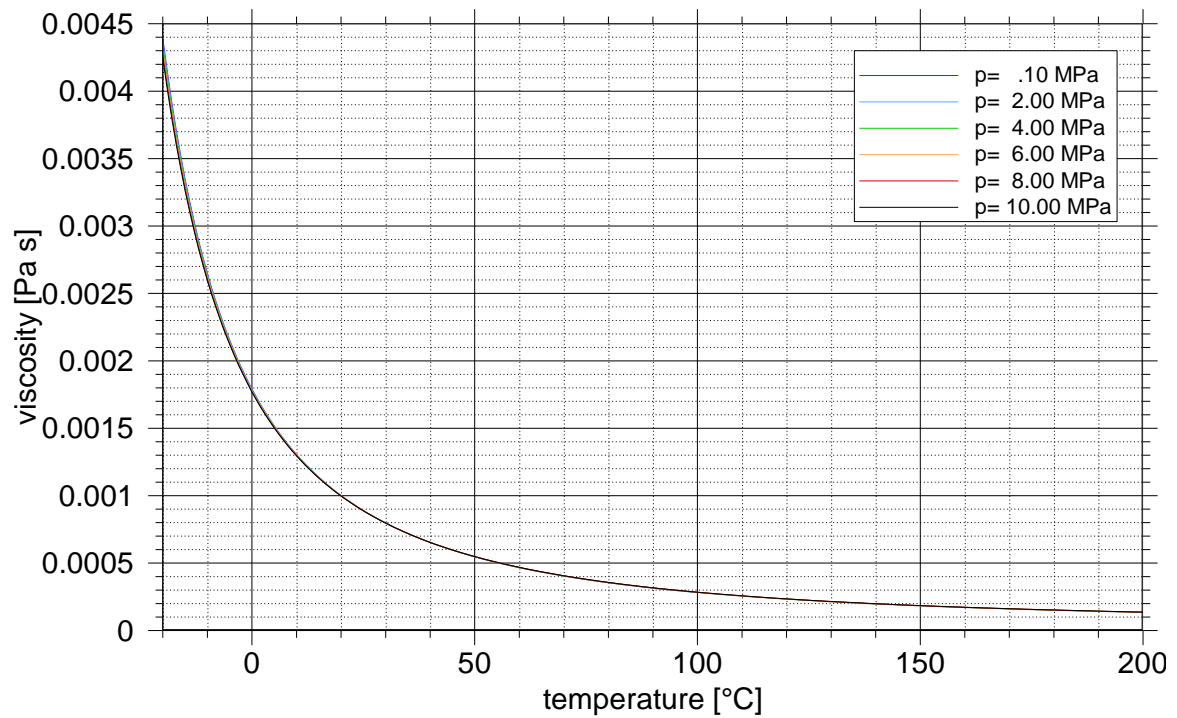


Fig. B.15 Viscosity of water in the whole considered temperature range

B.2.3 Thermal conductivity

Water and ice

The analytical formulations from /IAP 11/ for water (see appendix D.3) as well as the approach (B.8) for ice are shown together in Fig. B.16. An influence of pressure on the thermal conductivity in the range up to 5 MPa can hardly be observed. Much more important is the considerable relative change of values in case of a phase change.

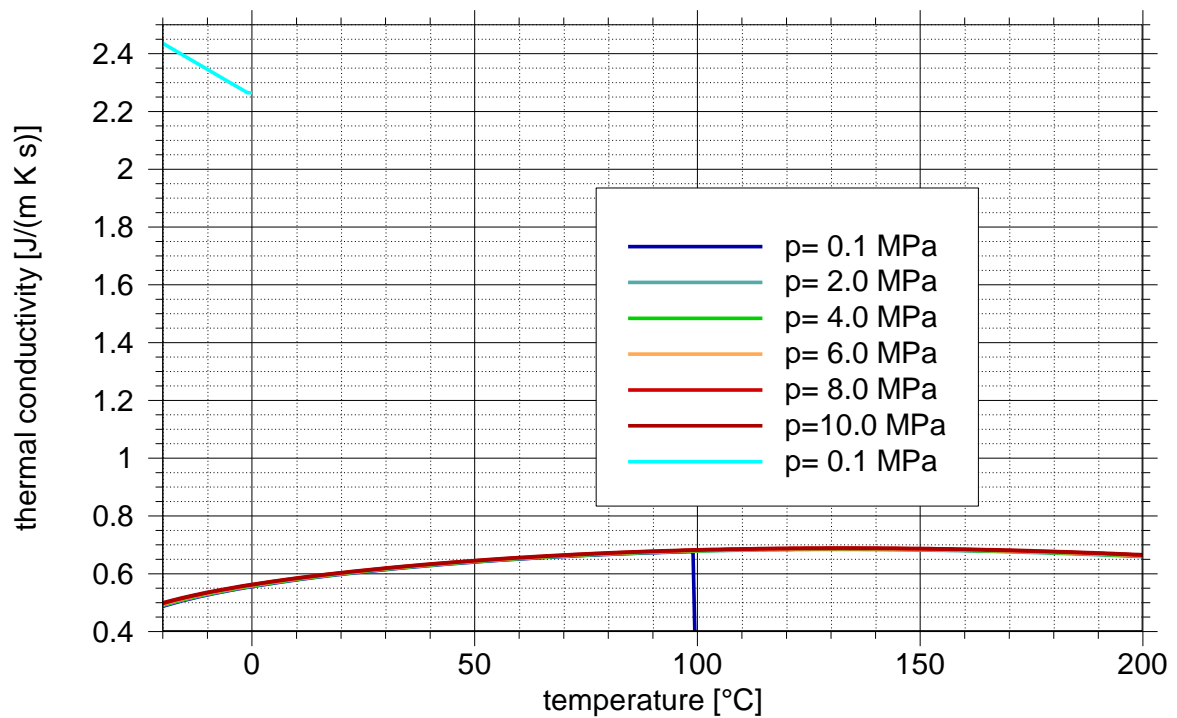


Fig. B.16 Thermal conductivity of water and ice in the whole temperature range

Rock

As pointed out in section B.1.3, formula (B.9) from /LAN 82/, depicted in Fig. B.17 is adopted here but can be treated only as a first approximation as the thermal conductivity is quite rock specific even if only ingenuous rock is considered.

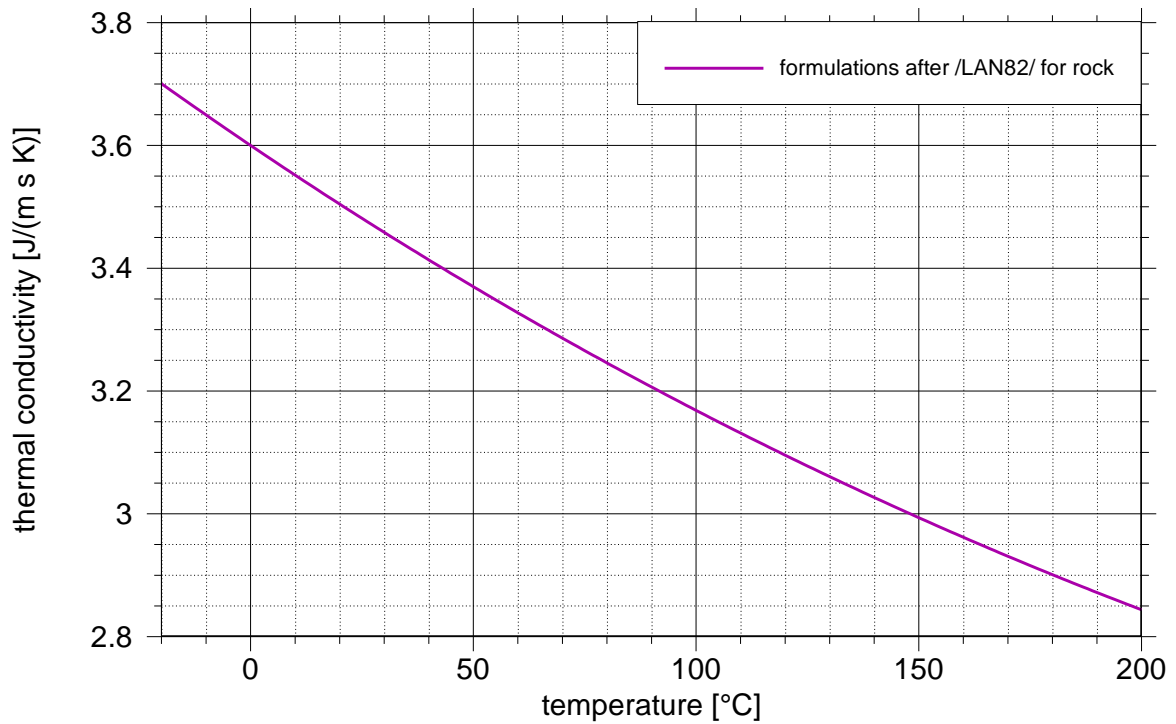


Fig. B.17 Thermal conductivity of the rock

B.2.4 Heat capacity

Water and ice

The full spectrum of the specific heat capacity for water and ice between -20 °C and 200 °C as well as 0.1 MPa and 10 MPa calculated after /IAP 15/ (see appendix D.4) and after the new approach for ice (B.12), respectively, is shown in Fig. B.18. Towards the lower temperatures, the pressure dependency becomes more pronounced. To a somewhat lesser extent this applies also to temperatures above 150 °C.

Rock

After the discussion in section B.1.4, formulation (B.15) as depicted in Fig. B.19, is adopted for the specific heat of igneous rock. Note that this formulation should be replaced if specific data for a particular problem are known.

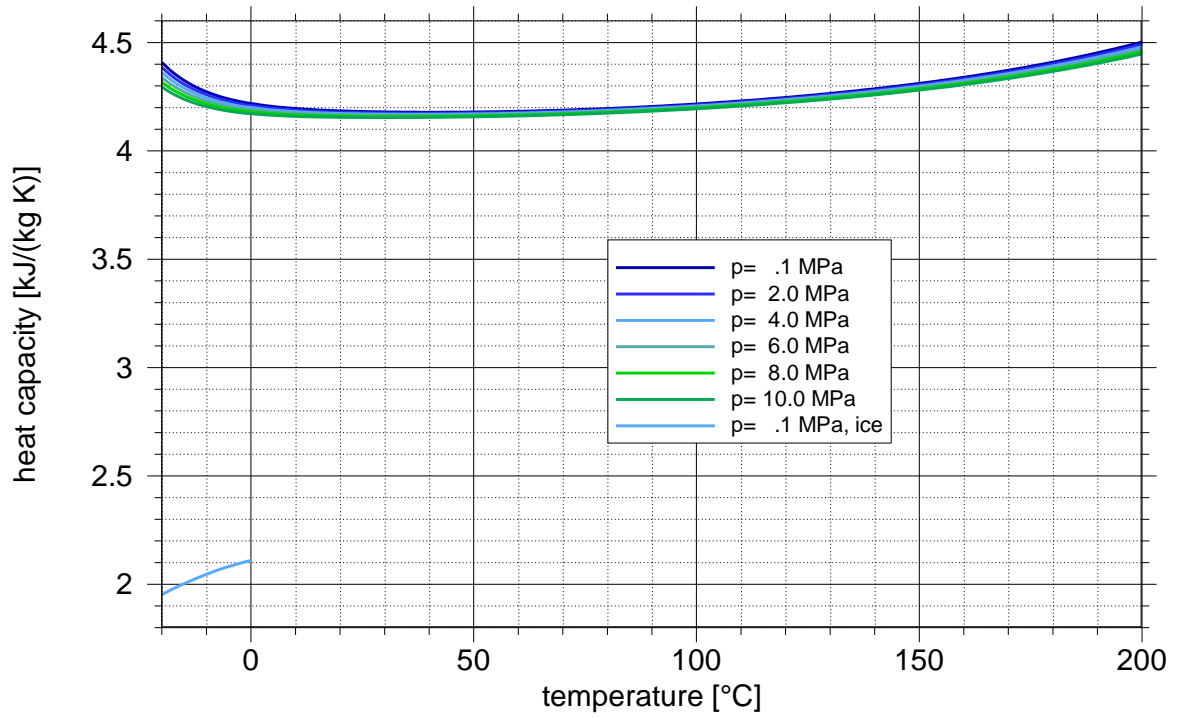


Fig. B.18 Heat capacity of water and ice in the whole considered temperature range

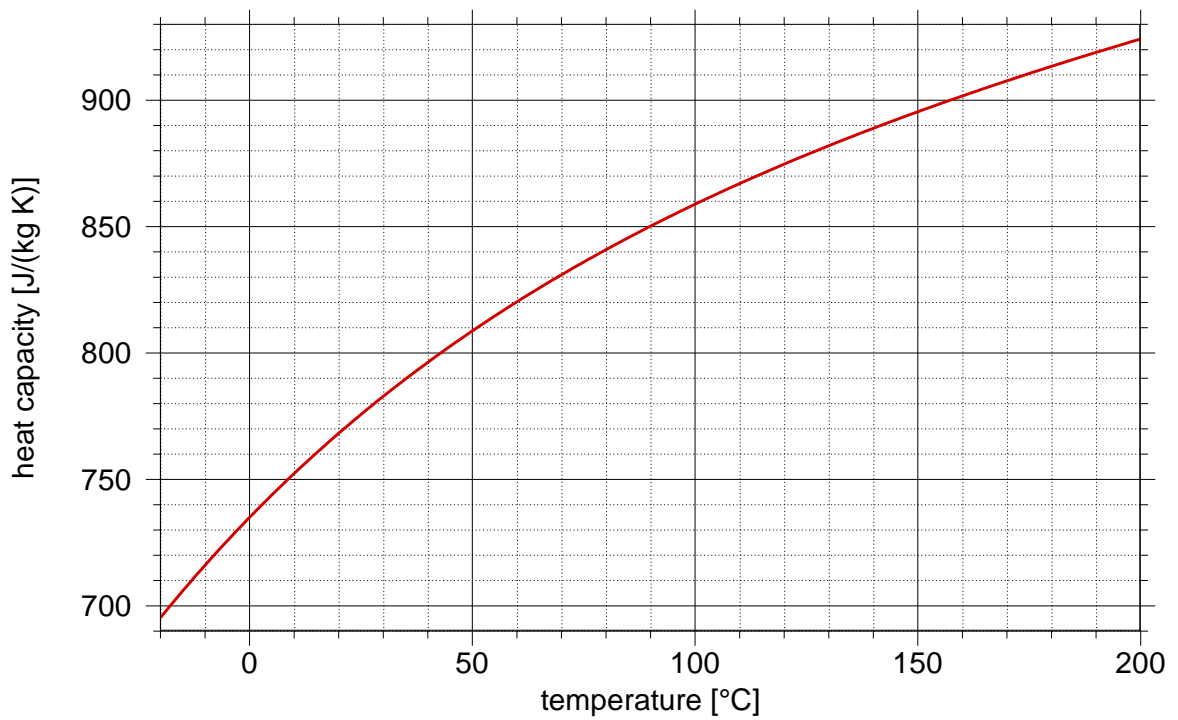


Fig. B.19 Heat capacity of the rock

B.3 Discussion of cases 1 to 3

B.3.1 Choice of formulations

The full ranges of temperature and pressure considered in this work are identical with the ranges adopted for case 1. While the state variables for ice are naturally defined for subzero temperatures only, approaches for water including supercooled water and for rock are continuous for the whole range of temperatures.

As pointed out in the previous subsections, the mathematical description of the EOS can be given at different levels of complexity and accuracy. There are the powerful formulations of the IAPWS, other already existing approaches from the literature, the new formulations developed here for case 3 that are obviously also applicable to case 2. The related equations are compiled in Tab. B.1. There may even be simple but reasonably chosen constants.

Tab. B.1 Compilation of formulations for the EOS

state variable	medium	existing	new
density	water	(D.1)	(B.1)
	ice	-*)	(B.3)
	rock	constant**)	constant**)
viscosity	water	(D.12)	(B.5)
	ice ⁺)	-	-
	rock ⁺)	-	-
thermal conductivity	water	(D.18)	(B.7)
	ice	-*)	(B.8)
	rock	(B.9)	(B.9)***)
heat capacity	water	(D.22)	(B.11)
	ice	-*)	(B.12)
	rock	(B.13)	(B.15)

*) no other formulation known to the author

***) see section B.1.1

***) adopted for subzero conditions

An appropriate set of formulations depends on the problem at hand and such criteria like temperature and pressure limitations or the sensitivity of the processes involved on changes of temperature and pressure. Such sets are chosen in the following for cases 1 to 3. The decision process leading to these sets may be of help for finding different sets

for other problems that are not appropriately covered by the cases 1 to 3 as presented here.

B.3.2 Variability of EOS in cases 1 to 3

With a view to computational efficiency, it is of interest to describe the state variables as simple as possible, preferably by constants. Using constants requires that the inaccuracies introduced by the inherent error are acceptably small. In order to establish means for quantification of deviations, the analytical formulations are evaluated with respect to maximum and minimum values over the defined ranges for cases 1 to 3, firstly at constant pressure, and secondly at constant temperature, where applicable. The related data are compiled in Tab. B.2 to Tab. B.4. Note, that as a general rule, a phase change between water and ice affects all considered state variables to a quite noticeable extent.

Based on the arithmetic mean of maximum and minimum value, variability in the considered temperature or pressure range can be expressed as the percentage of the deviation of the maximum (or minimum) value from the mean. The calculated variabilities of the state variables are compiled for all three cases in Tab. B.5. For classification, a critical variability can be defined that indicates where constants can safely be used instead of the more precise functions. Here, more or less arbitrarily, the critical variability is set to 1 %. All values below the critical value are marked in Tab. B.5 in green.

Tab. B.2 Data for calculation of variability of state variables in case 1

case 1	density [kg/m ³]	viscosity [Pa s]	thermal conductivity [W/(kg K)]	heat capacity [kJ/(kg K)]
water	min. 865.01 200 °C max. 1000.91 4 °C	min. 0.0001263 200 °C max. 0.0043631 -20 °C	min. 0.48988 -20 °C max. 0.68404 131 °C	min. 4.179 36 °C max. 4.409 -20 °C
	min. 999.97 0.1 MPa max. 1004.82 10 Mpa	min. 0.0043170 0.1 MPa max. 0.0042434 10 MPa	min. 0.48749 0.1 MPa max. 0.49966 10 MPa	min. 4.409 0.1 MPa max. 4.295 5 MPa
	min. 865.01 2 MPa max. 870.95 10 MPa	min. 0.0001344 2 MPa max. 0.0001533 10 MPa	min. 0.68404 2 MPa max. 0.68905 10 MPa	min. 4.179 0.1 MPa max. 4.154 10 MPa
	min. 917.00 0 max. 920.00 -20	(assumption: $\eta=0$)	min. 2.26480 0 °C max. 2.43580 -20 °C	min. 1.952 -20 °C max. 2.110 0 °C
	(assumption: $\rho=\text{const.}$)	(assumption: $\eta=0$)	min. 2.84175 200 °C max. 3.70066 -20 °C	min. 0.695 -20 °C max. 0.924 200 °C

Tab. B.3 Data for calculation of variability of state variables in case 2

case 2	density [kg/m ³]	viscosity [Pa s]	thermal conductivity [W/(kg K)]	heat capacity [kJ/(kg K)]
water	0.10 MPa	0.10 MPa	0.10 MPa	0.10 MPa
	min. 999.256 -5 °C	min. 0.001518 5 °C	min. 0.54205 5 °C	min. 4.2050 5 °C
	max. 999.975 4 °C	max. 0.002154 -5 °C	max. 0.56779 -5 °C	max. 4.2398 -5 °C
	4 °C	-5 °C	-5 °C	-5 °C
	min. 999.975 0.10 MPa	min. 0.002154 0.10 MPa	min. 0.54205 0.10 MPa	min. 4.2397 0.11 MPa
	max. 999.980 0.11 MPa	max. 0.002154 0.11 MPa	max. 0.54206 0.11 MPa	max. 4.2398 0.10 MPa
-5 °C	+5 °C	+5 °C	+5 °C	
min. 999.256 0.10 MPa	min. 0.001518 0.1 MPa	min. 0.56779 0.10 MPa	min. 4.2049 0.11 MPa	
max. 999.261 0.11 MPa	max. 0.001518 0.11 MPa	max. 0.56780 0.11 MPa	max. 4.2050 0.10 MPa	
ice	min. 917 0 °C	(assumption: $\eta=0$)	min. 2.2648 0 °C	min. 2.082 -5 °C
	max. 917.75 -5 °C		max. 2.3008 -5 °C	max. 2.110 0 °C
rock	(assumption: $\rho=\text{const.}$)	(assumption: $\eta=0$)	min. 3.5756 5 °C	min. 0.726 -5 °C
			max. 3.6247 -5 °C	max. 0.744 5 °C

Tab. B.4 Data for calculation of variability of state variables in case 3

case 3	density [kg/m ³]	viscosity [Pa s]	thermal conductivity [W/(kg K)]	heat capacity [kJ/(kg K)]
water	min. 993.52948 max. 999.97467	min. 0.0010016 max. 0.0043931	min. 0.4874900 max. 0.5980100	min. 4.18480 max. 4.40900
	0.1 MPa -20 °C 4 °C	0.1 MPa 20 °C -20 °C	0.1 MPa -20 °C 20 °C	0.1 MPa 20 °C -20 °C
	min. 999.97467 max. 1004.82257	min. 0.0042434 max. 0.0043931	min. 0.4874900 max. 0.4996600	min. 4.29510 max. 4.40900
	4 °C 0.1 10	-20 °C 10 MPa 0.1 MPa	-20 °C 0.1 MPa 10 MPa	-20 °C 10 MPa 0.1 MPa
	min. 993.52948 max. 999.77307	min. 0.0009977 max. 0.0010016	min. 0.5980100 max. 0.6037400	min. 4.15510 max. 4.18480
	-20 °C 0.1 10	+20 °C 10 MPa 0.1 MPa	+20 °C 0.1 MPa 10 MPa	+20 °C 10 MPa 0.1 MPa
ice	min. 917 max. 920	(assumption: $\eta=0$)	min. 2.264800 max. 2.435800	min. 1.95200 max. 2.11000
	0 °C -20 °C		0 °C -20 °C	-20 °C 0 °C
rock	(assumption: $\rho=\text{const.}$)	(assumption: $\eta=0$)	min. 3.504223 max. 3.700665	min. 695.316 max. 768.237
			+20 °C -20 °C	-20 °C 20 °C

Tab. B.5 Data for calculation of variability of state variables

		variability [%]			variability [%]			
	independent variable	case 1	case 2	case 3		case 1	case 2	case 3
	density	T (water)	7.28	0.04		0.32	thermal conductivity	16.54
p (water)		0.34	0.00	0.31	1.23	0.00		1.23
T (ice)		0.16	0.04	0.16	3.64	0.79		3.64
T (rock)		-	-	-	13.13	0.68		2.73
viscosity	T (water)	94.37	17.31	62.87	heat capacity	2.68	0.41	2.61
	p (water)	1.73	0.00	1.73		1.31	0.00	1.31
	T (ice)	-	-	-		3.89	0.67	3.89
	T (rock)	-	-	-		14.14	1.23	4.98

(all values below 1% are highlighted in green)

B.3.3 Choice of EOS in cases 1 to 3

While looking rather boring, Tab. B.5 provides a quite illuminating diagnosis of the variability of the state variables:

- dependence on pressure
 - In case 2, the admissible pressure range is so narrow that none of the state variables depends seriously on pressure. In case of density, this applies also for the other cases
 - All other state variables are slightly dependent on pressure, meaning by a variability of 1 to 2 %.
- dependence on temperature
 - Only for water in case 1, the **density** is significantly depending on temperature. It can be neglected in cases 2 and 3 as well as for ice in all cases.
 - A strong dependence of water **viscosity** on temperature can be observed for all cases.
 - The dependence of **thermal conductivity** on temperature can only be neglected for rock and ice in case 2. Otherwise, the variability must be taken into account.

- The variability of the **heat capacity** with temperature calls for sticking to functions for the EOS rather than using constants except for water and ice in case 2.

Based on these results, it can be decided in which case which state variable can be approximated by a constant and where an analytical function should be used instead. As a constant, the arithmetic mean of maximum and minimum in the considered temperature range at atmospheric pressure is defined here. The applicable formulations are referenced by the equation number.

Tab. B.6 Chosen expressions for the state variables in cases 1 to 3

state variable	dimension	medium	case 1	case 2	case 3
density	kg/m ³	water ^{*)}	(D.1)	999.6	996.8
		ice ^{**)}	918.5	917.4	918.5
		rock ^{***)}	constant	constant	constant
viscosity	Pa·s	water	(D.12)	(B.5)	(B.5)
		ice ^{+))}	-	-	-
		rock ^{+))}	-	-	-
thermal conductivity	W/(kg·K)	water	(D.18)	(B.7)	(B.7)
		ice ^{†))}	(B.8)	2.283	2.350
		rock ^{††))}	(B.9)	3.600	(B.9)
heat capacity	kJ/(kg·K)	water ^{‡))}	(D.22)	4.222	(B.11)
		ice	(B.12)	2.096	(B.12)
		rock	(B.15)	(B.15)	(B.15)

- ^{*)} eq. (B.1) may be considered instead of a constant
- ^{**)} eq. (B.3) may be considered instead of a constant
- ^{***)} see section B.1.1
- ^{+))} not applicable, see section B.1.2
- ^{†))} eq. (B.8) may be considered instead of a constant
- ^{††))} rather an indication; see discussion in subsection B.1.3
- ^{‡))} eq. (B.11) may be considered instead of a constant

C Appendix: Treatment of freezing soils after /AUK 16/

C.1 General assumptions

The approach of /AUK 16/ is formulated for granular soils based on the assumptions that

- the geometric mean of the grain diameter d_g can be determined,
- the bulk temperature T_{bulk} is known, and
- partly frozen pores have a similar effect on water flow as air filled pores.

C.2 Characterizing soil parameters

Some of the subsequently derived relations require the **geometric mean of the grain diameter d_g** as well as the **geometric standard deviation σ_g** . These two quantities can be approximated by data from the soil composition. The soils discussed in the following are assumed to consist of arbitrary fractions of three subclasses of soils, namely clay, silt, and sand. These subclasses are characterized by a range of particle diameters as for instance defined by the U.S.D.A. according to Tab. C.1. Based on work of /SHI 84/ who assumed that the grain size distribution is approximately log-normal, it is possible to derive diameter d_g and the standard deviation σ_g using the following equations:

$$d_g = e^{(\sum_{i=1}^3 m_i \ln d_i)} \quad (\text{C.1})$$

$$\sigma_g = e^{\sqrt{\sum_{i=1}^3 m_i (\ln d_i)^2 - (\sum_{i=1}^3 m_i \ln d_i)^2}} \quad (\text{C.2})$$

where the index i stands for the three subclasses. Note that if the grain size distribution is a step function, meaning that all grains have the same diameter, $d_g = d_i$ and $\sigma_g = 1$.

Tab. C.1 Ranges of grain sizes characterizing clay, silt and sand; after U.S.D.A.

Soil	Particle size d [mm]
Clay	$d < 0.002$
Silt	$0.002 \leq d < 0.05$
Sand	$0.05 \leq d < 2.0$

Furthermore, required is the **specific surface area A_{spec}** of the soil defined as the particle surface per gram material. This property has been formulated as a pedotransfer func-

tion of the mean grain diameter d_g by /SEP 10/ (for further discussion of this function see /AUK 16/):

$$A_{spec} = 3.89 d_g^{(-0.905)} \quad (C.3)$$

C.3 Effective hydraulic conductivity

The **hydraulic conductivity of a water saturated unfrozen soil** K_{sat} has been described by /CAM 85/ based on a literature review and later modified by /TAR 96/ eventually reading:

$$K_{sat} = 4 \cdot 10^{-5} \left(\frac{0.5}{1 - \Theta_{sat}} \right)^{1.3 b} \cdot e^{(-6.88 m_{clay} - 3.63 m_{silt} - 0.025)} \quad (C.4)$$

with

$$b = d_g^{-0.5} + 0.2 \sigma_g \quad (C.5)$$

When the hydraulic conductivity decreases under freezing conditions, the **effective hydraulic conductivity** K_{eff} is given as the product of the saturated conductivity K_{sat} and the relative permeability K_{rel}

$$K_{eff} = K_{rel} \cdot K_{sat} \quad (C.6)$$

where

$$K_{rel} = S_{uw}^{2b+3} \quad (C.7)$$

and

$$S_w = \frac{\Theta_w}{\Theta_{sat}} \quad (C.8)$$

C.4 Cryosuction

In a system of unfrozen pore water and ice, the difference of free energy in the two phases leads to a water migration towards the ice until thermodynamic equilibrium is reached (eg. /MÜL 19/). This **cryosuction** s_c can be described starting out with the Clausius-Clapeyron relation. Ignoring the difference between the density of water at 4 °C

of about 1000 kg/m³ and the density of air-free ice at 0°C of 918 kg/m³, /THO 09/ present an approximation for the cryogenic suction:

$$s_c \approx -\rho_{ice} L \ln \frac{T}{T_f} \quad (C.9)$$

C.5 Freezing temperature

Formulation (C.9) contains the **pressure-dependent freezing temperature of water** T_f for a given soil. For linking the freezing temperature to a mechanical pressure, the melting-pressure equation from /WAG 11/ is favoured by /AUK 16/. Originally intended to calculate the melting pressure of ice for a given temperature T , the inverse provides the melting temperature T_f for a given pressure. The parameters employed by eq. (C.10) are given in Tab. C.2.

$$\frac{p_{melt}}{p_t} = 1 + \sum_{i=1}^3 \left\{ a_i \left[1 - \left(\frac{T}{T_t} \right)^{b_i} \right] \right\} \quad (C.10)$$

Tab. C.2 Parameters for eq. (C.10)

	i =	1	2	3
a_i		$0.119539337 * 10^7$	$0.808183159 * 10^5$	$0.333826860 * 10^4$
b_i		$0.300000 * 10^1$	$0.257500 * 10^2$	$0.103750 * 10^3$

Porewater pressure and cryosuction add up to the **melting pressure** p_{melt} or ice pressure p_{ice} :

$$p_{ice} = p_{melt} = p_w + s_c \quad (C.11)$$

C.6 Water saturation

The **effective porosity** Φ_{eff} is defined as the fraction of the total porosity that is still available for flow under freezing conditions. It thus relates to the volumetric water content θ_{uw} of unfrozen water and definition (C.8) can be expanded to

$$S_w = \frac{\theta_w}{\theta_{sat}} = \frac{\Phi_{eff}}{\Phi} \quad (C.12)$$

or expressed explicitly

$$\Phi_{\text{eff}} = S_w \Phi = \Theta_w; \quad \Phi = \Theta_{\text{sat}} \quad (\text{C.13})$$

According to /AUK 16/, the volumetric content of unfrozen water and thereby the effective porosity can be expressed in different ways. The authors suggest to use “an empirical formulation based on test results of Anderson & Tice (1972)” (/AND 72/) which is also called soil freezing characteristic curve (SFCC). This formulation is basically a function of the local temperature T and the specific surface area A_{spec} expressed in the following as the volumetric unfrozen water content $\Theta_{\text{u emp}}$.

$$\Theta_{\text{u emp}} = \frac{\rho_w}{\rho_b} e^{(0.2618+0.5519 \cdot \ln(A_{\text{spec}}) - 1.4495(A_{\text{spec}})^{-0.2640} \ln|T_c|)} \quad (\text{C.14})$$

where

$$|T_c| = T_{f\text{bulk}} - T \quad \text{valid only for } T < T_{f\text{bulk}} \quad (\text{C.15})$$

With the help of definition (C.13), equation (C.14) can easily be expressed in terms of the water saturation:

$$S_w = \frac{1}{\Phi} \frac{\rho_w}{\rho_b} e^{(0.2618+0.5519 \cdot \ln(A_{\text{spec}}) - 1.4495(A_{\text{spec}})^{-0.2640} \ln|T_c|)} \quad (\text{C.16})$$

The unfrozen water content $\Theta_{\text{u emp}}$ calculated by eq. (C.14) may result in values that exceed Θ_{sat} (and thereby the total porosity Φ) when the actual temperature T comes close to the bulk freezing temperature $T_{f\text{bulk}}$. The value from Θ_{emp} has therefore to be limited to Θ_{sat} (and thereby the total porosity Φ). For practical purposes, the content of unfrozen water Θ_w is thus evaluated as

$$\Theta_w = \begin{cases} \Theta_{\text{emp}} & \text{for } \Theta_{\text{emp}} < \Theta_{\text{sat}} \\ \Theta_{\text{sat}} & \text{for } \Theta_{\text{emp}} \geq \Theta_{\text{sat}} \end{cases} \quad (\text{C.17})$$

In this context $\Theta_w = \Theta_{\text{sat}}$ is also called cutoff-value. According to /AUK 16/ the conditions at reaching the cut-off value are of particular significance as the related temperature T_f is assumed to represent the freezing point of a particular soil-water system at a pore water pressure of 0.

C.7 Explanation of variables

- A_{spec} - specific surface area of the grainy material [m^2/g]
- K_{sat} - hydraulic conductivity of the saturated soil in unfrozen state [m/s]
- K_{eff} - effective hydraulic conductivity in a frozen state [m/s]
- K_{rel} - relative hydraulic conductivity [-]
- L - latent heat [J/kg]; $L = 333.55$ kJ/kg for freezing/melting water
- S_{uw} - degree of unfrozen water saturation [-]
- T_{fbulk} - bulk freezing point [K]; $T_{fbulk} = 273.16$ K
- T_{bulk} - bulk temperature [K]
- T - local temperature [K]
- T_c - local temperature [$^{\circ}C$]
- T_f - local freezing point [K]
- T_t - reference temperature for eq. (C.10) [K]; $T_t = 273.16$ K
- a_i - parameters for eq. (C.10) [-]
- b_i - parameters for eq. (C.10) [-]
- b - empirical auxiliary function [-]
- d_g - geometric mean of the grain diameter [m]
- d_i - arithmetic mean diameter of soil class i [mm];
 $d_{clay} = 0.001$ mm, $d_{silt} = 0.026$ mm and $d_{sand} = 1.025$ mm
- m_i - mass fraction of soil class i [-]
- p_{ice} - pressure on the ice [Pa]
- p_{melt} - melting-pressure of ice [Pa]
- p_w - pore water pressure [Pa]
- p_t - reference pressure for eq. (C.10) [Pa]; $p_t = 611.657$ Pa
- s_c - cryogenic suction [Pa]
- Φ - total porosity of the soil [-]
- Φ_{eff} - effective porosity of the soil allowing for flow [-]
- θ_{sat} - volumetric water content of an unfrozen saturated soil (=porosity) [-]
- θ_{uw} - volumetric content of unfrozen water [-]
- $\theta_{u emp}$ - volumetric content of unfrozen water according to empirical eq. (C.14) [-]
- σ_g - geometric standard deviation of the grain diameter [m]
- ρ_{ice} - density of ice [kg/m^3]; $\rho_{ice} = 918$ kg/ m^3
- ρ_w - density of water [kg/m^3]; $\rho_w = 1000$ kg/ m^3
- ρ_b - density of unfrozen soil [kg/m^3]

D Appendix: Reference formulations from the literature

D.1 Density from /IAP 15/

The density of water ρ_w is given by /IAP 15/ as

$$\rho_w(p, T) = 1 / \left(\frac{1}{\rho_0} \left\{ \frac{\tau + 1}{2} \left[\frac{\omega_0}{2} (1 - \Phi^2) + L_\pi (\Phi + 1) \right] + \Psi_\pi^r \right\} \right) \quad (\text{D.1})$$

ρ_w - density of water [kg/m³]

ρ_0 - reference density [kg/m³]; $\rho_0 = 1081.6482$ [kg/m³]

τ - scaled temperature; see (D.2) [-]

ω_0 - parameter [-]; $\omega_0 = 0.5212269$

Φ - order parameter; see (D.3) [-]

L_π - partial derivative of function L (cp. (D.10)) with respect to π ; see (D.4) [-]

Ψ_π^r - partial derivative of function Ψ^r with respect to π ; see (D.8) [-]

with the scaled temperature τ

$$\tau = \frac{T}{T_{LL}} - 1 \quad (\text{D.2})$$

T - temperature [K]

T_{LL} - reference temperature [K]; $T_{LL} = 228.2$ K

the order parameter Φ

$$\Phi = 2x - 1 \quad (\text{D.3})$$

x - mole fraction (cp. (D.9)) [-]

the funktion L_π

$$L_\pi = \frac{L_0 K_2 (K_1 + k_0 k_2 - k_1 \pi + k_1 k_2 \tau - 1)}{2 k_2 K_1} \quad (\text{D.4})$$

L_0 – parameter [-]; $L_0 = 0.76317954$

k_0 – parameter [-]; $k_0 = 0.072158686$

k_1 – parameter [-]; $k_1 = -0.31569232$

k_2 – parameter [-]; $k_2 = 5.2992608$

K_1 – supplemental function; see (D.5) [-]

K_2 – supplemental function; see (D.6) [-]

π - scaled pressure; see (D.7) [-]

with

$$K_1 = \sqrt{[1 + k_0 k_2 + k_1 (\pi - k_2 \tau)]^2 - 4 k_0 k_1 k_2 (\pi - k_2 \tau)} \quad (\text{D.5})$$

$$K_2 = \sqrt{1 + k_2^2} \quad (\text{D.6})$$

the scaled pressure π

$$\pi = \frac{p}{\rho_0 R T_{LL}} \quad (\text{D.7})$$

p - pressure [Pa]

R - specific gas constant [J/(kg K)]; $R = 461.523087$ [J/(kg K)]

and function Ψ_π^r

$$\Psi_\pi^r = \sum_{i=1}^{20} c_i \bar{\tau}^{a_i \bar{\pi}} (b_i - d_i \bar{\pi}) e^{-d_i \bar{\pi}} \quad (\text{D.8})$$

with $\bar{\tau} = \tau - 1$ and $\bar{\pi} = \pi + \pi_0$

a_i – parameter; s. Tab. D.1 [-]

b_i – parameter; s. Tab. D.1 [-]

c_i – parameter; s. Tab. D.1 [-]

d_i – parameter; s. Tab. D.1 [-]

π_0 – parameter [-]; $\pi_0 = \frac{3 \cdot 10^8 Pa}{\rho_0 R T_{LL}}$

The mole fraction x cannot be calculated directly but has to be determined iteratively with the help of equation (D.9)

$$L(\tau, \pi) + \ln \frac{x}{1-x} + \omega(\pi)(1-2x) = 0 \quad (D.9)$$

L – function; see (D.10) [-]

ω – interaction parameter; see (D.11) [-]

where

$$L(\tau, \pi) = L_0 \frac{K_2}{2k_1 k_2} [1 + k_0 k_2 + k_1(\pi + k_2 \tau) - K_1] \quad (D.10)$$

and

$$\omega(\pi) = 2 + \omega_0 \pi \quad (D.11)$$

ω_0 - parameter [-]; $\omega_0 = 0.5212269$

The parameters a_i to d_i as required for equation (D.8) are compiled in Tab. D.1.

Tab. D.1 Parameters a_i , b_i , c_i , and d_i for equation (D.8)

i	a_i	b_i	c_i	d_i
1	0	0	-8.157 068 138 165 5	0
2	0	1	1.287 503 2	0
3	1	0	7.090 167 359 801 2	0
4	-0.2555	2.1051	-3.277 916 1 $\times 10^{-2}$	-0.0016
5	1.5762	1.1422	7.370 394 9 $\times 10^{-1}$	0.6894
6	1.6400	0.9510	-2.162 862 2 $\times 10^{-1}$	0.0130
7	3.6385	0	-5.178 247 9	0.0002
8	-0.3828	3.6402	4.229 351 7 $\times 10^{-4}$	0.0435
9	1.6219	2.0760	2.359 210 9 $\times 10^{-2}$	0.0500
10	4.3287	-0.0016	4.377 375 4	0.0004
11	3.4763	2.2769	-2.996 777 0 $\times 10^{-3}$	0.0528
12	5.1556	0.0008	-9.655 801 8 $\times 10^{-1}$	0.0147
13	-0.3593	0.3706	3.759 528 6	0.8584
14	5.0361	-0.3975	1.263 244 1	0.9924
15	2.9786	2.9730	2.854 269 7 $\times 10^{-1}$	1.0041
16	6.2373	-0.3180	-8.599 494 7 $\times 10^{-1}$	1.0961
17	4.0460	2.9805	-3.291 615 3 $\times 10^{-1}$	1.0228
18	5.3558	2.9265	9.001 961 6 $\times 10^{-2}$	1.0303
19	9.0157	0.4456	8.114 972 6 $\times 10^{-2}$	1.6180
20	1.2194	0.1298	-3.278 821 3	0.5213

The stated uncertainty of the calculated water density amounts to 0.04%. Up to 300 K, the uncertainty lies rather in the range of 0.0001 %. Beyond this temperature, the formulations from /IAP 18/ are recommended, though.

D.2 Viscosity from /IAP 08/

The formulation from /IAP 08/ for calculation of the viscosity consists of three terms:

$$\bar{\mu} = \bar{\mu}_0(\bar{T}) \cdot \bar{\mu}_1(\bar{T}, \bar{\rho}) \cdot \bar{\mu}_2(\bar{T}, \bar{\rho}) \quad (\text{D.12})$$

$\bar{\mu}$ – dimensionless viscosity; see (D.13) [-]

\bar{T} – dimensionless temperature; see (D.14) [-]

$\bar{\rho}$ – dimensionless density; see (D.15) [-]

$\bar{\mu}_0$ – scaled viscosity in the dilute-gas limit; see (D.16) [-]

$\bar{\mu}_1$ – viscosity due to finite density; see (D.17) [-]

$\bar{\mu}_2$ – critical enhancement of the viscosity [-]

where

$$\bar{\mu} = \frac{\mu}{\mu^*} \quad (\text{D.13})$$

μ – viscosity [Pa·s]

μ^* – reference viscosity [Pa·s]; $\mu^* = 10^{-6}$ Pa·s

$$\bar{T} = \frac{T}{T^*} \quad (\text{D.14})$$

T – temperature [K]

T^* – reference temperature [K]; $T^* = 647.096$ K

$$\bar{\rho} = \frac{\rho}{\rho^*} \quad (\text{D.15})$$

ρ – density [kg/m³]

ρ^* – reference density [kg/m³]; $\rho^* = 322.0$ kg/m³

The function $\bar{\mu}_0$ is given as

$$\bar{\mu}_0 = \frac{100\sqrt{\bar{T}}}{\sum_{i=0}^3 \frac{H_i}{\bar{T}^i}} \quad (\text{D.16})$$

H_i – coefficients; see Tab. D.2 [-]

and function $\bar{\mu}_1$ as

$$\bar{\mu}_1 = e \left[\bar{\rho}^{\sum_{i=0}^5 \left(\frac{1}{\bar{T}} - 1 \right)^i} H_{ij} \sum_{j=0}^6 (\bar{\rho} - 1)^j \right] \quad (\text{D.17})$$

H_{ij} – coefficients; see Tab. D.2 [-]

Note that formulation (D.12) for the viscosity includes a third function $\bar{\mu}_2$ that represents a final necessary correction “in a very small region in density and temperature around the critical point” /IAP 08/. Since the critical point for water is far beyond the temperature range of interest here, the function $\bar{\mu}_2$ can safely be dropped for the purpose at hand.

Tab. D.2 Coefficients H_i for eq. (D.16)

i	H_i
0	1.67752
1	2.20462
2	0.6366564
3	-0.241605

Tab. D.3 Coefficients H_{ij} for eq. (D.17)

i	j	H_{ij}^{53}
0	0	$5.20094 \cdot 10^{-1}$
1	0	$8.50895 \cdot 10^{-2}$
2	0	-1.08374
3	0	$-2.89555 \cdot 10^{-1}$
0	1	$2.22531 \cdot 10^{-1}$
1	1	$9.99115 \cdot 10^{-1}$
2	1	1.88797
3	1	1.26613
5	1	$1.20573 \cdot 10^{-1}$
0	2	$-2.81378 \cdot 10^{-1}$
1	2	$-9.06851 \cdot 10^{-1}$
2	2	$-7.72479 \cdot 10^{-1}$
3	2	$-4.89837 \cdot 10^{-1}$
4	2	$-2.57040 \cdot 10^{-1}$
0	3	$1.61913 \cdot 10^{-1}$
1	3	$2.57399 \cdot 10^{-1}$
0	4	$-3.25372 \cdot 10^{-2}$
3	4	$6.98452 \cdot 10^{-2}$
4	5	$8.72102 \cdot 10^{-3}$
3	6	$-4.35673 \cdot 10^{-3}$
5	6	$-5.93264 \cdot 10^{-4}$

The formulation for the viscosity of water above 0 °C "... is in fair agreement (within 5 %) with available data down to 250 K" /IAP 08/. For higher temperatures, the estimated uncertainty of approach (D.12) amounts to 1 %.

⁵³ "Note: Coefficients H_{ij} omitted from Table 2 are identically equal to zero." /IAP 08/

D.3 Thermal conductivity from /IAP 11/

The formulation for thermal conductivity from /IAP 11/ is formally quite similar to the formulation of the viscosity:

$$\bar{\lambda} = \bar{\lambda}_0(\bar{T}) \cdot \bar{\lambda}_1(\bar{T}, \bar{\rho}) + \bar{\lambda}_2(\bar{T}, \bar{\rho}) \quad (\text{D.18})$$

$\bar{\lambda}$ – dimensionless thermal conductivity; see (D.19) [-]

\bar{T} – dimensionless temperature; see (D.14) [-]

$\bar{\rho}$ – dimensionless density; see (D.15) [-]

$\bar{\lambda}_0$ – scaled thermal conductivity limit; see (D.20) [-]

$\bar{\lambda}_1$ – thermal conductivity due to finite density; see (D.21) [-]

$\bar{\lambda}_2$ – critical enhancement of the thermal conductivity [-]

where

$$\bar{\lambda} = \frac{\lambda}{\lambda^*} \quad (\text{D.19})$$

λ – thermal conductivity [W/(m K)]

λ^* – reference thermal conductivity [W/(m K)]; $\lambda^* = 10^{-3}$ W/(m K)

The function $\bar{\lambda}_0$ is given as

$$\bar{\lambda}_0 = \frac{\sqrt{\bar{T}}}{\sum_{i=0}^4 \frac{L_i}{\bar{T}^i}} \quad (\text{D.20})$$

L_i – coefficients; see Tab. D.4 [-]

and function $\bar{\lambda}_1$ as

$$\bar{\lambda}_1 = e^{\left[\bar{\rho} \sum_{i=0}^4 \left(\left(\frac{1}{\bar{T}} - 1 \right)^i \sum_{j=0}^5 L_{ij} (\bar{\rho} - 1)^j \right) \right]} \quad (\text{D.21})$$

L_{ij} – coefficients; see Tab. D.5 [-]

Tab. D.4 Coefficients L_i for eq. (D.20)

i	L_i
0	$2.443\ 221 \cdot 10^{-3}$
1	$1.323\ 095 \cdot 10^{-2}$
2	$6.770\ 357 \cdot 10^{-3}$
3	$-3.454\ 586 \cdot 10^{-3}$
4	$4.096\ 266 \cdot 10^{-4}$

Tab. D.5 Coefficients L_{ij} for eq. (D.21)

i	j	L_{ij}
0	0	1.603 973 57
1	0	2.337 718 42
2	0	2.196 505 29
3	0	-1.210 513 78
4	0	-2.720 337 0
0	1	-0.646 013 523
1	1	-2.788 437 78
2	1	-4.545 807 85
3	1	1.608 129 89
4	1	4.575 863 31
0	2	0.111 443 906
1	2	1.536 161 67
2	2	3.557 772 44
3	2	-0.621 178 141
4	2	-3.183 692 45
0	3	0.102 997 357
1	3	-0.463 045 512
2	3	-1.409 449 78
3	3	0.071 637 322 4
4	3	1.116 834 8
0	4	-0.050 412 363 4
1	4	0.083 282 701 9
2	4	0.275 418 278
3	4	0
4	4	-0.192 683 05
0	5	0.006 098 592 58
1	5	-0.007 192 012 45
2	5	-0.020 593 881 6
3	5	0
4	5	0.012 913 842

Note that formulation (D.18) for the thermal conductivity includes a third function $\bar{\lambda}_2$ that represents a final necessary additive correction. This correction is quantified in IAP 11/ to amount to about 0.1 % or less of the total value for the thermal conductivity in the

temperature and pressure range that is of interest in the present work. The critical enhancement is therefore not considered here.

Uncertainty in the thermal conductivity of water below 0 °C is not quantified in /IAP 11/. It is stated, though, that equation (D.18) “behaves in a physically reasonable manner down to 250 K”. Otherwise, it is expected to be lower than 1.5 % in the temperature and pressured range considered in this work.

D.4 Heat capacity from /IAP 15/

Heat capacity of water is described in /IAP 15/ by

$$c_p = -R(\tau + 1) \left\{ L_\tau(\Phi + 1) + \frac{1}{2}(\tau + 1)[L_{\tau\tau}(\Phi + 1) - L_\tau^2\chi] + \psi_{\tau\tau}^r \right\} \quad (\text{D.22})$$

c_p – heat capacity [J/(kg K)]

R – specific gas constant [J/(kg K)]; $R = 461.523087$ [J/(kg K)]

τ – scaled temperature; see (D.2) [-]

Φ – order parameter; see (D.3) [-]

L_τ – partial derivative of function L (cp. (D.10)) with respect to τ ; see (D.23) [-]

$L_{\tau\tau}$ – second partial derivative of function L with respect to τ ; see (D.24) [-]

$\Psi_{\tau\tau}^r$ – partial derivative of function Ψ^r with respect to τ ; see (D.25) [-]

χ – susceptibility; see (D.26) [-]

with

$$L_\tau = \frac{L_0 K_2}{2} \left(1 + \frac{1 - k_0 k_2 + k_1(\pi - k_2 \tau)}{K_1} \right)$$

L_0 – parameter [-]; $L_0 = 0.76317954$

k_0 – parameter [-]; $k_0 = 0.072158686$

k_1 – parameter [-]; $k_1 = -0.31569232$

k_2 – parameter [-]; $k_2 = 5.2992608$

K_1 – supplemental function; see (D.5) [-]

K_2 – supplemental function; see (D.6) [-]

π – scaled pressure; see (D.7) [-]

$$L_{\tau\tau} = -\frac{2L_0 K_2 k_0 k_1 k_2^2}{K_1^3} \quad (\text{D.24})$$

$$\Psi_{\tau\tau}^r = \sum_{i=1}^{20} c_i a_i (a_i - 1) \bar{\tau}^{(a_i-2)} \bar{\pi}^{b_i} e^{-a_i \bar{\pi}} \quad (\text{D.25})$$

$\bar{\tau} = \tau - 1$ and $\bar{\pi} = \pi + \pi_0$

a_i – parameter; s. Tab. D.1 [-]

b_i – parameter; s. Tab. D.1 [-]

c_i – parameter; s. Tab. D.1 [-]

d_i – parameter; s. Tab. D.1 [-]

π_0 – parameter [-]; $\pi_0 = \frac{3 \cdot 10^8 Pa}{\rho_0 R T_{LL}}$

$$\chi = \left(\frac{2}{1 - \Phi^2} - \omega \right) \quad (D.26)$$

ω – interaction parameter; see (D.11) [-]

Since calculation of the heat capacity is based on the same formulations as those for density, the same accuracy of the calculated values is expected.

**Gesellschaft für Anlagen-
und Reaktorsicherheit
(GRS) gGmbH**

Schwertnergasse 1
50667 Köln

Telefon +49 221 2068-0

Telefax +49 221 2068-888

Boltzmannstraße 14

85748 Garching b. München

Telefon +49 89 32004-0

Telefax +49 89 32004-300

Kurfürstendamm 200

10719 Berlin

Telefon +49 30 88589-0

Telefax +49 30 88589-111

Theodor-Heuss-Straße 4

38122 Braunschweig

Telefon +49 531 8012-0

Telefax +49 531 8012-200

www.grs.de